SURFACE REACTIONS AND ELECTRICAL DOUBLE LAYER PROPERTIES OF CERAMIC OXIDES IN AQUEOUS SOLUTION

BY

WAYNE CHARLES HASZ
B.S. Ceramic Science, Rutgers University (1981)

Submitted to the Department of
Materials Science and Engineering
in Partial Fulfillment of the
Requirements of the Degree of
Master of Science in Ceramics

at the

Massachusetts Institute of Technology

December 1983

Signature of Author ______________________
Department of Materials Science and Eng.
December 27, 1983

Certified by ______________________
Alan Bleier
Thesis Supervisor

Accepted by ______________________
Bernhardt Wuensch
Chairman, Departmental Committee on
Graduate Students

SURFACE REACTIONS AND ELECTRICAL DOUBLE LAYER PROPERTIES OF CERAMIC OXIDES IN AQUEOUS SOLUTION

BY

WAYNE CHARLES HASZ
B.S. Ceramic Science, Rutgers University (1981)

Submitted to the Department of Materials Science and Engineering in partial fulfillment of the requirements of the degree of Master of Science in Ceramics

Abstract

Surface charge arising from interfacial reactions of electrolyte ions with SiO_2, Al_2O_3, $Al_2O_3 \cdot SiO_2$ (mullite), and ZrO_2 suspensions are analysed using potentiometric titration. Points of zero charge, p.z.c., are calculated and surface charge profiles are plotted for these oxides. The intrinsic surface ionization and complexation constants of electrolyte ions on the surface are determined from the surface charge data using the double extrapolation technique of Davis, James, and Leckie. Theoretical equilibrium calculations are employed to solve for the interfacial reactions at the oxide/solution interface using the experimentally determined ionization and complexation constants to estimate the concentration of charged species in the electrical double layer, e.d.l.. From this estimate, the charge and potential distribution in the e.d.l. are calculated. The theoretical surface charge curves for SiO_2 and Al_2O_3 are compared to those determined experimentally. ζ-potentials for Al_2O_3 are calculated from electrophoresis data are compared with the theoretical values of the diffuse layer potential, Ψ_d. The theoretical charge distributions predict the experimental surface charge data well, implying that the DJL model applies for these systems. Theoretical diffuse layer potentials predict the experimentally measured ζ-potential well for pH-values greater than the isoelectric point.

Thesis Supervisor: Dr. Alan Bleier

Title: Assistant Professor of Ceramics

Table of Contents

List of Figures

List of Tables

Acknowledgements

The author would like to express appreciation to Professor Alan Bleier for his guidance during the research and preparation of this thesis.

The author would also like to express graditude and appreciation to Dr. R. James for helpfull discussions concerning MINEQL and Mr. Thomas M. Kramer and Ms. Margaret M. O'Connor for their helpful comments and suggestions in proof reading this thesis.

Financial support under the U.S. Department of Energy, Division of Materials Sciences, Contract # DE-AC02-81ER10953 is gratefully acknowledged.

1) Introduction

Typical ceramic processing techniques such as milling, dispersing, and casting, often produce green bodies of poor quality that require excessively high temperatures to sinter fully (REF Brook-81a). Poor properties are the result of the final, nonuniform, fired microstructures that develop from the poorly controlled green microstructure (REF Evans-82a). This problem reflects the fact that standard ceramic processing techniques do not adequately control particle arrangement in suspension.

If a ceramic suspension settles into an ordered array, the resultant green body exhibits regular particle spacing, a desirable feature for homogeneous sintering. Agglomeration of individual particles must be prevented to eliminate randomly packed regions in the ordered green body (REF Evans-82b). Furthermore, the use of spherical, monodispersed particles promotes uniform packing, in contrast with the irregularities arising from the broad particle size and shape distributions of normally milled powders (REF Rhodes-81a). Control of agglomeration and particle size and shape distributions permits ordered particle arrangement and high density in ceramic suspensions and green bodies.

The major technological consequences of understanding and controlling powders and their packing, according to Bowen (REF Bowen-80a), are:

1) Reliably reproduced microstructures.
2) Elimination of warping and cracking in densified

pieces.

3) Reproducibly sintered complex parts that do not require final grinding or finishing steps since shrinkage is controlled and uniform.
4) Formation of very fine-grained microstructures with improved mechanical properties.
5) Reduced sintering time and temperature.
6) Improved physical properties.
7) Reduced need for sintering aids.

Studies by Jubb (REF Jubb-82a) and Barringer (REF Barringer-82a) support Bowen's contention show that monosized particles improve processing by promoting ordered particle packing in the green body, thus forming dense, sintered pieces.

The next question is, how do we control particles in ceramic systems prepared using less ideal, commercially available powders that are not monosized, spherical, or nonagglomerated? Agglomeration and most interactions in these suspensions originate with the electrical double layer (e.d.l.) surrounding suspended particles. Consequently, the control of flocculation involves the surface and diffuse layer charges and potentials that govern not only suspension stability, but also interparticle spacing and particle arrangement in the concentrated suspension. Knowledge of the e.d.l. and appropriate models for ceramic powders are required to control ceramic processes reproducibly and to predict material properties reliably (REF Bleier-83a).

The e.d.l. of a material in suspension depends on the predominant surface phase and on the reactions that occur between the surface and solution. Since the properties of single and multicomponent powders in suspension are governed by the surface phase, the major volumetric phase may not significantly influence the e.d.l. properties. This is especially true when minor phases or contaminants that are highly surface active are present. Surface charge and potential arise from reactions of surface sites with the electrolyte ions in solution. The e.d.l. properties can therefore be modeled by determining appropriate surface-solution equilibria. These reactions are described by:

1) Surface ionization and complexation coefficients.
2) Surface and bulk solution species concentrations.
3) Charge and potential distribution of the electrical double layer.

The nature and extent of these reactions must be understood in order to control the e.d.l. properties of the powder, thereby preventing agglomeration, ensuring suspension stability, and improving processing.

The Davis, James and Leckie (DJL) model (REF Davis-78a, James-82a) describes the reaction of H^+, OH^-, and electrolyte species at the surface and in the e.d.l. for simple, single component oxide suspensions. A double extrapolation technique is employed to calculate the ionization and complexation constants of surface species. Unfortunately, a simple model adequately describing surface reactions and development of the e.d.l. does not presently exist for powders with multicomponent surfaces.

The principal objective of this study was to determine the reactions that occur on several oxide powders in aqueous suspension and to model the change in the e.d.l. structure and properties that result from these reactions. Silica, alumina and zirconia were chosen for study since they are technologically important ceramic oxides. Mullite, $3Al_2O_3 \cdot 2SiO_2$, was chosen since it is a common mixed, multicomponent oxide. composed of two of the single oxides studied. The support electrolyte was NaCl because of the extensive literature available on it.

In this work, the surface charge of several silicas, aluminas, and mullite were measured in aqueous NaCl solutions using potentiometric titration. The DJL model was used to calculate the apparent surface ionization (for OH^- and H^+) and complexation (for Cl^- and Na^+) coefficients at various conditions of pH and salt concentration. From these values, intrinsic thermodynamic surface coefficients were determined via extrapolation to the conditions of zero surface charge condition. The computer program, SITECAL, was used to calculate the relative concentrations of charged species at the surface and in the e.d.l., for a wide range of pH and electrolyte concentrations, based on the intrinsic ionization and complexation constants. Electrical double layer charge and potential distributions were estimated and compared to the experimentally determined σ_o for silica and alumina to check the consistancy of the proposed reaction model for these oxides. Comparison between the theoretical Ψ_d and experimentally measured ζ-potential for alumina were made.

2.1) Models of the Oxide/Solution Interface

When an oxide powder is immersed in an electrolyte solution, ions distribute near the solid/solution interface creating the electrical double layer, e.d.l. This distribution occurs in response to the surface potential generated as a result of chemical reactions between surface sites and charged, solution species. Counterions, soluable species opposite in sign to that of the surface, distribute in the solution to balance or screen the surface charge. Several models propose to describe the locations of ions near a charged interface: the Gouy-Chapman model, the Stern-Grahame model, and various others derived from these two models.

2.1.1) Gouy-Chapman and Stern-Grahame Models

Gouy-10a and Chapman-13a derived equations, the GC model, relating the equilibrium concentration of ions surrounding a charged mercury electrode in solution. Ions distribute in solution near the electrode surface in response to the applied potential resulting in the electrical double layer. The simplified, pertinent equations that describe the distribution of charge, σ, and potential, Ψ, in the e.d.l. are:

e2.1.1 $$\sigma_o + \sigma_d = 0$$

e2.1.2 $$\sigma_d = -(8c\varepsilon kT)^{1/2}\sinh(-e\Psi_o/zkT)$$

where, c is the concentration;
o and d denote the surface and diffuse layer;
ε is the dielectric constant;

k is the Boltzman constant;
T is the temperature;
e is the charge on an electron;
z is the electrolyte ion charge;

The GC model predicts much higher charge densities for high surface potentials than is expected, since a finite ion size is not assumed. Thus, an infinite number of ions can approach the surface in response to the applied surface potential.

Stern-24a modified the GC model after realizing that ions have a finite size and that they can, therefore, only approach the surface to some finite distance, thereby limiting the maximum adsorption density. Stern divided the e.d.l. into two regions, one located adjacent to the surface containing specifically adsorbed ions (the Stern layer) and the other consisting of unoriented ions in a diffuse, GC type region. The thickness of the Stern plane, d, is approximately half the radius of a solvated ion. Important assumptions about the adsorbed layer at the surface are (REF Hiemenz-77a):

1) The adsorption follows a Langmuir adsorption isotherm which may be written:

e2.1.3 $$\theta = Kn_o/(1+Kn_o)$$

where, θ is the fraction of occupied surface sites;
K is a constant;
n_o is the concentration of the adsorbing ion.

This isotherm implies a state of surface saturation. The constant, K, is described by a Boltzmann factor where the potential energy is composed of electrical and chemical terms involved with adsorption in the Stern plane:

e2.1.4 $$K = \exp((ze\Psi_d+\Phi)/kT)$$

where, Φ is the chemical energy of adsorption;
Ψ_d is the electrostatic potential at the Stern plane.

2) A parallel plate capacitor model describes the linear potential profile in the Stern plane which can be formulated to include the fraction of occupied sites:

e2.1.5 $$\frac{\Psi_o-\Psi_d}{d} = \frac{4\pi}{\varepsilon_d}\sigma_d = \frac{4\pi}{\varepsilon_d}\frac{\sigma_d^{sat}\,Kn_o}{1+Kn_o}$$

where, d is the distance between the surface and the diffuse layer;
σ_d^{sat} is the maximum diffuse layer charge.

Grahame-47a refined Stern's model by considering the state of hydration of the surface and adsorbed ions to determine positions of the planes of adsorption. The physical picture of the Stern model remains intact, but an explanation of the locations of the adsorption planes is given in this SG model. The metal surface with charge, σ_o, and potential, Ψ_o, is considered covered by a layer of water molecules, in the inner most double layer region. Unhydrated electrolyte ions (usually anions or large cations) displace the hydrated layer and specifically adsorb at the surface such that their centers define a region known as the inner Helmholtz plane (IHP), some distance, B, from the surface. Hydrated ions, usually cations, do not displace the layer of hydration and the center of these ions defines the outer Helmholtz plane (OHP), some distance, d, from the metal surface. Farther from the surface, a region of unoriented, diffuse ions extends from the OHP into the bulk solution. This diffuse region of the e.d.l. has an ion concentration profile given by the Boltzmann distribution. The pertinent equations for the SG model are:

e2.1.6 $\sigma_o + \sigma_\beta + \sigma_d = 0$ (Charge Neutrality)

e2.1.7 $\Psi_o - \Psi_\beta = \sigma_o / C_1$ (IHP)

e2.1.8 $\Psi_\beta - \Psi_d = \dfrac{\sigma_o + \sigma_\beta}{C_2} = -\dfrac{\sigma_d}{C_2}$ (OHP)

where, $C_{1(2)}$ are the capacitances for the inner (outer) adsorption planes;
o, β and d respectively identify the surface, IHP and OHP.

Equations e2.1.7 and e2.1.8 upgrade Stern's capacitor model.

The variations of the Stern model are shown in Figure 2.1. In the basic Stern model, the outer capacitance is assumed zero hence $\Psi_\beta = \Psi_d$ (Figure 2.1c). In the extended Stern model, the outer capacitance is not zero resulting in the potential profile seen in Figure 2.1c. The Stern theory introduces terms, C_1 and K, that cannot be easily experimentally evaluated. The inner layer capacitance cannot be directly determined since the surface and IHP potentials cannot be measured. The constant K is difficult to determine from energy considerations since the chemical and electrical energy components of adsorption cannot be separated.

2.1.2) Surface Charge Development

To develop the GC and SG models, a potential was considered applied to a mercury electrode, so that Ψ_o was experimentally controlled. The development of surface charge was considered straightforward and given by relatively simple equations. Hence, detailed charging mechanisms were considered of minor interest due to the metallic properties of Hg(l) electrodes. Contrastingly, for oxide surfaces, charging mechanisms are of primary concern because the surface charge originates with reactions between solution species and discrete surface sites. Therefore site type, density, and the overall surface charge must be determined, in order to describe e.d.l.'s associated with metal oxides in terms of equations e2.1.1 through e2.1.6.

Dry oxide surfaces, by their insulating nature, are electrically neutral and have no net surface charge or potential. When oxide powders are placed in aqueous solution, H_2O and H^+ and OH^- ions react with the surface to generate a hydroxylated layer. If this hydroxylated layer is considered as the new surface, then H^+ and OH^- ions from solution equilibrate with the hydroxylated surface sites. Ionization reactions change the number of charged species on the surface, altering the surface charge and potential. The H^+ and OH^- ions are therefore considered potential-determining ions (p.d.i.) for ceramic oxides processed in aqueous solution. Electrolyte species may also adsorb specifically (unhydrated) or nonspecifically (hydrated) as discussed earlier. Adsorption of positive and negative p.d.i. is not usually stoichiometric and surface charging generally results. The net surface charge of an oxide in aqueous solution is described by the equation:

e2.1.9 $$\sigma_o = F(\Gamma_+ - \Gamma_-)$$

where, F is the Faraday constant;
Γ is the surface adsorption density of the positively and negatively charged species.

The pH at which the surface charge is zero is called the point of zero charge (p.z.c.). Since the surface potential is also considered zero at the p.z.c., the Nernst equation can be written to describe the surface potential at any pH. Note: in most cases, the hydrogen ion concentration is assumed equal to its activity:

e2.1.10 $$\Psi_o = \frac{2.3\ RT}{F}(pH_{p.z.c.} - pH)$$

where, pH is $-\log[H^+]$;
[ ] is the ion concentration;
R is the gas constant.

This approach is valid only if the solid and solution are in thermodynamic equilibrium and H^+ and OH^- are the effective p.d.i. Equilibrium is not usually attained in titration experiments designed to yield surface charge because solubility of the oxide in the electrolyte solution often invalidates the use ot the Nernst equation. Finally, the diffuse layer potential, Ψ_d, may be estimated for oxides from experimentally determined ζ-potentials.

2.1.3) Porous Surfaces

In order to explain very high surface charge and low ζ-potentials exhibited by some oxide powders, several authors have modeled the surface as a porous gel layer (REFS Lyklema-68a, 71a, Tadros-68a, 69b, and Perram-73a, 74a). Here, the surface is considered porous to potential-determining and counterions. Adsorption is enhanced by the surface's microporosity or gel layer formed via surface dissolution and reprecipitation. Penetration of counterions into this region neutralizes the charges developed by p.d.i. Thus, high surface charge can develop without the correspondingly high ζ-potential because of charge neutralization within the e.d.l.

2.1.4) Site-Binding Surface Models

Several authors model the surface of an oxide in solution as planar, impervious, and consisting of surface sites that undergo chemical reactions with the solution's electrolyte ions (REFS Berube-68a, Levine-71a, Wiese-71a, Hunter-71a, and Yates-74a). Reviews of surface-site models include those by Healy-78a, Westall-80a, Morel-81a, and Sposito-83a. According to these models, surface sites ionize to form positive and negative sites that then react with soluble counterions. All of the models employ surface reactions that may be represented by mass balance equations of the type:

e2.1.11a $SOH^{o} + H_s^{+} = SOH_2^{+}$ $K_1 = \frac{[SOH_2^{+}]}{[SOH^{o}][H_s^{+}]}$

e2.1.11b $SO^{-} + H_s^{+} = SOH^{o}$ $K_2 = \frac{[SOH^{o}]}{[SO^{-}][H_s^{+}]}$

where, S is a surface metal ion site;

SOH^{o} is a neutral, hydroxylated surface site;

SOH_2^{+} is a positive, ionized surface group;

SO^{-} is a negative, ionized surface group;

H_s^{+} is a hydrogen ion located at the surface.

The electrical potential developed at the particle surface and its decaying field in the adjacent solution result from these ionization reactions and cause the chemical potential of the e.d.l. species to change. This process requires the distribution of ions in the e.d.l. to obey the Boltzmann distribution, which describes the potential decay from the surface to bulk solution. Equations e2.1.11a and b are therefore modified to include:

e2.1.12 $[H_s^{+}] = [H_{aq}^{+}]\exp(-e\Psi_o/kT)$

where H_{aq}^{+} is the free H^{+} concentration in solution. Similar expressions pertain to each specie in the e.d.l. The concentration of each specie is normally used instead of activities since the latter are difficult to determine.

The material balance equations used to describe surface reactions are of the forms:

e2.1.13a $\Gamma(SOH) = [SOH] + [SO^{-}] + [SOH_2^{+}]$

e2.1.13b $\Gamma(H) = [H^{+}] - [OH^{-}] + [SOH_2^{+}] - [SO^{-}]$

where Γ is the total surface concentration of the specie.

All site-binding models include similar mass law and material balance equations to describe reactions in the double layer. However, the specific reactions thought to occur in the e.d.l. differ, changing an ion's position in the double layer and the local potential it experiences. These constraints generate detailed reactions that are specific to each model.

Since the surface potential of an oxide cannot be measured easily, as in the case of metallic electrodes, the separation of the ionic interaction energy into its chemical and electrostatic components is difficult. Thus, it is common to determine chemical interaction energies by extrapolation of experimental data to the condition of zero charge and potential.

The constant capacitance models of Stumm-76a, Schindler-72a, and Hohl-76a can be regarded as the high ionic strength case of the basic Stern model (see Figure 2.1a). The relationship between surface charge and potential is assumed to be linear:

e2.1.14 $\sigma = C\Psi \quad (Cm^{-2})$

This potential is used in the mass balance equations to correct the experimentally determined reaction pK-values that depend linearly on the charge:

e2.1.15a $pK_{a1}(\sigma) = pK^{i}_{a1} + b_{+}\sigma$ $\qquad K_{a1}(\sigma) = \frac{(SOH^{o})(H^{+})}{(SOH_2^{+})}$

e2.1.15b $pK_{a2}(\sigma) = pK^{i}_{a2} + b_{-}\sigma$ $\qquad K_{a2}(\sigma) = \frac{(SO^{-})(H^{+})}{(SOH^{o})}$

where, pK is -log(K);
i represent intrinsic values;
$b_{+(-)}$ is the experimentally derived slope in plots of pK vs surface charge for a positive (negative) surface.

Thus, all specifically adsorbed ions contribute to the net surface charge density, σ_o, and experience the same surface potential, Ψ_o. All other species are considered to be located in the solution far from the surface plane. The capacitances determined in this model are treated as being constant and depend on the specific electrolyte species in solution.

The models of Stumm, Huang and Jenkins (REF Stumm-70a and Huang-73a) combine the diffuse layer or GC-model with a surface complexation model (see Figure 2.1b). The capacitance is also considered constant here, but it is calculated from theory and not experimentally determined. Specifically adsorbed ions contribute to the surface charge and experience a potential Ψ_o. The charge-potential relation is given by the GC equation e2.1.2, however, the concentration of ionized surface sites may approach a saturation level, corresponding to a maximum charge.

The variable surface charge-variable surface potential (VSC-VSP) model of Bowden, Posner and Quirk (REF Bowden-77a) is an extension of the Stern's model and is applicable at all ionic strengths (see Figure 2.1c). Here, H^+ and OH^- ions are considered to reside at the surface, to contribute to the surface charge, σ_o, and to experience a potential, Ψ_o. Specifically adsorbed ions are located in the IHP where they contribute to σ_β and experience the potential, Ψ_β. All other ions are located in the diffuse layer. The capacitance between the surface and IHP and the potential between the IHP and OHP are considered constant.

The triple layer model of Davis, James, and Leckie (the DJL model, REF Davis-78a,b and James-82a) is a further revision of the VSC-VSP model of Bowden-77a (Figure 2.1d) which is applicable at all ionic strengths. This model considers two regions of constant capacitance and a diffuse, GC type layer. H^+ and OH^- ions react at the oxide surface, contribute to the surface charge, σ_o, and experience a surface potential, Ψ_o. Counterions situated in the IHP are considered bound to charged surface sites. These complexed ions contribute to σ_β and experience a potential, Ψ_β. The OHP with potential, Ψ_d, and diffuse layer charge, σ_d, is separated from the IHP by a region of constant capacitance, C_2. Since the triple layer model considers ionization of surface sites and complexation of electrolyte ions in the e.d.l., chemical reaction constants can be derived for both types of reactions. These reaction constants apply over a wide range of electrolyte concentrations and may be used to predict Ψ_d, an estimate of the ζ-potential.

All of the models discussed make reasonable predictions regarding surface charge vs pH data, assuming appropriate values for the constants are employed (REF Westall-80a). Of all the models discussed, only the DJL model has been employed to predict ζ-potential experiments. One of several problems with these models is that descriptions of ion locations in the e.d.l. are based on theory and have not been experimentally observed. Even though the DJL model predicts the data well, this success does not mean that it accurately predicts details of the adsorption process for an oxide-electrolyte interface. To account for the effects of charge on intrinsic reaction constants, Davis et al. (REF Davis-78a) extrapolate experimentally derived reaction coefficients to the zero-charge condition. This procedure may be misleading since the assumptions inherent in the DJL model affect the extrapolation and hence the intrinsic extrapolated value, K^i.

Since the DJL model is one of the more recent and interesting models of the oxide e.d.l., it was chosen as the basic framework for this study on ceramic suspensions. Inclusion of surface ionization and complexation reactions is desired to predict ceramic suspension properties accurately for improved processing. The next section discusses the DJL model in detail.

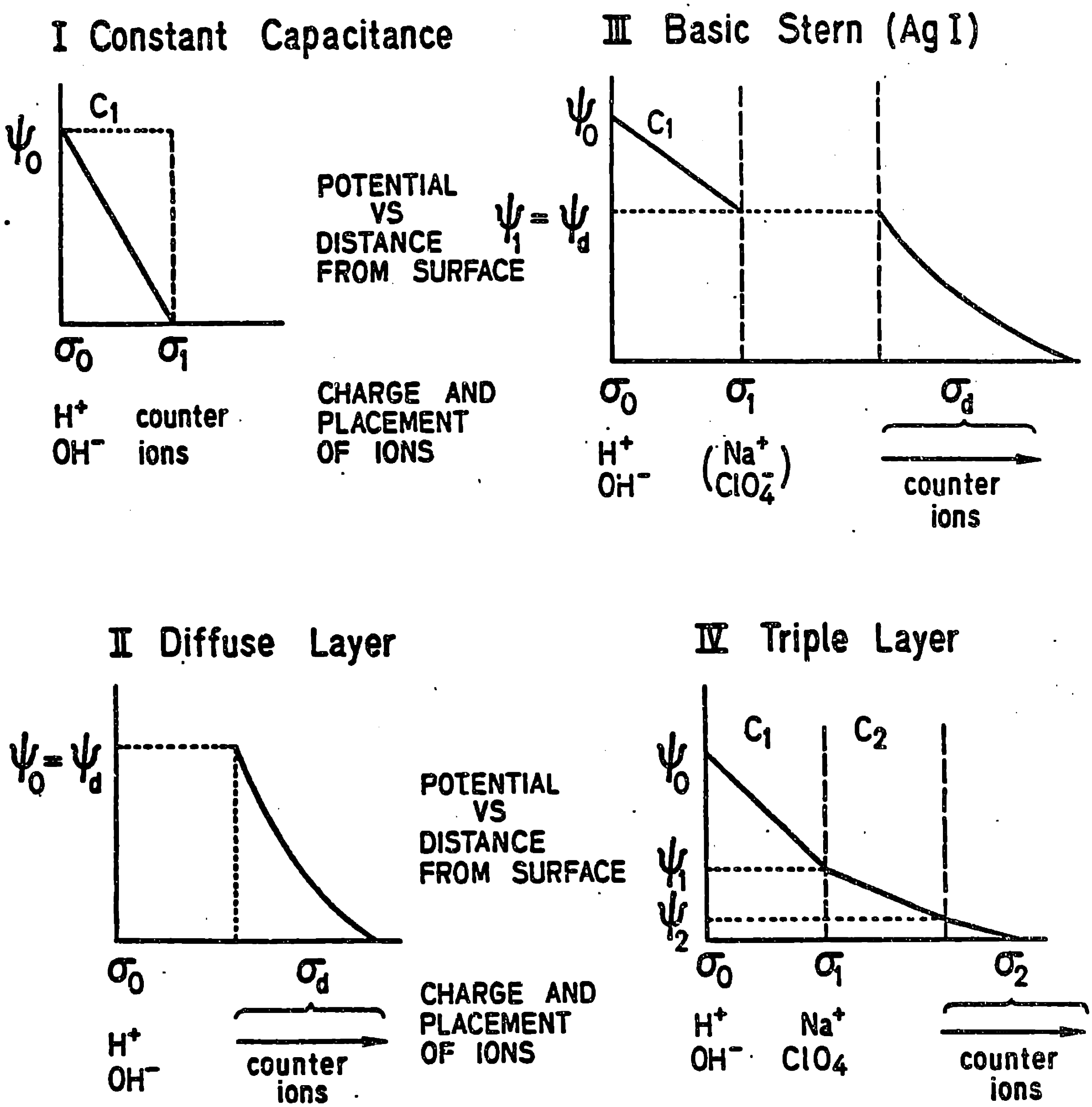

Figure 2.1 The electrical double layer models of the oxide/electrolyte interface. (after Westall-80a)

a) constant capacitance model (high ionic strength limit).

b) diffuse layer model (low ionic strength low potential limit).

c) Bowden, Posner, and Quirk model (Basic Stern).

d) DJL Triple layer model (extended Stern model).

2.2) The Davis, James, and Leckie Model

2.2.1) Ionization Model

The oxide/solution electrical double layer model of Davis etal. (REF Davis-78a,b and James-82a) was used in this study. According to the DJL model, several simultaneous equations must be solved in order to describe the charge, potential, and ion distribution around a particle in solution. They are (REF James-82a):

1) Mass-action expressions for all possible ionization and complexation reactions at the surface and in the electrical double layer;

2) Boundary conditions on the saturation of surface charge that depends on the total number of surface sites including un-ionized, ionized and complexed sites;

3) Charge balance description of σ_o using all surface sites;

4) Charge balance description of σ_β using complexed sites;

5) Bulk solution elecroneutrality;

6) Relationships relating e.d.l. propertes σ_o, σ_β, σ_d, Ψ_o, Ψ_β and Ψ_d;

7) Experimental parameters such as uptake of H^+ and OH^-, zeta potential, and surface area.

For most ceramic materials, three types of surfaces are possible: amphoteric, monofunctional, and zwitterionic. Neutral, amphoteric surfaces have a single ion-type that generates both positive and negative sites. Neutral, monofunctional surfaces also contain only one type of site that has only two states, neutral/negative or neutral/positive. Zwitterionic colloids contain two or more types of surface ions that independently undergo reactions.

Since most oxide surfaces are amphoteric in nature, the equations for this surface type will be discussed.

Surface charge develops on amphoteric surfaces via dissociation reactions of the type, assuming unit activity coefficents:

e2.2.1a $SOH_2^+ = SOH^o + H_s^+$ $K_{a1} = \frac{[SOH^o][H_s^+]}{[SOH_2^+]}$

e2.2.1b $SOH^o = SO^- + H_s^+$ $K_{a2} = \frac{[SO^-][H_s^+]}{[SOH^o]}$

The ionization pK-values describe the pH at which the predominating surface specie changes. In a plot of logarithm of the species surface concentration versus pH, the condition at which pH = pK's define the transition from the ionized to the unionized state (see Figure 2.2a). Monofunctional surfaces have only one ionization and are represented by one side of Figure 2.2a. Zwitterionic surfaces have two different surface species that undergo separate reactions (see Figure 2.2b).

Surface protons, H_s^+, have a different chemical potential and activity than do bulk solution protons, H_{aq}^+, due to the work required to move the charged species through the potential gradient from the bulk solution to the charged surface. The equation describing this effect is given in e2.2.2. When combined with e2.2.1, the ionization reactions are described in terms of bulk solution pH.

e2.2.2 $[H_s^+] = [H_{aq}^+]\exp(-e\Psi_o/kT) = [H_{aq}^+]\exp(-y_o)$

where $y_o = e\Psi/kT$ is the reduced surface potential.

The net surface charge, σ_o, results from the concentration difference of charged surface sites developed in response to the two ionization reactions in e2.2.1:

e2.2.3 $$\sigma_o = F[\Gamma(SOH_2^+) - \Gamma(SO^-)]$$

The fraction of ionized surface sites is:

e2.2.4a $$\alpha = \frac{\sigma_o}{eN_s} = \frac{[SOH_2^+] - [SO^-]}{[SOH_2^+] + [SO^-] + [SOH^o]}$$

where N_s is the surface site density. Equations defining the concentrations of SO^-, SOH^o, and SOH_2^+ modify e2.2.4:

e2.2.4b $$\alpha = \frac{([H_{aq}^+]/K_{a1})\exp(-y_o) - (K_{a2}/[H_{aq}^+])\exp(y_o)}{1 + ([H_{aq}^+]/K_{a1})\exp(-y_o) - (K_{a2}/[H_{aq}^+])\exp(y_o)}$$

The Nernst equation, e2.1.10, can be rewritten as:

e2.2.5a $$\exp(y_N) = \exp(e\Psi_N/kT) = [H^+]/[H^+]_{p.z.c.}$$

e2.2.5b $$y_N = 2.303(pH_{p.z.c.} - pH)$$

where y_N is the reduced Nernst potential. $\sigma_o = 0$ at the p.z.c. because the concentrations of positive and negative surface sites are equal, $[SOH_2^+]_{p.z.c.} = [SO^-]_{p.z.c.}$. The activity and concentration of surface and bulk solution H^+ ions are also equal, i.e. $[H_s^+]_{p.z.c.} = [H_{aq}^+]_{p.z.c.}$, since the surface potential is zero. Equating e2.2.1a and 1b, the $[H^+]$ at the p.z.c. becomes:

e2.2.6 $$[H_s^+]_{p.z.c.} = (K_{a1}K_{a2})^{1/2}$$

Defining:

e2.2.7 $$\delta = 2(K_{a2}/K_{a1})^{1/2} = 2\times10^{pK/2}$$

it is found that:

e2.2.8 $$\alpha = \frac{\sigma_o}{eN_s} = \frac{\delta\sinh(y_N-y_o)}{1+\delta\cosh(y_N-y_o)}$$

This equation contains all the thermodynamic and e.d.l. parameters needed to describe the system in the DJL model.

Combining the expressions for electroneutrality (e2.1.1), the Gouy-Chapman expression relating surface potential, Ψ_o, to diffuse layer charge, σ_d, (e2.1.2), and e2.2.8 completely describes the e.d.l. of and oxide powder in aqueous media. If we define:

e2.2.9 $$\frac{1}{\gamma} = \frac{0.1174(c)^{1/2}}{eN_s} \quad \text{at } 25\ ^{o}C$$

then the system is completely described by:

e2.2.10 $$\frac{1}{\gamma}\sinh(y_o/2) = \alpha' = \frac{\delta\sinh(y_N-y_o)}{1+\delta\cosh(y_N-y_o)}$$

For a given set of pH, electrolyte concentration, and fixed solid parameters N_s, K_{a1} and K_{a2}, the surface charge and potential, σ_o and Ψ_o, can be solved by independently calculating the RHS and LHS of equation e2.2.10 and applying a graphing routine. The reduced Nernst potential, y_N, is calculated and graphs for the RHS and LHS are overlayed such that $y_N = 0$ at $-(y_N - y_o) = y_o$. The curves for γ and δ intersect at specific points and these values are resubstituted into equations e2.2.4 and e2.2.10 to yield values for σ_o and Ψ_o.

This method allows the determination of σ_o and Ψ_o for a system even though the oxide surface does not obey the Nernst equation, e2.1.10. The surface potential of oxides is usually less at a given pH than the Nernst value, Ψ_N, where the difference $\Psi_o - \Psi_N$, increases as either the difference between the two ionization constants, ΔpK_a ($= pK_{a1} - pK_{a2}$), or the electrolyte concentration increases (REF Hunter-81a). Nernstian behavior is observed with small surface potentials if ΔpK_a is also small, implying a small pH range for which surface sites are predominantly neutral. If the Nernst equation applies, then $d\Psi_o/dpH$ should be 59.3 mV at 25 ^oC, but for most oxides this value is not found, e.g. $d\Psi_o/dpH = 40$ mV for silica.

2.2.2) <u>Complexation Model</u>

When electrolyte ions complex with the surface, a more complicated model of the oxide-aqueous solution interface must be applied to the experimental data. In addition to site ionization reactions, electrolyte complexing reactions occur of the nature:

e2.2.11a $SO^- + Na^+ = SO^-Na^+$

e2.2.11b $SOH_2^+ + Cl^- = SOH_2^+Cl^-$

where SO^-Na^+ and $SOH_2^+Cl^-$ are complexed surface sites.

These reactions are usually expressed as ion exchange reactions:

e2.2.11c $SOH^{o} + Na^{+} = SO^{-}Na^{+} + H_{s}^{+}$ $\quad K^{*}_{Na} = \frac{[SO^{-}Na^{+}][H_{s}^{+}]}{[SOH^{o}][Na_{s}^{+}]}$

e2.2.11d $SOH_2^{+}Cl^{-} = SOH^{o} + H_{s}^{+} + Cl^{-}$ $\quad K^{*}_{Cl} = \frac{[SOH^{o}][H_{s}^{+}][Cl^{-}]}{[SOH_2^{+}Cl^{-}]}$

where $K^{*}_{Na(Cl)}$ are complexation constants for sodium (chlorine).

In this form of the DJL model, soluble protons are bound to the surface forming ionized sites. Electrolyte counterions complex with these sites at the IHP, located at a distance β from the surface but within the compact layer (Figure 2.3). As in the case of ionization reactions, when the pH = pK* a transition occurs for surface sites from the complexed to the uncomplexed state.

The transition from the state in which the predominating surface species is the negative, uncomplexed site, SOH, to one dominated by the Na^{+} complexed site occurs at a pH greater than the p.z.c., when pH = pK^{*}_{Na}. The Na^{+} complexation reactions are:

e2.2.12a $SO^{-} + Na^{+} = SO^{-}Na^{+}$

e2.2.12b $SOH^{o} + Na^{+} = SO^{-}Na^{+} + H^{+}$

In the first reaction, negative SO^{-} sites complex with sodium ions yielding a complex which is neutral relative to the diffuse layer plane. The concentration of charged surface sites and therefore the surface charge remain constant, but the diffuse layer potential decreases due to electrostatic shielding by Na^+. In the second complexation reaction, a neutral surface site complexes forming a negative site, SO^-, combined with a positive Na ion located in the β plane of the e.d.l. The surface charge becomes increasingly negative due to the SOH^o to SO^- transition, while the Ψ_d remains the same since the neutral SOH site is replaced by a net neutral complex. Thus, the effect of Na^+ complexation on a negatively charged surface is to increase surface charge, σ_o, while decreasing diffuse layer potential, Ψ_d.

The corresponding chloride complexation reactions are:

e2.2.12c $SOH_2^+ + Cl^- = SOH_2^+Cl^-$

e2.2.12d $SOH^o + Cl^- + H^+ = SOH_2^+Cl^-$

The complexation of Cl^- occurs at a pH below the p.z.c., pH = pK^*_{Cl}, for which the surface sites are predominatly positive. Since the complexation reactions reduce the concentration of neutral, SOH^o sites and generate positive surface species, the net surface charge increases with complexation. The diffuse layer charge of the e.d.l. decreases with complexation since the resultant surface complex ion is oppositely charged that of the surface site, annihilating the charge at the β plane.

In general, the complexation of cations and anions at an aqueous oxide interface increases surface charge and decreases diffuse layer potential. These effects are experimentally observed: the measured surface charge increases with salt concentration and the ζ-potential, an experimentally determined Ψ_d, decreases for increasing salt concentration.

The activity of the Na^+ and Cl^- ions is modified by the electrcal work required to bring them from bulk solution to the adsorption plane, some distance β from the charged interface. Thus, expressions of the type:

e2.2.13a $[Na_s^+] = [Na_{aq}^+]\exp(-y_\beta)$

e2.2.13b $[Cl_s^-] = [Cl_{aq}^-]\exp(+y_\beta)$

must be included in the equilibrium equation. In general, for multicharged species:

e2.2.13c $[i_s^z] = [i_{aq}^z]\exp(-zy_\beta)$

where, i is the species;
z is the charge on the i^{th} species.

With this replacement in eqs. e2.2.11c and 11d we obtain:

e2.2.14a $$K^*_{Na} = \frac{[SO^-Na^+][H_{aq}^+]}{[Na_{aq}^+][SOH^o]} \exp(-y_o) \exp(y_\beta)$$

e2.2.14b $$K^*_{Cl} = \frac{[SOH^o][H_{aq}^+][Cl_{aq}^-]}{[SOH_2^+Cl^-]} \exp(-y_o) \exp(y_\beta)$$

where y_β is the reduced potential at the β plane.

The surface charge, when expressed in terms of charged sites, must now include the new positive and negative surface sites, the SO^- and SOH_2^+ components of SO^-Na^+ and $SOH_2^+Cl^-$, brought about by the addition of complexation reactions (see Figure 2.3). The diffuse layer charge changes with the addition of Cl^- and Na^+ ions aligned in this plane from the newly formed complexed species, SO^-Na^+ and $SOH_2^+Cl^-$. Likewise, the mass balance equations for the surface and adsorbed counterion plane change due to charged species aligning in these regions from the complexation reactions:

e2.2.15a $$N_s = N_a[\Gamma(SOH^o) + \Gamma(SOH_2^+) + \Gamma(SOH_2^+Cl^-) + \Gamma(SO^-) + \Gamma(SO^-Na^+)]$$

e2.2.15b $$\sigma_o = eN_a[\Gamma(SOH_2^+)+\Gamma(SOH_2^+Cl^-)-\Gamma(SO^-)-\Gamma(SO^-Na^+)]$$

e2.2.15c $$\sigma_\beta = eN_a[\Gamma(SOH_2^+Cl^-) - \Gamma(SO^-Na^+)]$$

where: N_s is the surface site density;

N_a is Avogadro's number.

Equations e2.2.1, 2, 14, and 15 define the electroneutrality, stoichiometry and thermodynamics of the e.d.l. for electrolyte complexation. The general relationship between the diffuse charge and potential for $z_1^+:z_2^-$ electrolytes is:

e2.2.16 $$\sigma_d = -0.0587c^{1/2} \frac{\Psi_d}{|\Psi_d|}\left(\frac{1}{z_+}[\exp(-z_+y_d)-1] - \frac{1}{z_+}[\exp(-z_-y_d)-1] \right)^{1/2}$$

The charged regions of the surface, denoted o, and counterion adsorption plane, denoted β, are considered separated by a dielectric region. The description of the e.d.l. surrounding the particle is completed by the GC-SG equations relating σ_o, σ_d, Ψ_o, Ψ_d, Ψ_β, C_1 and C_2:

e2.2.17a $$\Psi_o-\Psi_\beta = \frac{\sigma_o}{C_1} = + \frac{\beta}{\varepsilon_1}\sigma_o$$

e2.2.17b $$\Psi_\beta-\Psi_d = - \frac{\sigma_d}{C_2} = - \frac{(d-\beta)}{\varepsilon_2}\sigma_d$$

If the complete set of equations describing electroneutrality and chemical reactions in the electrical double layer can be silmultaneously solved, then the dynamic equilbria of oxide powders in solution can be expressed.

2.2.3) Numerical Evaluation

Two methods exist for evaluating the e.d.l. charge and potential distribution based on these principles. The graphical method employed for the uncomplexed case becomes cumbersome to use when complexation must be included. The double extrapolation method used in this study (REF James-82a) employs a numerical analysis that yields pK-values for the ionization and comlexation reactions. The concentration profiles of surface and e.d.l. species are calculated and used to estimate the e.d.l. charge and potential.

Operational reaction coefficients, Q, are defined for the equilibrium reactions:

e2.2.18a $$Q_{a1} = \frac{[SOH^o][H_{aq}^+]}{[SOH_2^+]} = K_{a1}\exp(y_o)$$

e2.2.18b $$Q_{a2} = \frac{[SO^-][H_{aq}^+]}{[SOH^o]} = K_{a2}\exp(y_o)$$

e2.2.18c $$^*Q_{Na} = \frac{[SO^-Na^+][H_{aq}^+]}{[SOH^o][Na_{aq}^+]} = K^*_{Na}\exp(y_\beta - y_o)$$

e2.2.18d $$^*Q_{Cl} = \frac{[SOH^o][H_{aq}^+][Cl_{aq}^-]}{[SOH_2^+Cl^-]} = K^*_{Cl}\exp(y_\beta - y_o)$$

By equating the activities and concentrations of species, experimentally measured surface charge as a funtion of pH and electrolyte concentration can be used to estimate the reaction pQ's. The values of y_o and y_β depend on surface and diffuse layer potential, Ψ_o and Ψ_β, that can not be experimentally measured. However, as surface charge decreases toward zero, y_o for dilute and $y_\beta - y_o$ for concentrated salt solutions approach zero. Thus, if pQ is evaluated for both low and high electrolyte concentration, extrapolation to the zero-charge condition yields the reaction coefficients, i.e. pK-values.

When the pH is greater than the p.z.c., the surface is net negative. The surface charge is essentially produced via ionization reactions forming SO^- sites at low salt concentrations and complexation reactions forming SO^-Na^+ sites at high salt concentrations. For pH-values below the p.z.c. the surface is positive, chlorine complexation occurs, and charge developes in a similar manner. Extrapolation of the pQ-values to conditions where $\sigma_o=0$, to remove the effect of potential, and salt concentration to 0 N and 1 N, yields estimates of the reaction constants, $pK_{a1,a2}$ and $pK^*_{Na,Cl}$, that apply for the predominating surface species present. This approach is valid since ionization can be ignored at high ionic strengths and complexation can be ignored at low ionic strengths.

Intrinsic ionization constants K_{a1} and K_{a2} are determined by plotting pQ_{a1} and pQ_{a2} versus α^*, where:

e2.2.19a $pQ_{a1} = pH + \log(\alpha/1-\alpha)$

e2.2.19b $pQ_{a2} = pH - \log(\alpha/1-\alpha)$

e2.2.19c $\alpha^* = 10\alpha + c^{1/2}$

e2.2.19d $\alpha = \sigma_o/eN_s$

Such plots yield the intrinsic ionization constants after extrapolation to the zero charge and ionic strength. Data of James-82a are shown in Figure 2.4a for a pyrogenic silica.

Intrinsic complexation constants are determined by plotting pQ^*_{Na} and pQ^*_{Cl} versus α^*_{ion}, where:

e2.2.20a $pQ^*_{Na} = pH + \log(\alpha/(1-\alpha)C_{ion})$

e2.2.20b $pQ^*_{Cl} = pH - \log(\alpha/(1-\alpha)C_{ion})$

e2.2.20c $\alpha^*_{ion} = 10\alpha - \log(c)$

and extrapolating the data to the zero charge and 1N ($\log[C_{ion}]$) conditions. Data of James-82a for pyrogenic silica are shown in Figure 2.4b. These extrapolations yield the intrinsic complexation constants K^*_{cation} and K^*_{anion} for the electrolyte ions on the oxide surface.

The values of σ_o and Ψ_ζ are determined from potentiometric titration and ζ-potential measurements, respectively. The electrokinetic ζ-potential has been used by several authors to approximate Ψ_d. Titration data directly yields the surface ionization and complexation constants from which the intrinsic constants are derived by appropriate extrapolations. The concentration of species in the electrical double layer at given pH and electrolyte concentration conditions are estimated using computer techniques once the intrinsic values of N_s, K_{a1}, K_{a2}, K^*_{Na} and K^*_{Cl} are determined.

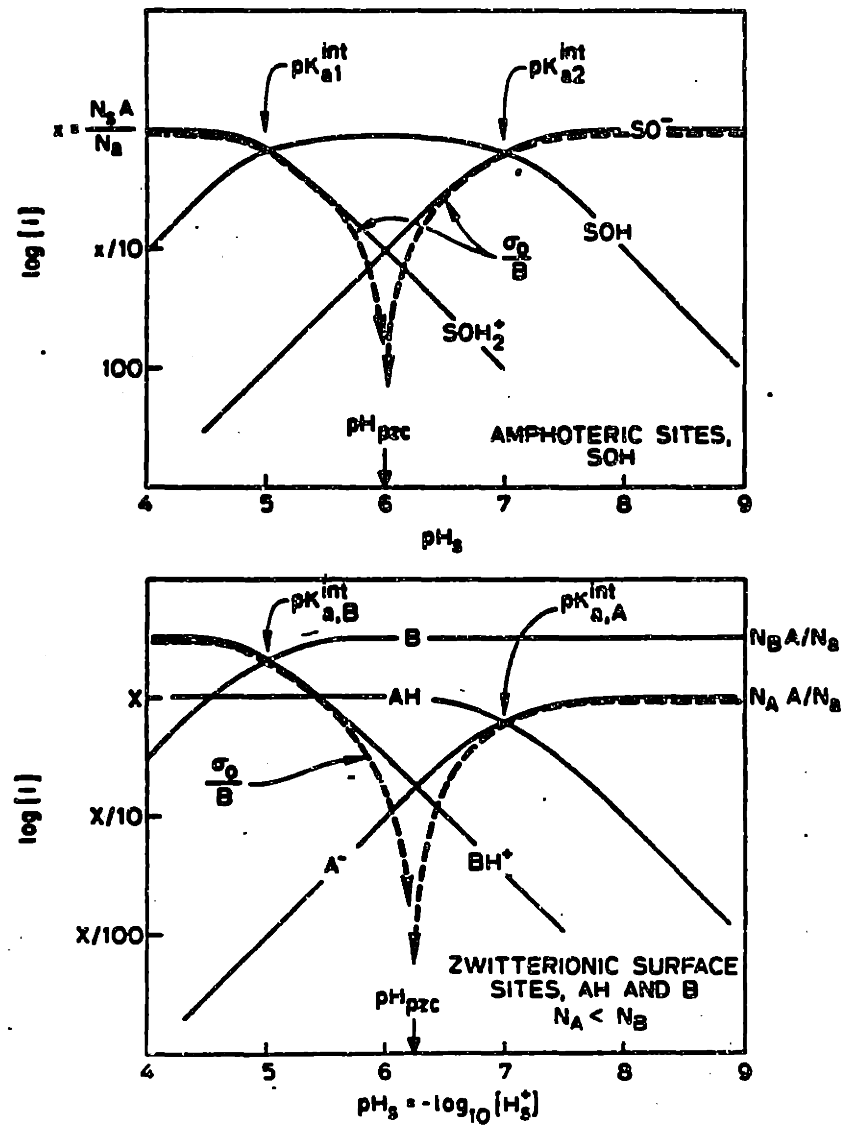

Figure 2.2 Schematic illustration of the surface pH dependence of charged and uncharged site densities on amphoteric and zwitterionic surfaces. The pK_a-values define the transition of surface charged species as a function of pH. (After James-82a)

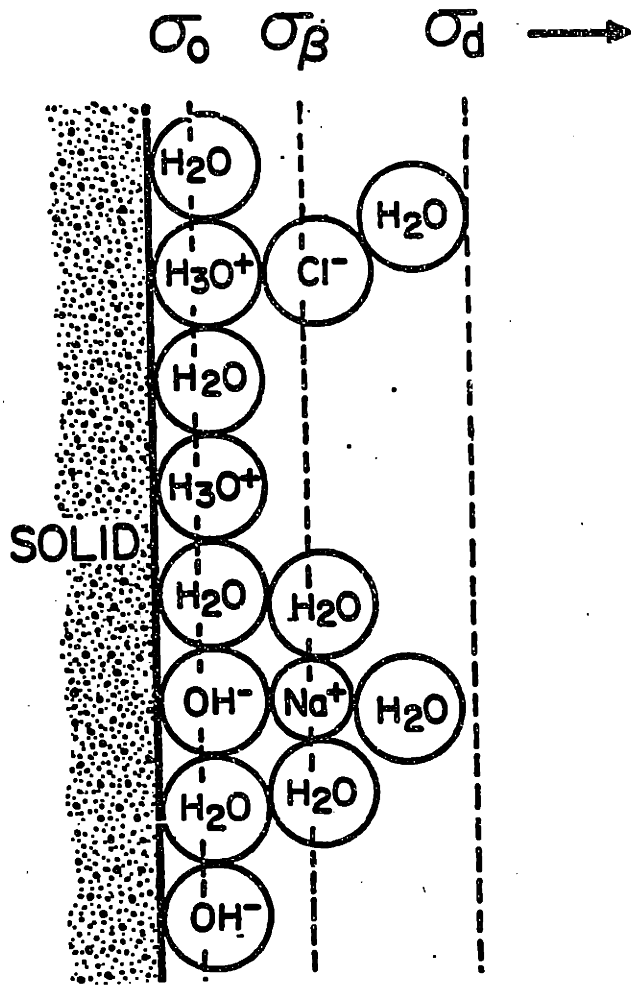

$$\sigma_0 = [SOH_2^+] + [SOH_2^+ - Cl^-] - [SO^-] - [SO^- - Na^+]$$

$$\sigma_\beta = [SO^- - Na^+] - [SOH_2^+ - Cl^-]$$

$$\sigma_0 + \sigma_\beta + \sigma_d = 0$$

Figure 2.3 Schematic representation of an oxide interface showing possible locations for molecules comprising the places of charge. Ionization reactions occur in the inner layer, o, while complexation reactions occur at the β layer. (After James-78a)

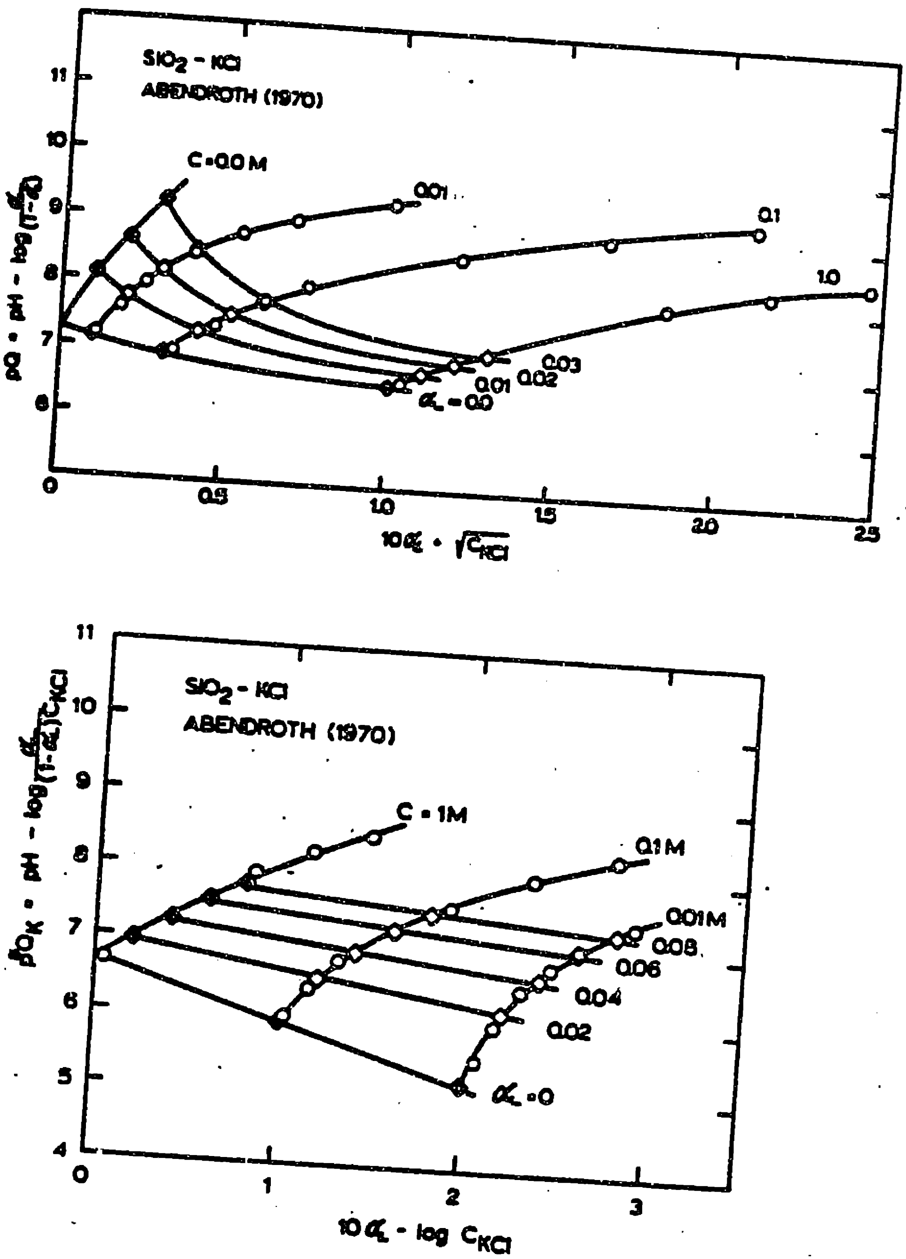

Figure 2.4 Graphical method of James et. al. to yield intrinsic ionization and complexation constants for the oxide surface. (after James-82a)

a) Extrapolation of pQ's yield $pK_{a1,a2}$ for BHD silica.

b) Extrapolation of pQ*'s yield $pK^*_{Na,Cl}$.

2.3) Methods to Determine Suspension Properties

Potentiometric acid/base titrations of oxide powder surfaces are used to calculate surface charge, potential, and reaction constants. Bolt (REF Bolt-57a) and Parks and de Bruyn (REF Parks-62a) were among the first investigators to use potentiometric titrations to study the interaction of acids and bases with the oxide-electrolyte interface.

In this method, a control electrolyte solution, e.g. 10^{-3} to 1 N NaCl, is titrated with the corresponding acid or base, HCl or NaOH, and the volume of titrant required to attain various pH-values is recorded. A sample of the electrolyte solution is equilibrated with an oxide powder of known surface area. This dispersion is titrated and the two titration curves are compared; see Figure 2.5. The difference in volume of acid or base required to obtain a given pH for each sample relates to the net uptake of H^+ and OH^- at the powder's surface. If supporting electrolyte does not specifically adsorb and if the potential-determining ions, H^+ and OH^-, have equal affinity for the surface, then the net uptake of H^+ and OH^- is given by:

e2.3.1 $$\Gamma' = [(C_a - C_b) - (C_{H+} - C_{OH-})] \ / \ A$$

where, Γ' is the net uptake per cm^2 of surface;
$C_{a(b)}$ is the concentration of acid(base) required to attain a given pH;
$C_{H+(OH-)}$ is the concentration of $H^+(OH^-)$ species at a given pH;
A is the surface area in $m^2\ gm^{-1}$.

The relative surface charge, $R\sigma_o$, can be calculated from equation e2.3.2:

e2.3.2 $R\sigma_o = F(\Gamma_{H+} - \Gamma_{OH-})$

where F is the Faraday constant. If a series of $R\sigma_o$ versus pH isotherms are plotted for different electrolyte concentrations, the curves intersect at a unique pH called the point of zero charge, p.z.c., as in Figure 2.6. The surface charge is independent of the concentration of non-adsorbing electrolyte at the p.z.c. implying that the surface density of positive equals that of negative sites:

e2.3.3 $\Gamma_{H+} = \Gamma_{OH-}$

The intersection of the relative surface charge curves may not occur at $R\sigma_o=0$, see Figure 2.6a. To compensate for this effect, the axis is shifted by a value, $\Delta\sigma_o$, such that the intersection occurs at $\sigma_o=0$ as shown in Figure 2.6b. The second plot defines the actual value of the surface charge as a function of pH. The shift, $\Delta\sigma_o$, in the relative surface charge results from a release or uptake of charged species from the surface during solid-solution equilibration prior to titration. This release or uptake of species results from either dissolution of surface impurities or initial hydroxylation of the oxide surface if dry powder is placed in solution. The magnitude of $\Delta\sigma_o$ relates to the amount of surface impurity or the extent of hydroxylation.

The p.z.c. corresponds to the average of the surface ionization constants, pK_a's, as was described earlier and in Figure 2.1a. At this pH, the overall surface is uncharged since the concentration of neutral sites is high and those of positive and negative sites are small and equal. Thus:

e2.3.4 $[SOH_2^+] = [SO^-] << [SOH^o]$

Titration data directly yield the area-average concentration difference between positive and negative groups on the surface. It is quantitatively impossible to distinguish between the actual types of sites.

Oxides that are strong acids generally have low p.z.c.-values and those that are strong bases have high p.z.c.-values (REF Parks-67a). Examples are SiO_2 with a p.z.c. of 2 and MgO with a p.z.c. of 11. The p.z.c. can be predicted from electrostatic considerations and is found to be related to the cationic charge and radius (REFs Parks-67a and Yoon-79a). Shifts in the p.z.c. occur due to changes in the state of hydration, crystal cleavage habit, and crystallinity, making the actual value difficult to predict. Thus, the experimentally determined p.z.c.-values may differ from that expected due to changes in sample preparation technique.

Potentiometric titrations can also be used to measure the concentration of electrolyte species adsorbed at the oxide surface. Ions such as Na^+, Cl^-, Br^-, I^-, CN^-, F^-, Cu^{2-}, S^{2-}, Ag^+, Ca^{2+}, and K^+ can be studied with the use of specific ion electrodes. The procedure is similar to that for a pH-titration: the pX-titration for a suspension is compared with that of the control electrolyte, where X is the ion of interest.

The suspension effect may cause problems in measuring the pH of a suspension (REF Cherbonowski-82a). Errors result from an interaction between the junction potential at the glass electrode and the charged ion cloud (e.d.l.) surrounding particles in suspension. The magnitude of this effect depends on particle size and concentration, electrical double layer properties, and the electrode junction potential. The suspension effect is greatest for very concentrated, low ionic strength suspensions containing highly charged particles. Large errors between the measured pH in the suspension and true solution pH result if the suspension effect is not properly taken into account. Fortunately, use of a second junction electrode; see Figure 2.7, eliminates the suspension effect. The outer reservior is filled with the control electrolyte, eliminating the concentration gradient that normally exists between the suspension and the electrode's reservoir. Thus, a second junction potential is not developed and the particles do not interact with the electrode.

Electrophoresis is another technique used to explore the electrical double layer at the oxide-solution interface. In this technique, an applied voltage interacts with the charged particles, creating a hydrodynamic shear plane in the e.d.l. and causing the particle to move towards the oppositely charged electrode. The motion of particles is observed through a thin-walled capillary using a side-illuminated microscope. The electrophoretic mobility of the particle, μ, is calculated and the electrostatic potential, ζ, at the shear plane is estimated. This ζ-potential is thought to be identical to the diffuse layer potential, Ψ_d, even at high electrolyte concentrations (0.1 N) and low potentials (<25 mV- REF Smith-81a). The ζ-potential is calculated from the particle mobility using the equations:

e2.3.4a $\quad \zeta = 4\pi\eta\mu\varepsilon^{-1}$

e2.3.4b $\quad \zeta = 6\pi\eta\mu\varepsilon^{-1}[1+f(\kappa a)]$

where, ε is the solution dielectric constant;
η is the solution viscosity;
κ is the Debye-Huckel parameter;
a is the particle radius.

The specific equation used depends on the double layer properties. The Smoluchowski equation, e2.3.4a, is used for $\kappa a > 200$ and the Henry equation, e2.3.4b, is used for $0.1 < \kappa a < 200$ (REF Hunter-81a).

The ζ-potential is found to decrease as the pH approaches the isoelectric point since the concentration of charged surface, sites and thus the induced OHP potential, decreases. The ζ-potential also decreases as the electrolyte concentration increases since complexing ions neutralize the diffuse layer charge. If the p.z.c. equals the iep, then the electrolyte ions do not specifically adsorb. In this case, only the OH^- and H^+ ions contribute to the charge developed at the surface.

Errors introduced in the measurement of surface charge, zeta potential, and other e.d.l. properties may be significant and occur from several causes:

1) Dissolved CO_2 produces carbonic acids which changes the pH and which may specificall adsorb at the powder surface;

2) Dissolution at extreme pH may consume titrant or induce surface reprecipitation;

3) Variability in surface site density measurements;

4) Lack of independent experimental checks on the titration data.

Carbonic acid formed by the dissolution of atmospheric CO_2 decreases the solution pH. The concentration of carbonate species in water as a function of pH is shown in Figure 2.8. These species may specifically adsorb onto oxide surfaces, changing the e.d.l. charge and potential distribution. Adsorption of this type has been observed for MgO, Al_2O_3, and TiO_2 (REF Boehm-71a). Also, the addition of the carbonate equilibria to an already complex system further complicates calculations of surface pK's. The time for carbonate species to attain equilibrium is usually rapid, within five minutes, so precautions for its exclusion must be rigorous. A titration cell that excludes CO_2 by continuous bubling is shown in Figure 2.7.

Dissolution of the oxide powder introduces free metal species into solution that may react with H^+ and OH^- ions, changing the volume of titrant required to attain a certain pH. Also, as powder dissolves, the surface area continually changes and the correct value for calculation purposes may infact be unknown. Dissolution and reprecipitation can also lead to a surface gel layer where counterions may imbed, introducing kinetic limitations on equilibrium attainment.

The surface site density, N_s, of the oxides should be determined independently for the calculations. This is usually done via:

1) calculation from crystal structure;
2) isotopic exchange at the surface;
3) IR-studies using H_2O-desorption;
4) acid/base titration.

Since each of these methods leads to a slightly different value of the N_s (REF James-82a), the "correct" value to be used in the calculation is in doubt.

Once the ionization and complexation reaction constants have been estimated from the pH titration data, the calculation of the distribution of species in the e.d.l. can be attempted. The simultaneous evaluation of expressions for the bulk solution and e.d.l. equilibria can be made using computer programs such as MINEQL (REF Westall-76a) or MICROQL (REF Westall-79a,79b). The incorporation of surface charge effects and the exp(eΨ/kT)-terms that must be included can be handled by a subroutine in the computer programs. These programs determine the concentration distribution of species in the e.d.l. from which the charge and potential distribution may be estimated. These values are then compared to the experimentally determined surface charge and diffuse layer potential to verify the model employed.

Conductometric titration can be used to check the computer calculated ion adsorption density on the particle surface. These titrations are carried out in a manner similar to potentiometric titration, except that the conductivity of the bulk solution is measured as a function of titrant added. If the calculated conductivity equals the actual conductivity, then the proposed model of adsorption is substantiated. The calculation for the conductometric titration basically accounts for all species in bulk solution by the equation:

$$K = \Sigma_i \, [\lambda_i C_i |z_i| / 1000] \qquad \text{e2.3.5}$$

where, C_i is the concentration of ion i;
z_i is the charge of ion i;
λ_i is the equivalent ionic conductance.

The value of λ_i is usually estimated from the limiting ionic conductance using the relation:

$$\lambda_i = \lambda_i^o - [.23\lambda_i^o + 30.32|z|] \frac{I^{1/2}}{3.29\times10^7 (I)^{1/a}} \qquad \text{e.2.3.6}$$

where, a_i is an atomic size parameter;
I is the ionic strength.

Ignoring surface conduction effects, calculated values of the conductivity are in accord with experimental results (REF James-82a). However, Baran-83a has shown that for certain ionic strengths, the effects of surface conduction outweigh those of the dispersing medium and caution must be employed.

The next section discusses experimental results for the e.d.l. of oxides employed in this study.

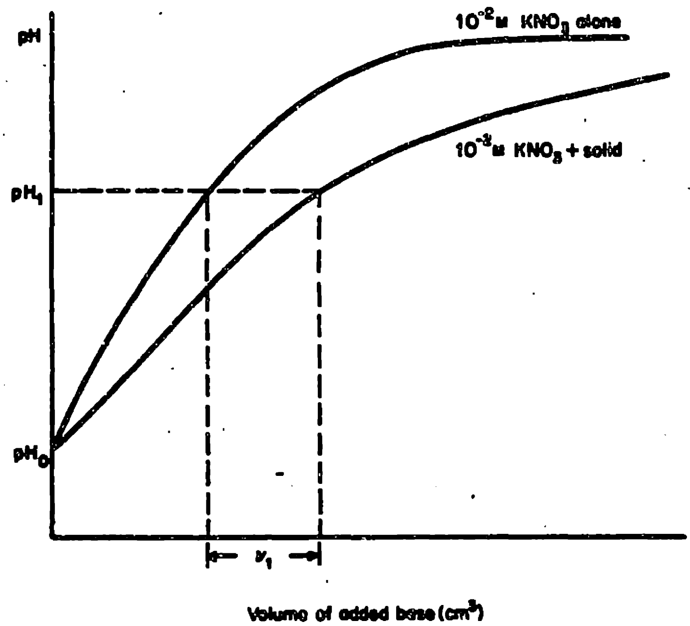

Figure 2.5 Potentiometric titration of electrolyte control and suspension to yield surface charge. (after Hunter-81a)

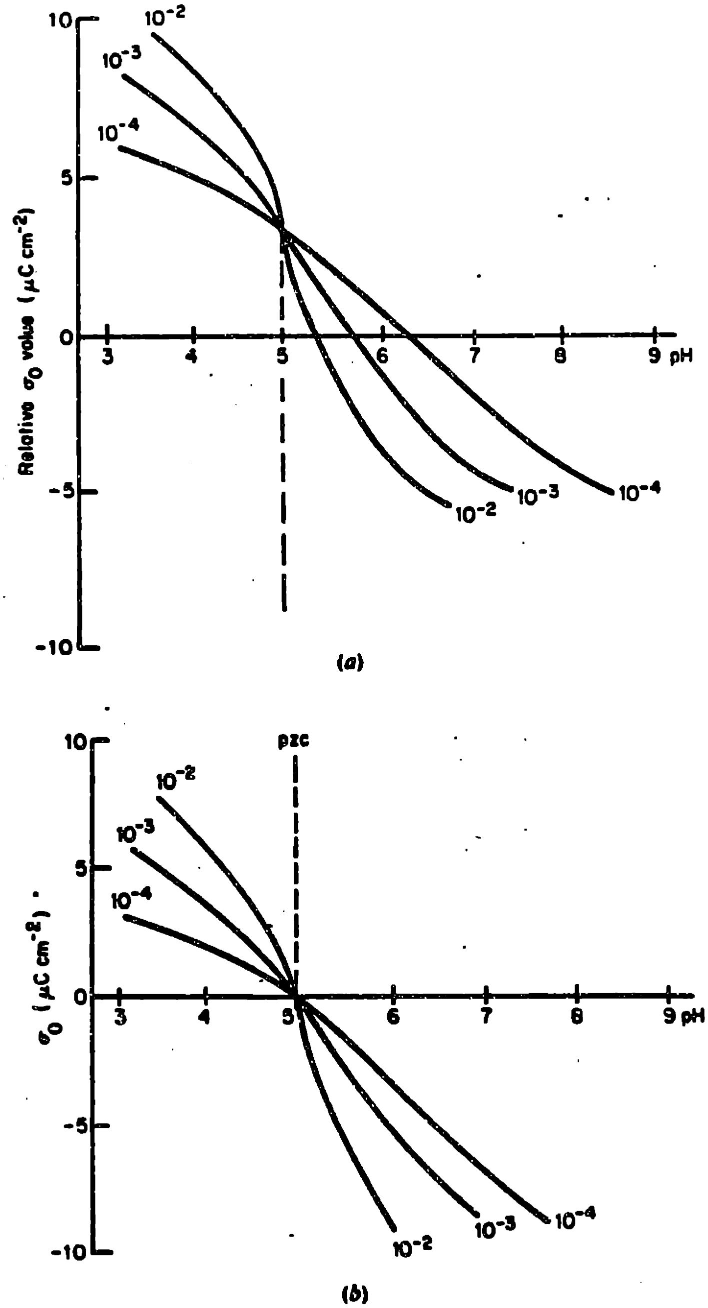

Figure 2.6 Method to determine the point of zero charge of the oxide surface. (after Hunter-81a)

a) the intercept of the Rσ versus pH as a function of electrolyte yields the pzc.

b) once the pzc is known, a correction factor, $\Delta\sigma$, is applied to remove the effect of solubility, impurity, etc.

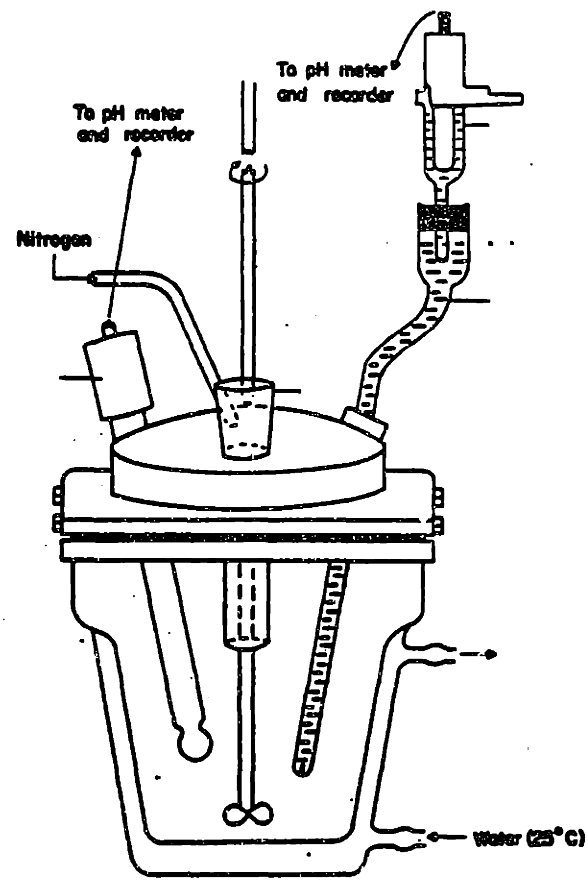

Figure 2.7 Schematic of a titration setup with a second junction electrode and N_2 injection system. The inner electrode reservoir is filled with a saturated KCl solutions while the outer reservoir is filled with the same electrolyte as in the suspension. (after Ahmed-75a)

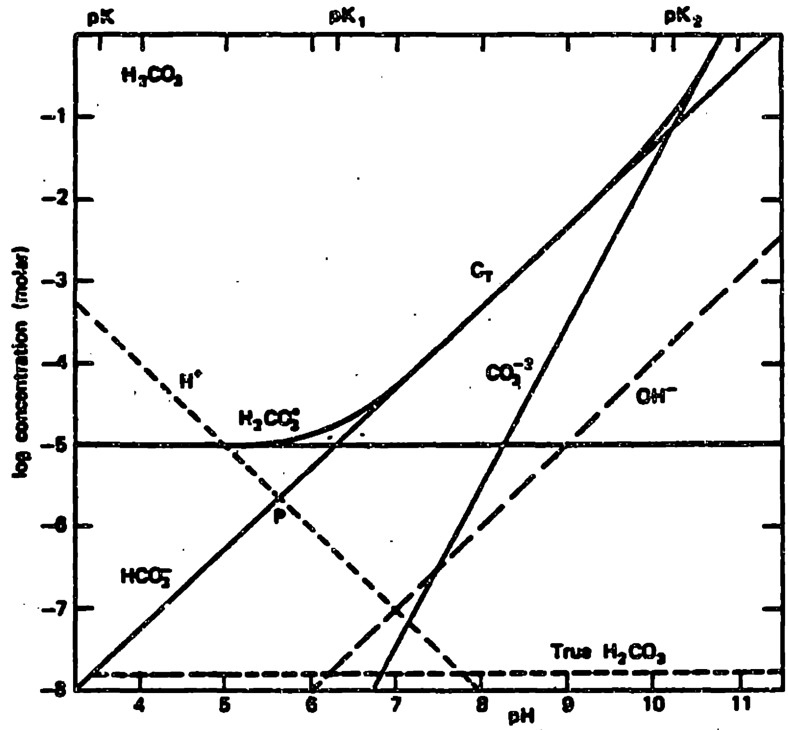

Figure 2.8 The concentration of carbonate species in solution as a function of pH. (after Stumm-81a)

2.4) Chemistry of Oxides

Previous studies of the electrical double layer, dissolution and crystal structure of the oxides used in this study are discussed in this section. The cited e.d.l. studies were conducted in a N_2-atmosphere to prevent carbonate-related pH-problems, allowing proper comparison.

2.4.1) Silica

2.4.1.1) Silica- Electrical Double Layer Studies

Several investigators have studied the surface charge and related properties of silica in aqueous solutions. Parks-65a tabulated the p.z.c.-values of SiO_2, quartz, silica sols, and gels as being between pH 1 and 3.7 depending on the nature of preparation. A wide range of reported values is probably due to differences in preparation, surface treatment, and surface impurities.

Tadros-68a studied the role of potential determining ions, p.d.i., at the silica/electrolyte interface using BHD silica suspended in aqueous KCl solutions determining the p.z.c. to be 3.0. The effect of oxide concentration on potentiometric titration was using a series of suspensions with different oxide concentrations in the same volume of support electrolyte. No effect was seen on the absolute charge density. The adsorption of OH^- at a level greater than the surface concentration of silanol groups and the low ζ-potential was explained by invoking a porous, gel-layer model where OH^- and cationic counter-ions penetrate the solid matrix, pores or gel-layer. Owing to this process, most of the surface charge is neutralized by the penetrating cations in the porous layer where the extent of ion-penetration depends on the size of the ion. This adsorption scheme was borne out by OH^- adsorption that increased in the order, $(C_2H_5)N^+ < Li^+ < Na^+ < K^+ < Cs^+$, which is in accord with predictions based on hydrated ionic radius. A model of specific adsorption model also predicts the determined order of adsorption.

Allen-71a studied the exchange of protons for Na^+ in silica sols. A single dissociation constant for the silanol sites was inadequate to describe surface ionization and ion-exchange. A best fit to experimental data was obtained using a model that considered three reaction equilibria; two ionization reactions of silica surface sites and ion-exchange of Na^+ with the surface.

Yates-76a studied the structure of the silica-electrolyte interface using titration, tritium exchange, gas adsorption, and dissolution measurements. Very high surface charge values were obtained for uncalcined powder, however upon calcination to 500-800 ^oC, the surface charge decreased to more usual values. Gas adsorption measurements did not detect significant porosity; however, tritium exchange studies indicated a significantly higher concentration of surface hydroxyl groups than was expected from crystallographic calculations. The authors postulated the formation of a gel-layer containing incompletely condensed polysilisic acid groups that allow penetration by counterions to explain their results. As the calcination temperature increased, condensation of free silanol groups and some sintering of the surface pores and gel-layer was thought to occur, explaining the decrease in apparent surface charge. Tritium exchange experiments indicated that gel-layers on calcined silicas do not grow during titration.

Davis-78a studied the ionization and complexation properties of silica. The data of Abendroth-70a was recalculated according to the model of Davis-78a yielding pK_{a2} = 7.2 and pK^*_K = 6.7 for BHD precipitated silica in KCl solutions. A site density of 5 sites nm^{-2} and inner layer capacitance of 125 uF cm^{-2} was used for the calculations. The experimental and calculated surface charge densities are shown in Figure 2.9, adapted from James-82a based on the determined pK and pK^*_{ion}-values given earlier in Figures 2.4a and 2.4b.

Finally, Smit-78a showed experimentally that Na^+ specifically adsorbs within the IHP for SiO_2. This evidence supports a site binding model rather than a gel layer model for the silica studied.

2.4.1.2) Silica- Dissolution Studies

The concentration of aqueous silicate species equilibrated with amorphous silica as a function of pH is given in Figure 2.10. For pH-values less than ~9.0 the uncharged species, $Si(OH)_4$, predominates at a concentration of approximately $10^{-2.7}$ M. At higher pH, the concentration of soluble, charged silicate species increases until they dominate. Reaction constants from which these concentrations were calculated are listed in Table 2.1. The mononuclear "wall" shown in the figure represents the minimum concentration at which aqueous, multinuclear silica species are thermodynamically stable. Greenberg and Price (REF Greenberg-57a) concluded that electrolyte concentration below 0.1 N has no effect on the solubility of amorphous silica for suspensions in the pH range 7 to 10.

2.4.1.3) Silica- Crystal Structure Studies

The crystal and surface structures of silica have been discussed by Boehm-71a, Yates-75a, and Iler-79a. The surface of freshly annealed and subsequently hydroxylated silica contains two distinct types of sites. The surface silicon is bound to either isolated, type A, or paired, type B, hydroxyl groups (REF Boehm-71a). When the oxide is heated, hydroxyls are removed first from the B site and then from the A site, with the removal of hydroxyls being reversible to approximately 450 ^{o}C. The site density of silica is between 3 and 6 sites nm^{-2} (REF Yates-75a). The postulated surface of amorphous silica is composed of a mixture of the (0001) β-tridymite and the (100) β-cristobalite surface planes.

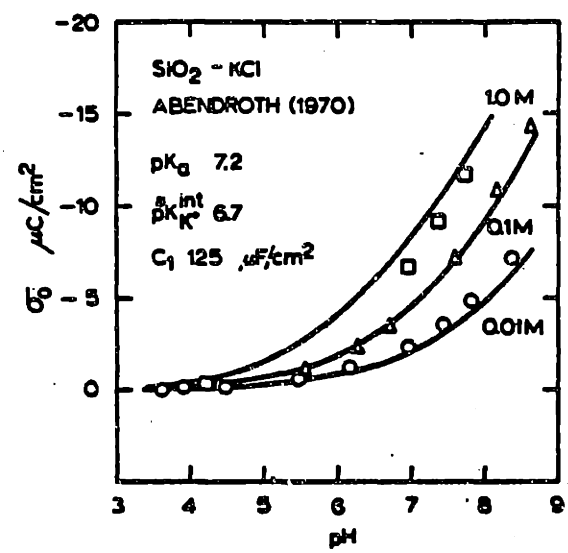

Figure 2.9 Surface charge density of pyrogenic silica. (after James-82a)

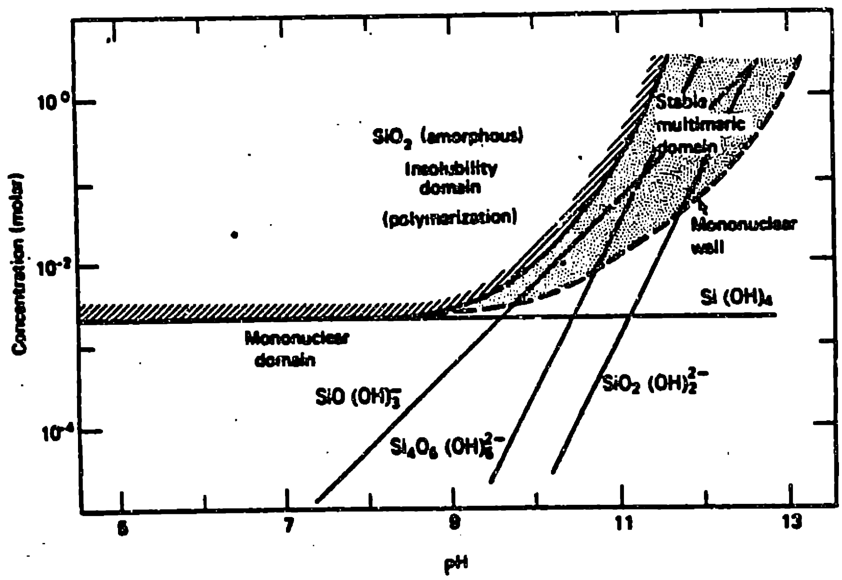

Figure 2.10 Concentration of dissolved silica species as a function of pH. (after Weise-73a)

<u>Table 2.1</u>

Solubility equilibria for the SiO_2-H_2O system at 25 °C.

SiO_2 (α-quartz) + $2H_2O$ = $Si(OH)_4$	log K = -3.7
SiO_2 (s, amorphous) + $2H_2O$ = $Si(OH)_4$	log K = -2.7
$Si(OH)_4$ = $SiO(OH)_3^-$ + H^+	log K = -9.46
$SiO(OH)_3^-$ = $Si_2(OH)_2^{2-}$ + H^+	log K = -12.56
$4Si(OH)_4$ = $Si_4O_6(OH)_6^{2-}$ + $2H^+$ + $4H_2O$	log K = -12.57

(after Yates-75a)

2.4.2) Alumina

2.4.2.1) Alumina- Electrical Double Layer Studies

Huang-71a,73a studied the specific adsorption of cations on γ-Al_2O_3. A p.z.c. of 8.5 and surface ionization constants of pK_{a1}= 7.9 and pK_{a2}= 9.1 were determined for NaCl solutions at 25 °C. A site-binding model was employed to describe the reaction of cations with the surface. The titration technique developed by these investigators compared the amount of titrant consumed by the alumina suspension to its centrifugate in order to calculate the surface charge. This technique removes most of the problems related to impurity and dissolution since these effects are included in both titrations and are cancelled upon comparison. Dissolution effects occuring during the titration are not removed and must be accounted for.

Tschapek-76a determined that KCl is an indifferent electrolyte for γ-Al_2O_3 while LiCl and $CaCl_2$ are specifically adsorbed. The p.z.c. of their alumina in KCl is 9.1 and in $CaCl_2$ is 7.4. The i.e.p. of all suspensions with 10^{-3} M salt were occurred at pH 9.1 +/- 0.1, coinciding with the p.z.c. in KCl. The amount of cation substitution for OH^- and H^+ in 1 M salt solutions was only 10% or approximately 10 uC cm^{-2}. These authors found no difference between fast and slow titrations in KCl, but a p.z.c.-difference of 0.8 was found for $CaCl_2$ and LiCl solutions. These findings were attributed to the effects of specific adsorption.

Davis-78a recalculated the data of Huang-71a determining ionization constants of 5.7 and 11.5 for γ-Al_2O_3 in NaCl solutions. The corresponding complexation constants are 9.2 and 7.9 using an assumed inner layer capacitance of 100 to 120 uF cm^{-2} and site density of 8 sites nm^{-2} (Peri-65a). The calculated and determined surface charges are shown in Figure 2.11.

Smit-78b proved experimentally that Na^+ ions specifically adsorb on the alumina surface, thus supporting a site-binding model for alumina. Smit-80a also studied the radiotracer adsorption of NaBr on α-Al_2O_3 single crystals and found that Na^+ and Br^- ions specifically adsorb slightly on the oxide surface. The p.z.c. and i.e.p. were found to be 4.5 and 3.1 to 3.5 respectively, with the discrepancy attributed to the greater complexating ability of Br^- compared to that of Na^+ at the surface.

Mikami-83a studied the specific adsorption-desorption of phosphate ions on the γ-AL_2O_3 surface using a pressure-jump technique. This technique follows the adsorption-desorption kinetics of specifically adsorbed ions by measuring suspension conductivity. The DJL model was found to most closely predict the experimental data.

2.4.2.2) Alumina- Dissolution Studies

Dissolution studies on alumina have been discussed by Wiese-73a. The concentration profiles of dissolved, aqueous species, as a function of pH, for freshly precipitated and aged $Al(OH)_3$ is shown in Figure 2.12. Reaction constants from which these concentrations were calculated are listed in Table 2.2. Gibbsite is the most thermodynamically stable phase of solid aluminum hydroxide in solution.

2.4.2.3) Alumina- Crystal Structure Studies

Knozinger-78a developed a surface model for alumina based on a crystalline spinel lattice. The γ-Al_2O_3 structure is considered a defective, tetragonally distorted, spinel lattice with a unit cell composed of 32 oxygen, 23 1/2 aluminum atoms, and 2 2/3 cation vacancies. The oxygen lattice is well ordered with an average Al-O bond length 1.819 A and a stacking sequence ABCABCABC. Octahedral sites are preferentially occupied with respect to tetrahedral sites for γ-Al_2O_3 while α-alumina has only octahedrally coordinated aluminum ions.

The expected surface of γ-Al_2O_3 is composed of (110) and (100) planes, however most calculations use values for the (110) face (Kozinger-78a). Parkyns-72a has described a model for microcrystalline particle aluminas for which the particles are approximated by rhombooctahedrons of 26 sides having low index spinel planes (100), (110), and (111). Five types of site are recorded and correspond to the five IR absorption maxima observed at 3800, 3780, 3744, 3733, and 3700 cm^{-1}. Morterra-76a assigned the IR-stretching frequencies of 3760-3800 cm^{-1} to OH ions bound to tetrahedrally coordinated Al^{3+} and those of 3700-3750 cm^{-1} to OH groups bound to both octahedrally and tetrahedrally coordinated Al^{3+}.

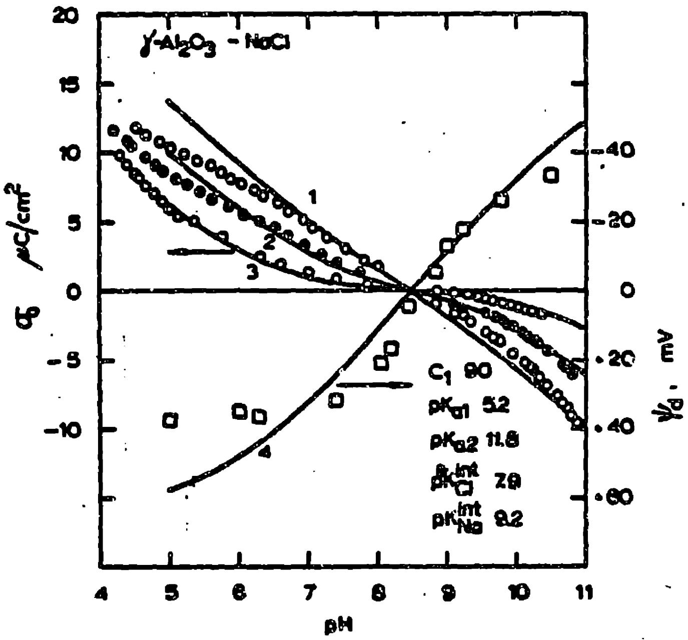

Figure 2.11 pH and ionic strength dependence of surface charge and zeta potential for γ-Al_2O_3. (after James-82a)

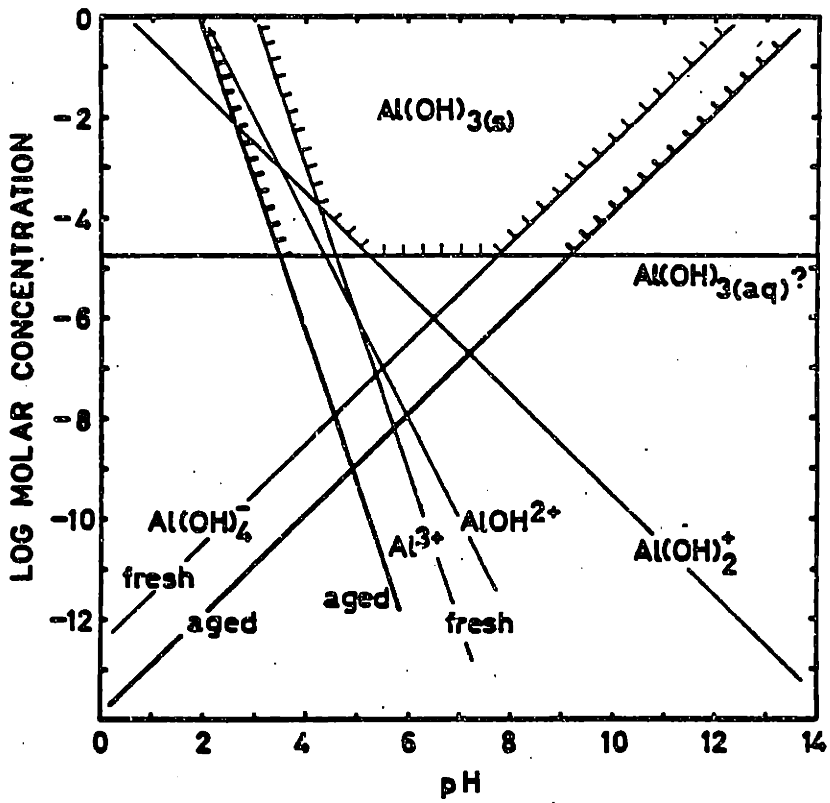

Figure 2.12 Concentration of dissolved alumina species as a function of pH. (after Weise-73a)

Table 2.2

Solubility equilibria for the Al_2O_3-H_2O system at 25 °C.

α-$Al(OH)_3(s) + 3H^+ = Al^{3+} + 3H_2O$	log K = 8.5
$Al(OH)_3(amorph) + 3H^+ = Al^{3+} + 3H_2O$	log K = 10.8
$Al^{3+} + H_2O = AlOH^{2+} + H^+$	log K = - 4.97
$Al^{3+} + 2H_2O = Al(OH)_2^+ + 2H^+$	log K = - 9.3
$Al^{3+} + 3H_2O = Al(OH)_3(aq) + 3H^+$	log K = -15.0
$Al^{3+} + 4H_2O = Al(OH)_4^- + 4H^+$	log K = -23.0

(after Stumm-81a)

2.4.3) Mullite

2.4.3.1) Mullite- Electrical Double Layer Studies

Mullite, $3Al_2O_3.2SiO_2$ or $Al_6Si_2O_{13}$, is the most stable phase in the silica-alumina system. Smolik-66a evaluated the p.z.c. of mullite to be 8.1, while Parks-67a calculated the p.z.c. to be 7.1 for hydrous and 5.3 for anhydrous mullite from electrostatic considerations.

Tschapek-74a studied the p.z.c. of kaolinite and SiO_2/Al_2O_3 mixtures by comparing the p.z.c.-values with those of the individual oxides; 2.0 for silica and 9.0 for alumina. Mechanical mixtures of alumina and silica did not yield linear relationships between p.z.c. and composition as predicted by Parks-67a (Figure 2.13a); rather alumina dominated the surface properties of the mixtures. The explaination given was that Al_2O_3 is more sensitive to pH change than silica.

Pyman-79a also studied the p.z.c. of mechanically mixed and coprecipitated aluminosilicates that were not fired, Figure 2.13b. The anticipated p.z.c.-value for a composition with mullite's stoichiometry of Al/Al+Si= 6/8=.75 is 8.6 for a mechanical mixture and 6.3 for the coprecipitate. The low value for the coprecipitate probably results from preferential precipitation of silica on the alumina surface sites. Similar results were obtained by Perrott-77a.

At some pH between 2.0 and 9.0, the p.z.c.-values of silica and alumina, silica sites are negatively charged while alumina surface sites are positively charged. A composite p.z.c. is anticipated at a pH for which the negative charge on the silica portion exactly neutralizes the positive charge on the alumina portion of the surface. This property need not follow a linear composition relationship as expressed by Parks-67a if the width of the pH range where charged species predominate differs for the Al and Si surface sites due to different ΔpK's.

2.4.3.2) Mullite- Dissolution Studies

No dissolution data on mullite could be found in the technical literature, probably due to this solid's very low solubility. Iler-79a states that the very low solubility of aluminosilicates implies a strong interaction between the two constituant oxides. This interaction may result from the fact that both ions can have either 4 and 6-fold coordination with oxygen and have appproximately the same diameter. Moreover, $Al(OH)_4^-$ is geometrically similar to $Si(OH)_4$, meaning that the ion can substitute into a silica surface creating an aluminosilicate site with fixed negative charge.

2.4.3.3) Mullite- Crystal Structure Studies

The mullite phase forms for compositions between (0.6-0.67) Al_2O_3/(0.4-.33) SiO_2. Accordingly, Gray-71a has expressed doubt in experimentally determined crystal structures and their relation to surface properties for mullite. Ratnasamy-71a describes the mullite structure as being composed of alumina tetrahedra sharing one corner with a silica tetrahedron and the three other others with alumina octahedra.

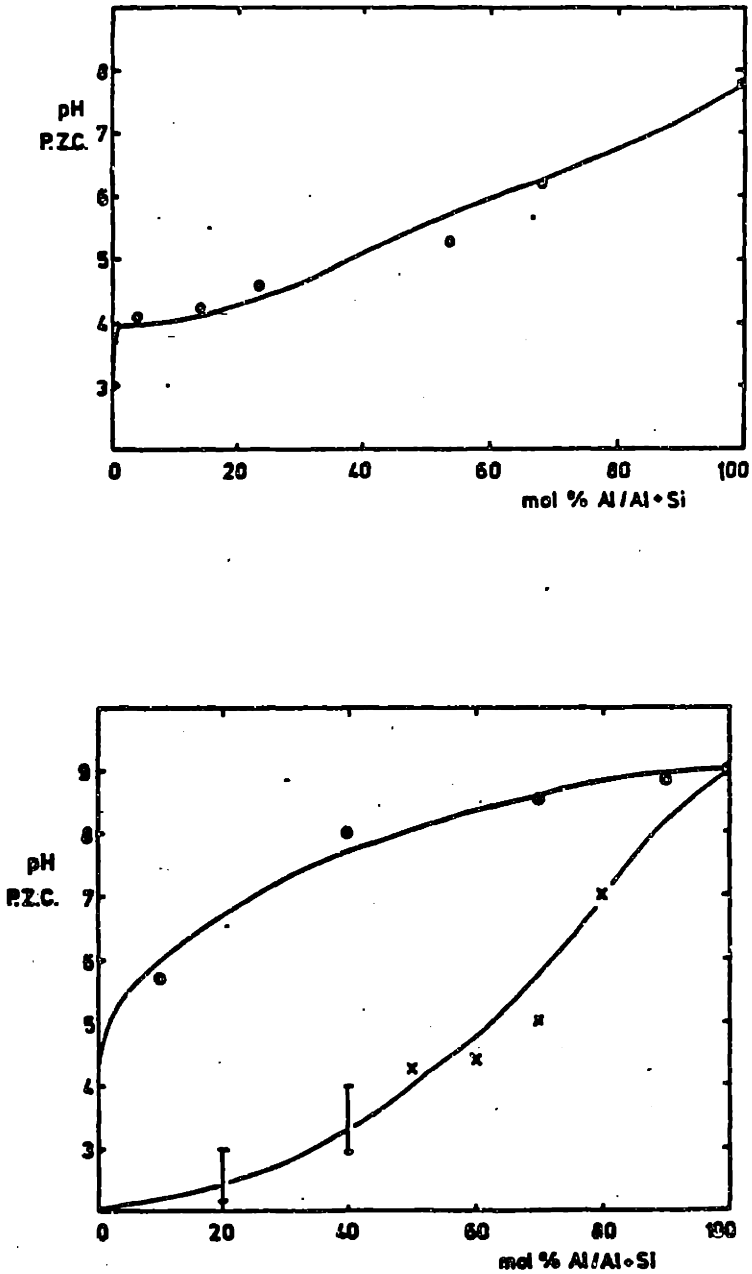

Figure 2.13 The p.z.c. of mixtures of alumina and silica.

a) Mechanical mixtures. (after Tschapek-74a)

b) Coprecipitated and calcined mixtures of alumina and silica. (after Pyman-79a)

2.4.4) Zirconia

2.4.4.1) Zirconia- Electrical Double Layer Studies

Ahmed-66a found that K^+ and NO_3^- specifically adsorb on the ZrO_2 surface with a p.z.c. of 6.0. Ahmed-75a also determined that Cl^-, NO_3^- and ClO_4^- specifically adsorbed onto ZrO_2 but not onto Al_2O_3, TiO_2 or SiO_2. Ray-75a found identical p.z.c. and i.e.p.-values of ZrO_2 to be 6.7 in NaCl solutions, corresponding to the solubility minimum in aqueous solution. Since Na^+ and Cl^- ions were found to be indifferent to the surface, differential capacitances of the double layer were calculated from the σ_o curves.

Yoon-79a calculated the p.z.c. of ZrO_2 in the high temperature, 8-fold coordination to be 10.1 from crystallographic data. The p.z.c. for the low temperature, 7-fold form would be expected to be much less and close to that of the hydrous oxide (REF Mandel-80a). Mandel-80a studied the p.z.c. of synthetic hydrous ZrO_2 oxide sols using potentiometric titration. The p.z.c. was determined to be between 6.0 and 6.3 in KNO_3 depending on preparation technique.

Milonjic-83a interpreted the adsorption of lithium, sodium, and potassium ions onto zirconia using the DJL model. The p.z.c. of the hydrous zirconia was determined to be 4.0. Surface ionization pK-values were reported for LiCl, NaCl, and KCl. Two ZrOH sites were found on the ZrO_2 surface using IR-spectroscopy and were labeled ZrO_I-H and ZrO_{II}-H. The ionization constants in NaCl solution were 5.8

and 7.2, while the complexation constants were 5.3 and 6.8 for sites I and II respectively. These intrinsic ionization and complexation constants are similar, indicating that the ions only weakly complex with the surface. Equilibria during potentiometric titration entail a two-step process that involves the rapid sorption of H^+ and OH^- requiring a 2-minute equilibration time and a slow equilibrium process. Surface complexation or specific adsorption was found to be markedly less for ZrO_2 than for most other oxides.

Regazzoni-83b, studying the interfacial proprties of ZrO_2, applied the DJL model to obtain surface pk-values. The p.z.c. and i.e.p. were determined to be 6.4 and 6.5. The outer capacitance, K_1 = 140 uF cm^{-2}, inner capacitance, K_2 = 20 uF cm^{-2}, and site density, 5 nm^{-2}, were used for calculation purposes. The ionization and complexation constants determined using the DJL model, pK_{a1} = 4.2, pK_{a2} = 8.6, pK^*_{anion} = 5.2, and pK^*_{cation} = 7.6 for KNO_3 solutions, imply that ionization dominates over complexation. The relative fractions of charged sites arising from these reactions were calculated, and are given in Figure 2.14. The concentration of surface sites is dominated by complexed sites for high electrolyte concentration, while ionized surface sites are seen to dominate for low electrolyte concentrations.

2.4.4.2) <u>Zirconia- Dissolution Studies</u>

Ray-75a has shown that for a logarithmic plot of concentration versus pH for zirconia in aqueous solution, shown in Figure 2.15, the point of minimum solubility occurs at a pH of 6.7 corresponding to the determined p.z.c. For pH-values between 3.0 and 12.0 the concentration of dissolved species remains less than 10^{-5} M, so dissolution plays a minor role in the titration of zirconia. The dissolution reaction equations for zirconia are listed in Table 2.3.

2.4.4.3) Zirconia- Crystal Structure Studies

The crystal structure of zirconia was discussed by Rijnten-70a. Zirconia can be present in three forms; monoclinic (m), tetragonal (t), and cubic (c). Monoclinic zirconia contains four ZrO_2 groups per unit cell, with two types of oxygen sites; O_I with four Zr-O bonds and O_{II} with three Zr-O bonds. The tetragonal form is represented by a slightly distorted CaF_2-structure with a unit cell size between 5.07 and 5.16 A. This phase is normally present only above 1200 °C but may be obtained in fine powder precipitation. The cubic phase is apparently stable only above 2285 °C and hence will not be discussed further.

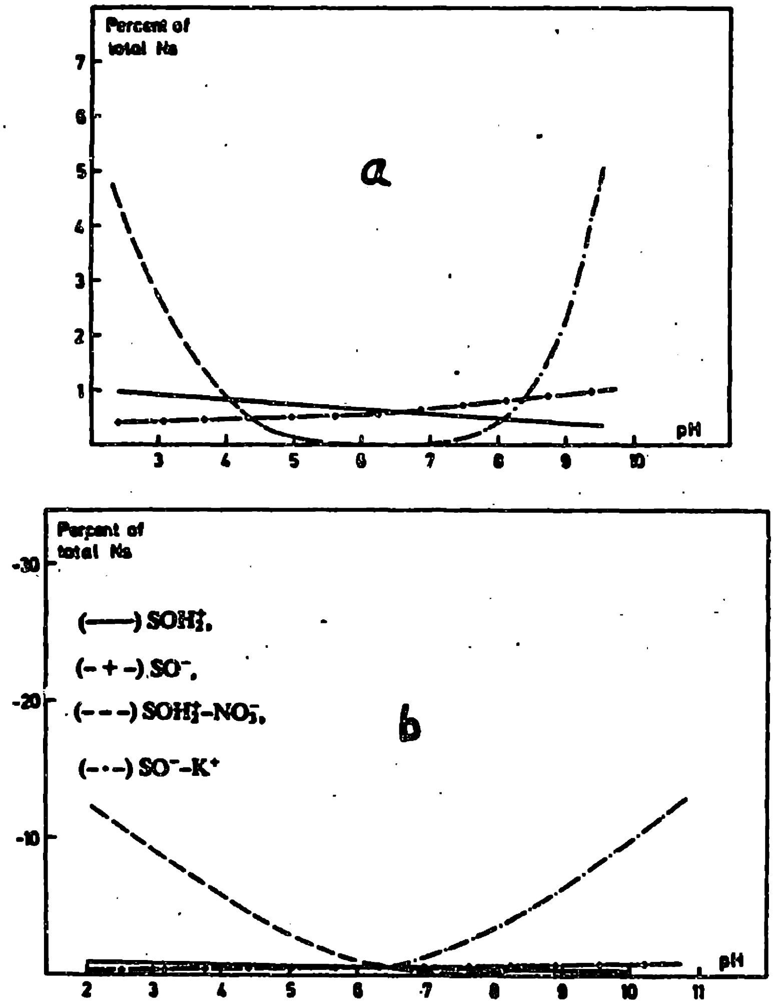

Figure 2.14 Surface speciation of ZrO_2 as a function of pH. (after Regazzoni-83b)

a) in 0.001 N KNO_3

b) in 0.1 N KNO_3

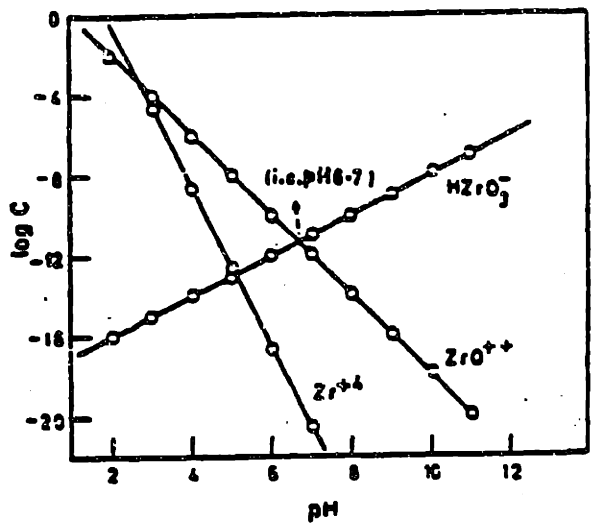

Figure 2.15 Concentration of dissolved zirconia species as a function of pH. (after Ray-75a)

Table 2.3

Solubility equilibria for the ZrO_2-H_2O system at 25 °C.

$ZrO_2(s) + 2H^+ = ZrO^{2+} + H_2O$	log K = -2.02
$ZrO_2(s) + OH^- = HZrO_3^-$	log K = 4.0
$ZrO_2(s) + H^+ = Zr^{4+}$	log K = -7.3

(after Ray-75a)

3) Experimental Materials and Techniques

3.1) Experimental Materials

3.1.1) Oxides

Two silicas were used in this study. Quso G30 was obtained from the PQ Corporation, Valley Forge, PA. It is a precipitated silica produced by depolymerizing a high purity sand to yield soluble silicate. The soluble silicate is then repolymerized to precipitate fine, particulate, amorphous silica (REF PQ-78a). Yates (REF Yates-76a) states that most commercial precipitated silicas are usually prepared by the addition of acid to a sodium silicate solution under controlled conditions yielding a hydrous silica which is filtered, washed and dried.

The second silica was prepared based on the method of Stober (REF Stober-68a) and is amorphous, spherical, and essentially monosized. It was prepared for this study by hydrolysis of tetraethyl orthosilicate (TEOS) following Jubb's (REF Jubb-82a) modification of Stober's method. In this technique, 360 ml of ethanol, 57 ml NH_4OH, and 30 ml TEOS are separately filtered, then combined and mixed for 24 hours at room temperature (~25 ^oC) in a sealed container. The resulting suspension of precipitated monosized, spherical SiO_2 particles is cleaned by repeated centrifuging, decanting, and redispersing in deionized (DI) water.

The aluminas were obtained from Adolf Meller Co., Providence, RI. Both alpha and gamma alumina are produced by the refining and thermal decomposition of a complex aluminum salt which is said to yield high purity alumina due to multiple recrystallizations and precise heating (REF Meller-83a). Meller 180 is a pure α-Al_2O_3 whereas Meller 182 is a transition $\alpha\gamma$-Al_2O_3 phase.

The high-purity mullite used in this study was provided by Baikowski International Corp., Charlotte, NC.

The zirconia used in this study was prepared in the laboratory using the technique of Bleier (REF Bleier-82a). A 0.2 F $ZrOCl_2 \cdot 8H_2O$ aqueous solution is placed in a sealed glass test tube and aged at 98 ^{o}C for 72 hours. The product, a turbid, white suspension of m-ZrO_2 is centrifuged and the resulting powder separated from the decant and resuspended in DI water. This step is repeated 12 to 14 times and produces the final, cleaned material.

3.1.2) Cleaning Procedure for Commercial Powders

The commercial SiO_2, Al_2O_3, and $3Al_2O_3 \cdot 2SiO_2$ powders were cleaned using soxhlet extraction. In this technique the powder is placed in a porous, filter paper cup which is placed in a siphon chamber. Freshly distilled, DI water flows through the powder removing soluble ions and filling the chamber. When the siphon height is obtained, the siphon tube drains the dirty water into the solvent container where it is redistilled and the process repeated. This allows continuous washing with hot, DI water where the washing solvent is replaced every few minutes. Parfitt and Wharton found that continuous extraction for 48 hours removes all traces of surface chloride from chloride-originated powders, e.g. SiO_2 from $SiCl_4$, TiO_2 from $TiCl_4$ and Al_2O_3 from $AlCl_3$ (REF Parfitt-72a). Titrations on nonsoxhleted Quso G30 powders yielded $R\sigma$ versus pH curves that did not reliably intersect at $R\sigma = 0$, whereas soxhleted powders did, as did those for Al_2O_3 and mullite. The $\Delta\sigma$ discrepency for SiO_2 apparently derives from the dissolution and then replacement of surface sodium ions with H^+ ions from solution in the uncleaned system. For the cleaned system, surface sodium was not present and hence no shift in the titration curves was evident. Soxhlet extraction also eliminated problems in the intersection of surface charge curves for Meller 180, α-alumina.

The cleaned powders were then dispersed in DI water and stored in cleaned polypropylene containers.

3.1.3) <u>Reagents</u>

All water used in this study was prepared by deionization of tap water to a resistivity of greater than 18 M Ω-cm.

All chemicals used in this study were of analytical grade unless otherwise specified. NaCl was used to maintain constant ionic strength in all titration, electrophoresis, and dissolution experiments. To avoid aging effects, dye solutions for the UV-determinations were made fresh daily.

Dilute solutions of 0.1 N HCl and 0.1 N NaOH were used for pH-control during all experiments. NaOH solutions were standardized using the phthalate technique of Vogel (REF Vogel-62a). The acid solutions were then standardized against these primary standards. All solutions were standardized to 0.001% at 25 ^{o}C.

Prepurified nitrogen, saturated with water vapor, was used as an inert atmosphere for all titration studies.

3.1.4) Glassware

Volumetric glassware used in this study was new. Polypropylene titration cells and reagent bottles were used to eliminate glass dissolution problems in basic solutions. Reagent bottles were fitted with two stopcocks leading to the titration system and to an ascarite container allowing solution removal without CO_2 intake. All glass and polypropyleneware was washed by first scrubbing in soapy water either by hand or with the use of an ultrasonic bath. The pieces were rinsed in DI water and soaked for one day in a bath which containing 1:1 parts 1N KOH to alcohol to remove organics. The pieces were then rinsed in DI water, washed in 1N HNO_3 to remove KOH and soluble metal ions, and rinsed vigourously several times in DI water before drying (REF Vogel-62a).

3.2) Experimental Techniques

3.2.1) General Measurements

The specific surface area of the powders were determined using the single-point BET method on a Quantasorb surface area instrument by Quantachrome. A 30% N_2-70% He mixture was used for the measurements. Approximately 0.2 g. of powder was placed in the microcell and outgassed in flowing nitrogen at 200 ^oC for two hours; however, the monosized silica was outgassed at selected temperatures up to 400 ^oC. Four measures of the desorption peak area were averaged to determine the sample surface area. The size of the nitrogen was assumed to be 16.2 A^2.

X-ray powder diffraction, XRD, patterns were obtained using a computer controlled GE 8000 unit for the 2θ-range of 10-80^o using CuK_α radiation and 35 kV and 15 mA. The powder was mulled in collodion and spread evenly on a glass slide where it was allowed to dry.

Transmission electron microscopy, TEM, was used to analyse the morphology of the powders used in this study using a Phillips 300 microscope. Samples were prepared by dipping carbon-coated, copper TEM grids into a very dilute, aqueous dispersion of powder. The grids were removed and allowed to dry before carbon-sputtering and analysis.

3.2.2) Potentiometric Titration

Potentiometric titrations were caried out using a Radiometer RTS822 system. This system includes a PHM84 scientific pH meter, TTT80 titrator controller, ABU80 autoburette, a TTA80 titration cell, and a REC80 servograph chart recorder with the REA160 titrgraph module. The electrodes included Radiometer's K701 double junction, G2040C glass, and T701 temperature sensor. This system allows for stepped titrations of oxides in electrolyte, where a known volume of titrant is added, a finite time is allowed for equilibrium to be obtained, and the pH of the sample is measured. The pH of the suspension was recorded as a function of acid or base added.

Titrations of control electrolyte were compared to those of samples prepared by pipetting 20 ml of stock dispersion and 20 ml of 2, 0.2, 0.02, and 0.002 N NaCl solution. The volume of powder in the final suspension was small. The samples were then subjected to N_2-bubbling for two hours in a glove bag. The bottles were capped and sealed with electrical tape to exclude CO_2. Samples were allowed to equilibrate for 10 hours and were titrated the next day.

Prior to titration, the burette was thoroughly cleaned by repeated flushings with fresh titrant to insure that contamination of the titrant due to solubility of the burrette's glass walls was minimized. The second junction of the K701 electrode was rinsed with DI water and similarly flushed with the electrolyte before the final filling. 1.0 N NaCl solutions were used for samples with 1.0 and 0.1 N electrolyte and 0.01 N for samples with 0.01 and 0.001 N electrolyte. The electrodes were placed in their holders and rinsed vigorously with distilled water. The pH meter was standardized against two buffers for the region to be titrated and the electrodes were rewashed. The nitrogen flow was started in the last step to ensure that no entrapped water or buffer remained in the nitrogen injection tube. The sample container was then rapidly (<5s) unsealed and placed in position and sealed against the TTA80 titration cell. The samples were N_2-bubbled for at least 10 minutes to ensure removal of any residual CO_2. The titration was started in the stepped titration mode with speeds of 70 min per full scale deflection for the recorder and titrant delivery speed of 5. At the end of the run, the final pH and volume added was recorded. The average titration time was 2 pH units per hour. The titrations for the control electrolyte and suspension are compared, yielding the net uptake of titrant by the powder's surface (see Figure 4.3). Differences in the titration data for oxide surfaces result because specific surface sites have different acid/base properties and reaction constants. This leads to changes in the specific amount of titrant required to obtain a certain pH (see Figure 3.1).

In the case of monosized silica and uniform zirconia, unacceptable experimental data was obtained when the suspension titration curves were compared to the salt solution titration curves. Possible solubility and impurity problems were assumed. In order to eliminate these problems, the titration method of Huang-71a was used, by which oxide is equilibrated with electrolyte, the sample is divided and one portion is titrated as described. The second portion is centrifuged and the supernatant is titrated. The titration of the suspension is compared to that of the supernatant liquid therebye providing a correction for the effects of impurity and backround solubility which were present. It is recognized that dissolution that occurs during the titration of the suspension will not be taken into account and must be treated in the final calculations.

3.2.3 Electrophoresis

Electrophoresis was carried out using a Rank Brothers Particle Micro-Electrophoresis Apparatus Mark II. Measurements were made at 25 ^{o}C in the cylindrical cell. At least ten measurements were made for each sample to ensure accuracy. Samples were titrated under nitrogen and allowed to equilibrate at the desired pH for two hours. The samples were removed and stored in polypropylene test tubes for 4 hours when electrophoresis measurements were made. Unfortunately the measurements were made in air, so pH shifts due to CO_2 absorption from the atmosphere may have occurred.

To overcome this problem, it is desired to do the experiments in nitrogen in order to remove the carbonate pH shift and possible adsorption problems. Meller 180 α-Al_2O_3 suspensions were titrated to the desired pHs under N_2 and pumped to the electrophoresis unit using a peristaltic pump to exclude CO_2. Unfortunately the measured mobilities remained approximately constant without the expected sign reversal near the expected i.e.p. of 9.0. Possible reasons for this problem would be dissolution of the PVC tubing to form PV monomers which adsorb on the powder surface causing fixed OHP potential. Another possible problem would result from CO_2 diffusion through the tubing causing downward pH shifts for higher pH-values. This problem would cause shifts in the ξ-potential, however it would not cause the observed constant ξ-potential, thus we have assumed that the first mechanism is causing the problems. Owing to time constraints, this experiment was not pursued, however discussions with Dr. R. James (REF James-83a) have outlined the solution to this problem.

3.2.4) Solubility Studies

The solubility of alumina and silica in aqueous solutions at different pH-values was determined using a Bausch and Lomb Spectronic 21 UVD and Bausch and Lomb matched cells. Samples consisted of equal volumes of stock suspension and 0.02 N NaCl solutions, titrated in air to different pH. The suspensions were allowed to equilibrate during the titration for at least 4 hours before supernatant sampling and measurement.

The proceedure used to determine the solubility of silica was that of Vogel (REF Vogel-62a). An ammonium molybdate solution was made by dissolving 8 g of ammonium molybdate in DI water, adding 9 ml of concentrated sulphuric acid, and diluting to 100 ml. A reducing solution was made from solutions A) 10 g sodium hydrogensulphite in 70 ml of water and B) 0.8 g anhydrous sodium hydrogensulphite and

0.16 g 1-amino-2-napthol-4-sulphonic acid in 20 ml of water. Solutions A and B are mixed and diluted to 100 ml. A 10% tartaric acid solution was prepared. Standards of Si were made from $Na_2Si_3 \cdot 5H_2O$.

2.5 ml of SiO_2-supernatant was placed in a 50-ml volumetric flask. To this sample, 0.5 ml of the ammonium molybdate solution is added. After five min, 2.5 ml of tartic acid solution was added and mixed producing the characteristic yellow molybdosilicic complex color. Next, 0.5 ml reducing agent was added turning the solution blue due to the formation of the molybendenum blue complex. The sample was then diluted to 50 ml. After 20 min, the absorbance was measured at 815 nm against that of a reagent blank. The absorbance of the silica standards was plotted versus concentration to establish a calibration curve.

The procedure to determine soluble alumina was also that of Vogel (REF Vogel-62a). An aliquot of the test solution was transfered to a 50 ml volumetric flask. 2.5 ml of 5-volume hydrogen peroxide was added and mixed. The pH was adjusted to 6.0 using 0.1 N NaOH or 0.1 N HCl. 2.5 ml of Eriochrome Cyanine R solution (0.1 g in 100 ml of DI water, then filtered) was added and mixed. 25 ml of dilute buffer solution was added, made by diluting concentrated buffer (27.5 g ammonium acetate and 11.0 g hydrated sodium acetate in 100 ml DI water plus 1.0 ml of acetic acid) with 5 times water and adjusting the pH to 6.1 using glacial acetic acid. The solution was then rapidly diluted to 50 ml and after 30 min, the absorbance was measured relative to that for a reagent blank establishing a calibration curve.

Centrifugation or filtration is used in the case where solids had to be separated from their solutions.

3.2.5) Calculations and Surface Property Determination

Calculations of the electrical double layer properties such as surface charge, effective ionization, and complexation constants were made on an Osborne 1 computer. All equations used in the calculations are listed in Appendix I.

Graphs of surface charge, σ_o, vs pH were made. The effective ionization constants, pQ-values, were calculated and plotted versus α^* $(10\alpha + c^{1/2})$. Extrapolation to the zero charge and infinitely dilute solution conditions yielded the intrinsic ionization constants, $pK_{a1,a2}$. Plots of pQ^*_{ion} versus α^*_{ion} $(10\alpha - \log(c))$, when extrapolated to the zero surface charge and log(c)=0 conditions yielded the intrinsic complexation constants, $pK^*_{Na,Cl}$.

Estimates of the distribution of e.d.l. species, charge, and potential were made using the program SITECAL, a modification of MINEQL, listed in Appendix II on a Tektronix 4052. The determined values for the ionization and complexation constants were entered into a reaction tableau describing the surface reactions between the oxide and electrolyte solution. The theoretical species, charge, and potential distributions were calculated and compared to the experimentally determined σ_o-values and Ψ_δ-values.

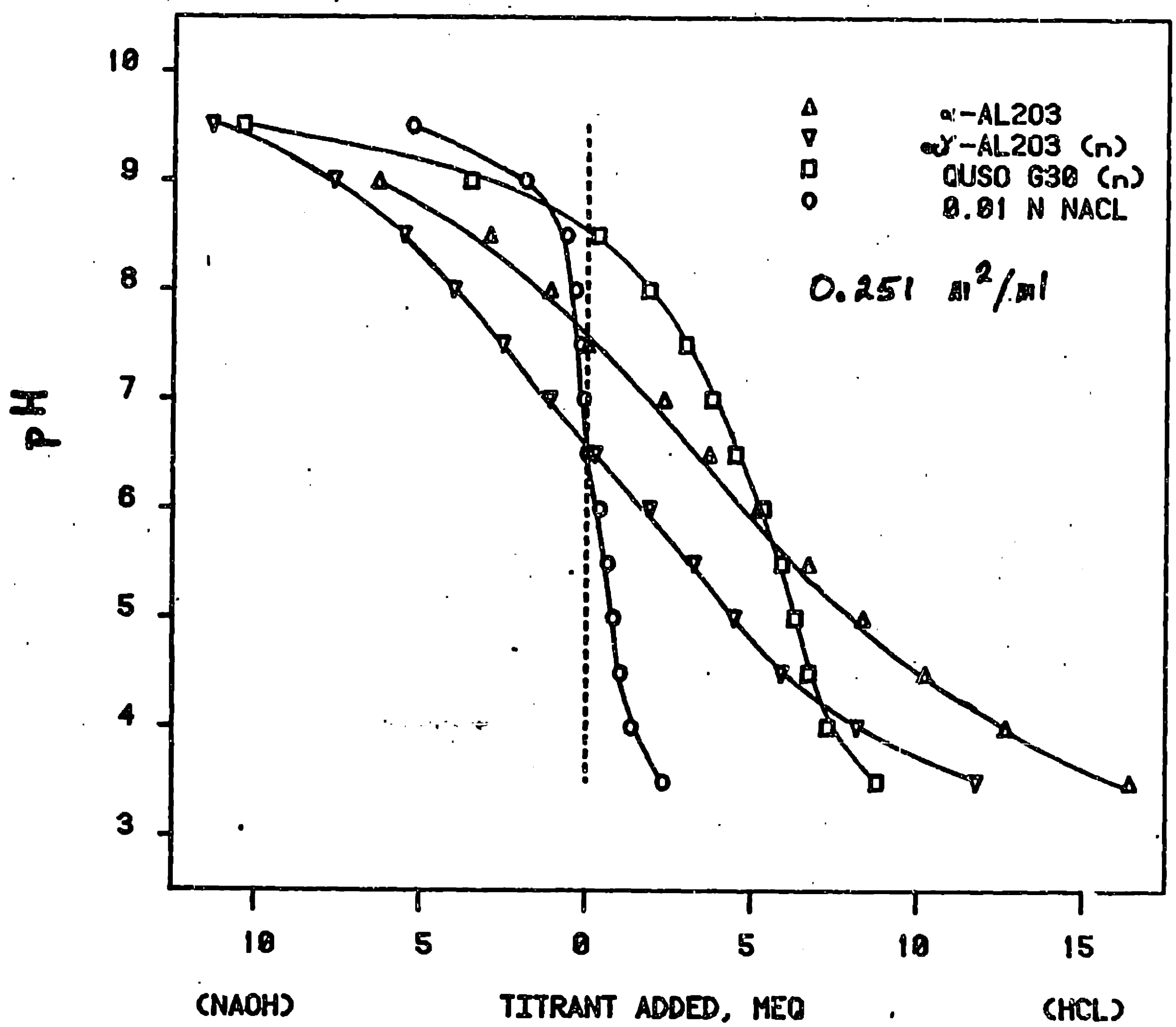

Figure 3.1 Examples of titration data for α-Al_2O_3, $\alpha\gamma$-Al_2O_3, and SiO_2 showing the differences between the data due to different reaction equilibria occurring between the solution and surface reactive sites.

4) Results and Discussion

4.1) General Properties and Morphology of Powders

The surface area of the oxides used in this study was determined by the BET method (REF Brunauer-38a) and are listed in Table 4.1. The area of the monosized silica increased with outgassing temperature, whereas that of Quso G30 was independent of outgassing temperature. This result implies that surface porosity was present in the former and that upon heating, the water was removed from these small pores, allowing for N_2 filling and hence increasing the experimental surface area. The maximum value of 41.46 m^2/gm was chosen for subsequent calculations.

The crystal structure of all powders was examined using TEM and XRD. The two silicas are amorphous. Meller 180 and 182 are crystalline α-Al_2O_3 and transition $\alpha\gamma$-Al_2O_3 phase respectively. Baikowski's mullite is crystalline mullite. The zirconia studied is crystalline, monoclinic ZrO_2.

Particulate morphology was examined using TEM. Figures 4.1 are representative micrographs of the morphology of Quso G30 silica, while the monosized SiO_2 is shown in Figures 4.2. The former silica consists of irregularly shaped particles exhibiting a broad size distribution whereas the particles in Figure 4.2 are spherical and have a narrow size distribution. Small particles located in the neck regions between particles and on the surface of particles indicate that reprecipitation may have occurred, perhaps during the washing procedure in which pH decreases significantly.

Meller 180, α-Al_2O_3 is shown in Figures 4.3. The material contains several forms of crystallites: large platelets, smaller particles that appear rounded due to melting, and very fine particles that are agglomerated. Meller 182, the transition $\alpha\gamma$-Al_2O_3, is shown in Figures 4.4 and contains a structure similar to that of the Meller α phase, implying a similar manufacturing technique. Baikowski's mullite, shown in Figures 4.5, has a mixed structure of large and small particles; dense, rounded particles implying a thermal production process. The m-ZrO_2 studied, shown in Figures 4.6, is essentially spherical and monosized. The "particles" appear, however, to consist of very fine particles that are agglomerated to form particulates on a scale of a few tenths fo a micron in diameter.

Solubility studies were conducted to determine appropriate corrections for the titration data to account for titrant uptake by soluble oxide species. The soluble silica data determined for Quso G30 and monosized silica are listed in Table 4.2. The change in solubility from baseline was approximately 1.0×10^{-4} M dissolved Si species represent approximately 1.0% of the 9.37×10^{-3} M SiO_2 sites for Quso G30 and 2.5% for the 4.00×10^{-3} M SiO_2 for the monosized material, using the reported N_s for silica of 5.0 sites/nm^2 (REF James-82a). No corrections were made for these two materials since the concentration of soluble silica remains low and essentially constant throughout the titration pH range. Thus, titrant is not significantly consumed by $Si(OH)_4$-species, the dominant specie for the entire titration pH range investigated. In the case of monosized silica, the Huang titration technique removes the effect of initial solubility before titration.

The total amounts of soluble Al-species for Meller 180 and 182 Al_2O_3 were determined and are listed in Table 4.2. Since the concentration of soluble species remains at approximately 10^{-5} M, solubility corrections were similarly unnecessary for Al_2O_3. This concentration corresponds to approximately 0.33% of the 2.99×10^{-3} M surface sites for Meller 180, and 0.13% of the 7.90×10^{-3} M surface sites for Meller 182 using N_s = 2.7 sites/nm^2 (REF James-82).

The concentration of soluble Al-species for Baikowski's mullite are listed in Table 4.2. The baseline solubility of 3.0×10^{-5} represents 0.58% of the total 5.18×10^{-3} M mullite sites assuming N_s = 5 sites/nm^2. The only pH for which solublility corrections apply for mullite is pH 3.0. No solubility of Si-species could be detected for mullite using the technique of Vogel (see section 3.2.4), implying that the concentration of dissolved Si-species is less than 10^{-5} M. Iler-79a states that the very low solubility of aluminosilicates implies strong interaction of aluminum and silicon oxides. This interaction possibly derives from the fact that both metal ions have coordination numbers of 4 or 6 oxygen and have approximately the same atomic diameter.

No solubility studies were conducted for the m-ZrO_2. Bleier and Cannon (REF Bleier-82a) found 100% precipitation of the reagent zirconium species for pH-values between 4 and 10, suggesting that the material does not significantly dissolve in this pH region. The solubility of ZrO_2 is small for the titration range studied, as seen earlier in Figure 2.15.

Table 4.1

XRD and BET Results for Cleaned Oxide Powders.

Oxide	Phase (XRD)	BET Surface Area (m^2/gm)	
SiO_2			
Quso G30	amorphous	118.73 ± 1.25	(200 °C)
monosized	amorphous	18.78 ± 2.33	(200 °C)
		36.23 ± 3.93	(300 °C)
		41.46 ± 5.17	(400 °C)
Al_2O_3			
Meller 180	α-Al_2O_3	21.31 ± 0.49	(200 °C)
Meller 182	$\alpha\gamma$-Al_2O_3	79.68 ± 1.57	(200 °C)
$3Al_2O_3.2SiO_3$			
Baikowski	crystalline	6.87 ± 0.03	(200 °C)
ZrO_2			
uniform	monoclinic	96.00	(200 °C)

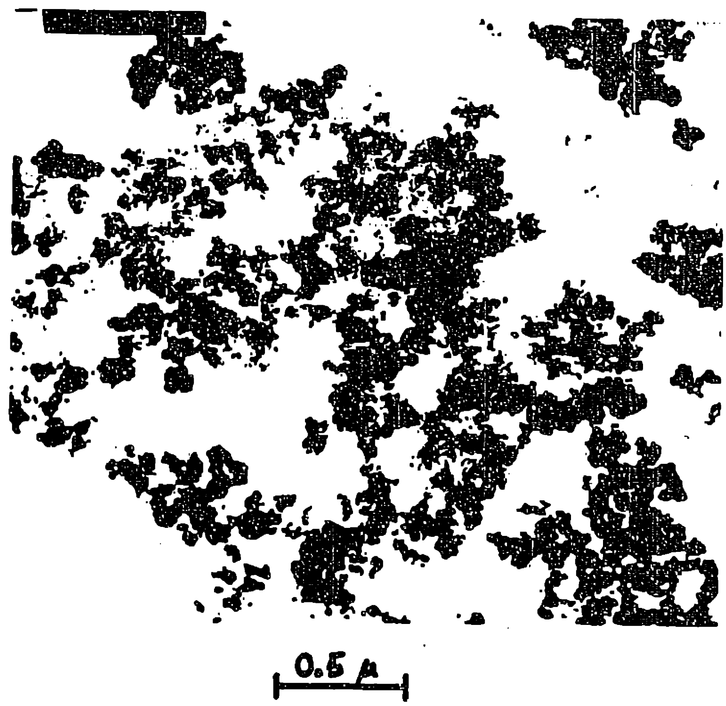

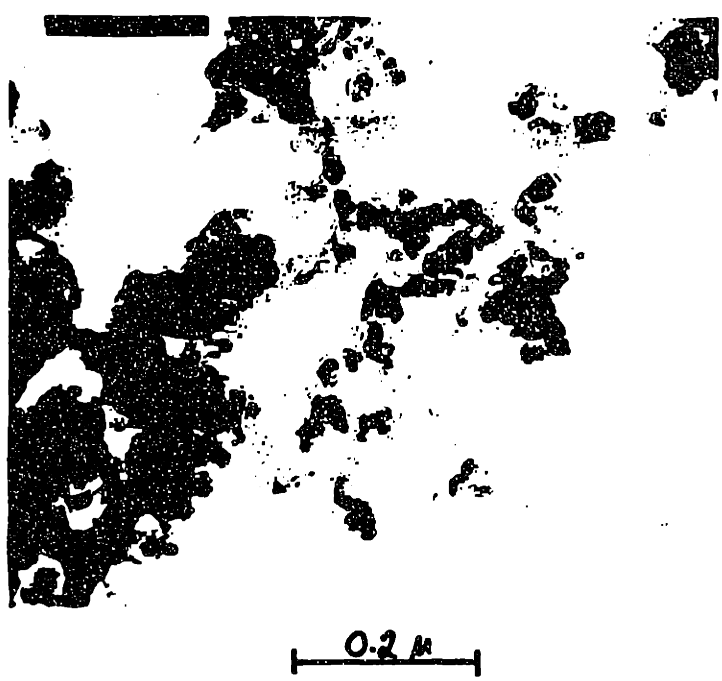

Figure 4.1 TEM micrographs of Quso G30, amorph-SiO_2.

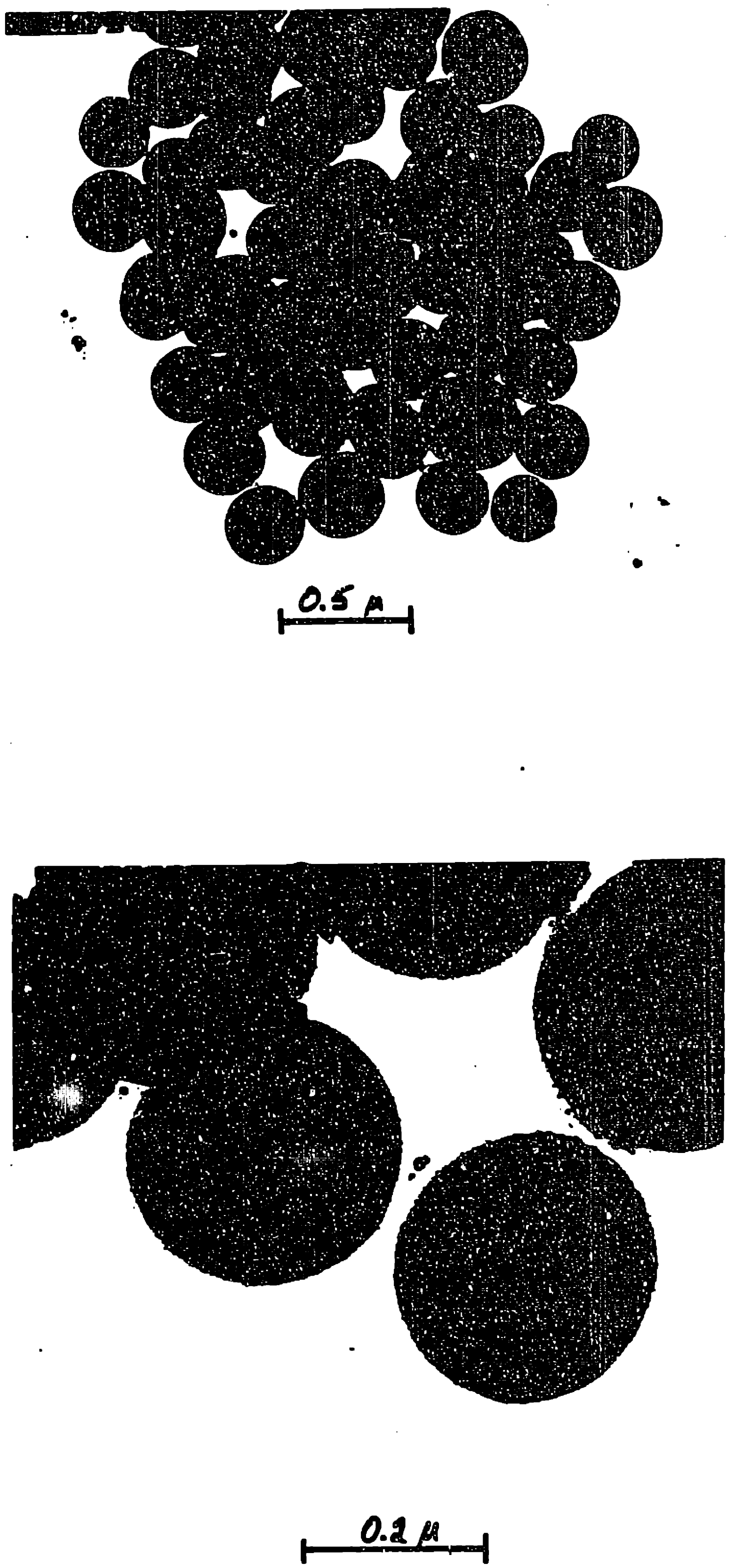

Figure 4.2 TEM micrographs of monosized, amorph-SiO_2.

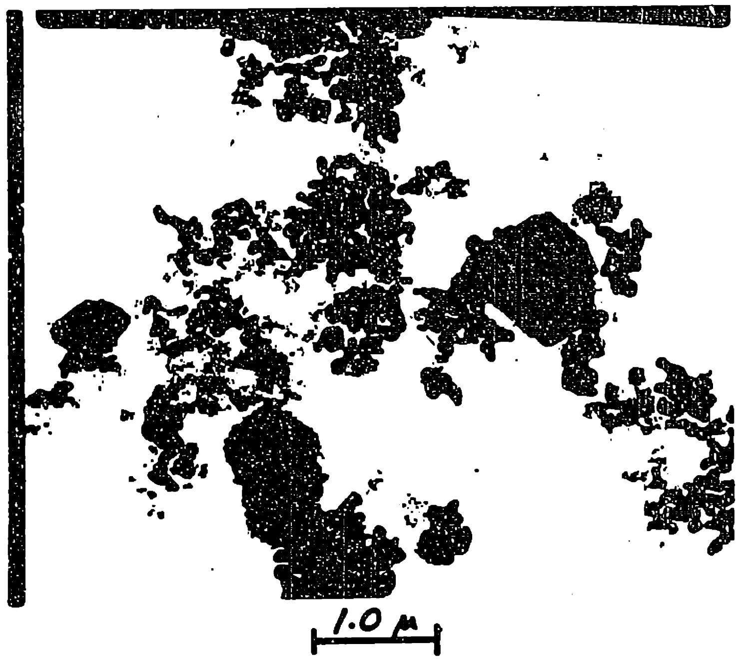

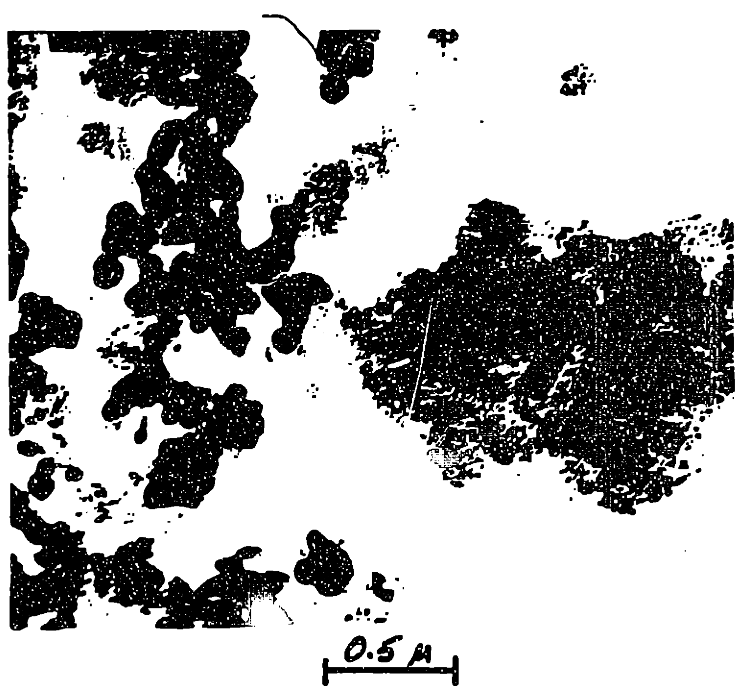

Figure 4.3 TEM micrographs of Meller 180, α-Al_2O_3.

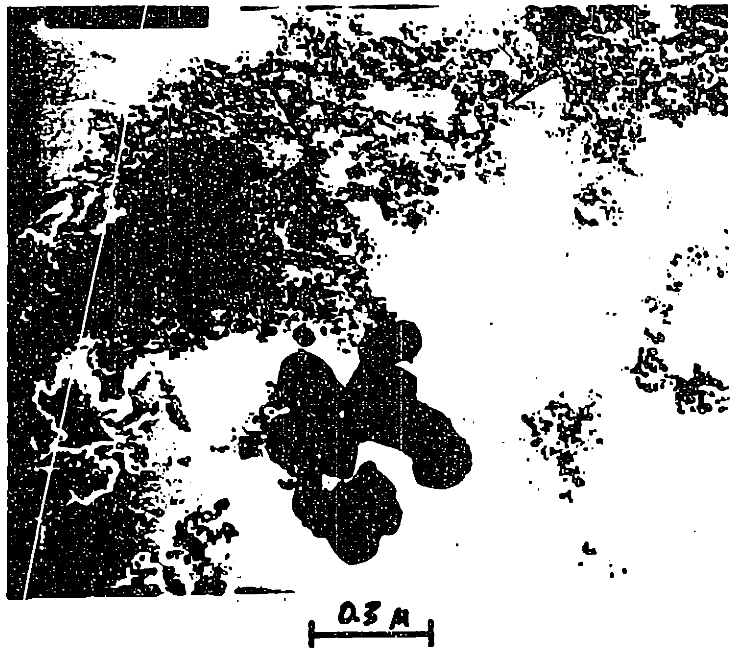

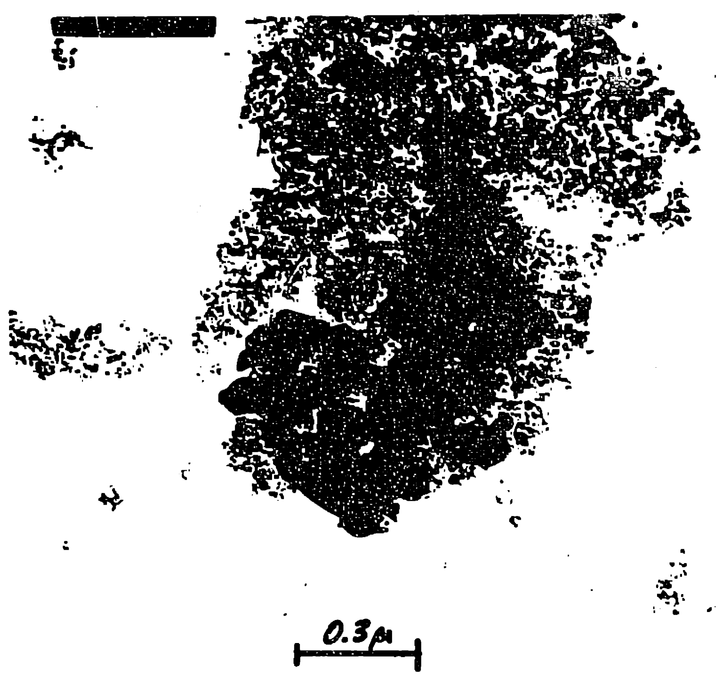

Figure 4.4 TEM micrographs of Meller 182, αγ-Al_2O_3.

Figure 4.5 TEM micrographs of Baikowski mullite, $3Al_2O_3.2SiO_2$.

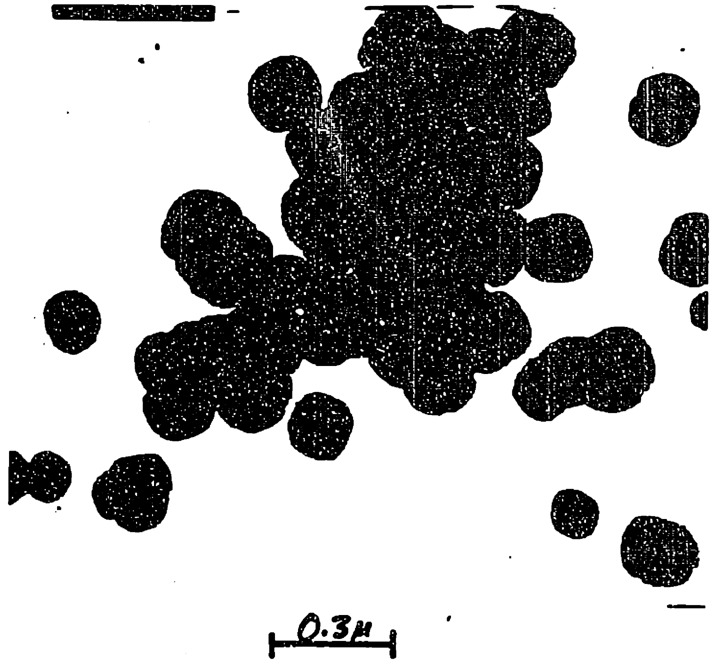

Figure 4.6 TEM micrographs of uniform, m-ZrO_2.

Table 4.2

Results of UV solubility studies for the cleaned oxides.[a]

Quso G30 (amorph-SiO_2)

pH	moles Si/l
2.99	8.95×10^{-4}
3.46	1.29×10^{-3}
5.5	1.26×10^{-3}
7.43	1.49×10^{-3}
9.03	1.61×10^{-3}
10.49	3.83×10^{-3}

monosized, amorph-SiO_2

pH	moles Si/l
2.47	2.00×10^{-3}
3.50	1.94×10^{-3}
4.48	1.75×10^{-3}
5.49	1.89×10^{-3}
6.49	2.67×10^{-3}
7.49	3.18×10^{-3}
8.49	2.90×10^{-3}
9.45	4.09×10^{-3}

Meller 180 (α-Al_2O_3)

pH	moles Al/l
3.00	3.46×10^{-4}
4.04	3.97×10^{-5}
4.96	$<3.15\times10^{-5}$
6.03	$<3.15\times10^{-5}$
6.96	3.54×10^{-5}
7.96	3.30×10^{-5}
8.76	3.38×10^{-5}
9.85	3.71×10^{-5}
11.07	4.46×10^{-4}

Meller 182 ($\alpha\gamma$-Al_2O_3)

pH	moles Al/l
3.08	1.51×10^{-3}
4.08	3.97×10^{-4}
4.97	$<3.15\times10^{-5}$
5.98	$<3.15\times10^{-5}$
6.74	$<3.15\times10^{-5}$
7.83	$<3.15\times10^{-5}$
8.89	$<3.15\times10^{-5}$
9.92	3.71×10^{-5}
11.00	5.61×10^{-4}

Baikowski Mullite $3Al_2O_3.2SiO_2$

pH	moles Al/l	moles Si/l
4.07	3.30×10^{-5}	$<6.25\times10^{-5}$
4.28	3.30×10^{-5}	$<6.25\times10^{-5}$
5.12	3.30×10^{-5}	$<6.25\times10^{-5}$
6.37	3.30×10^{-5}	$<6.25\times10^{-5}$
7.06	$<3.15\times10^{-5}$	$<6.25\times10^{-5}$
8.04	6.59×10^{-5}	$<6.25\times10^{-5}$
8.72	8.30×10^{-5}	$<6.25\times10^{-5}$
9.92	3.62×10^{-4}	$<6.25\times10^{-5}$
10.97	7.92×10^{-4}	$<6.25\times10^{-5}$

(a) < indicates the lower detection limit concentration.

4.2) Titration and Electrical Double Layer Calculations

Surface charge and surface reaction pK-values were calculated from titration experiments. All titration data and calculations are listed in Appendix III. The surface charge profiles were determined for oxide suspensions in 1.0, 0.1, 0.01, and 0.001 N NaCl solutions as a function of pH. All titration experiments for Quso G30 silica, Meller 180 and 182 alumina, and Baikowski mullite were made on soxhleted powders, unless specifically mentioned. Monosized silica and uniform zirconia were cleaned using the dilute, centrifuge, and decant method.

4.2.1) Silica

In the case of Quso G30, the p.z.c. is 4.25 and the corresponding surface charge profile shown in Figure 4.7. The σ_o curves have a unique intersection at $\sigma=0$, however, for unsoxhleted powder, the intersection occurs at $R\sigma$ = 4.74 uC/cm^2, requiring a $\Delta\sigma$-shift of the same amount to cause the intersection to occur at $\sigma = 0$. This $\Delta\sigma$ shift may be due to the dissolution of soluble surface impurities as the powder is placed in solution. Since Quso G30 is prepared from soluble Na-silicate solution, Na is the likely predominant impurity. Soluble Na is apparently removed upon soxhletion, thereby removing the cause of the surface charge shift, $\Delta\sigma$.

The second ionization constant for Quso G30, pK_{a2} is 6.6, determined by plotting pQ vs α and by extrapolating to the conditions of zero charge and infinite dilution; see

Figure 4.8a. The complexation constant for sodium, pK^*_{Na}, is 5.4, determined by plotting pQ* vs α^*_{ion} and by extrapolating to the conditions of zero charge and log[NaCl] = 0; as seen in Figure 4.8b. The first ionization and complexation constants for silica cannot be determined, in general, since the pH-conditions where the surface species transitions occur are pH = 1.90 and 3.10 for the pK_{a1} and pK^*_{Cl} (since p.z.c. = $(pK_1+pK_2)/2$). Thus, the experimental pH-values required to obtain these data are too low to be easily experimentally determined.

The surface charge versus pH profile for monosized silica is shown in Figure 4.9 yielding a p.z.c.-value of 3.20. Data for the lowest electrolyte concentration are not plotted due to poor experimental correlation with the results for higer concentrations. This discrepency may be due to residual alcohol from the initial precipitation reagents (REF Jubb-82a). The wash proceedure yielded sample supernatants that had the ionic conductivity of pure DI water, implying that no residual reagent ions were present. However, solution conductivity is not greatly affected by alcohol species, therefore residual alcohol could be present. Iler-79a states that alcohol can specifically adsorb onto the silica surface under conditions of low electrolyte concentration and effectively block surface sites from reacting with solution H^+-ions. This potential complication would affect the accuracy of Γ_{H+} used in subsequent calculations.

The data in Figure 4.9 were calculated using the method of Huang-71a, in which titrations of suspension and supernatant are compared. This method removes the effects of backround impurities and oxide solubility since these sources of error are present in both the suspension and supernatant. The correction technique does not remove either the effects of dynamic dissolution that may occur as the titration progresses or those of residual alcohol.

The surface charge for the precipitated, monosized silica is much higher than that for Quso G30. Possible explanations for the very high measured σ_o-values in the former system are surface porosity and surface gellation, suggested by the four-fold increase in the surface area upon outgassing at successively higher temperatures; see Table 4.1. Since the surface area increases with outgassing temperature, implying that bound or trapped water is present in small surface pores, it is possible that undetected micropores exist and lead to significantly higher p.d.i. adsorption than would otherwise be expected. If a surface gel-layer is present, coions adsorb in this layer neutralizing the charge developed from p.d.i.. This reduces the electrostatic repulsion that p.d.i. experience, allowing more p.d.i. to adsorb at the surface. Thus, higher adsorption densities and surface charges are calculated, that do not accurately describe the surface charge conditions.

The second ionization constant, pK_{a2}, for monosized silica is 4.9, determined from the plot of pQ vs α^*, as shown in Figure 4.10a. The corresponding sodium complexation constant, pK^*_{Na}, is 4.25, determined from the plot of pQ^* vs α^*_{Na}, as shown in Figure 4.10b. A comparison of the e.d.l. properties for the silicas in this study to those of other works is shown in Table 4.3. The differences in the properties of these materials are probably due to the variety of different preparation techniques that lead to different surface habits, i.e. site density, surface structure, and relative reactivity. Differences in reactivity change the relative amounts of sites ionized and complexed per unit area, and generate different surface charge profiles as a function of pH and electrolyte concentration. The extrapolated pK-values are then also shifted. Additionally, if the calculated σ_o-values are artificially high due to adsorption in a gel-layer, then the experimental pK-values will be incorrect, unless details of the gel are evaluated.

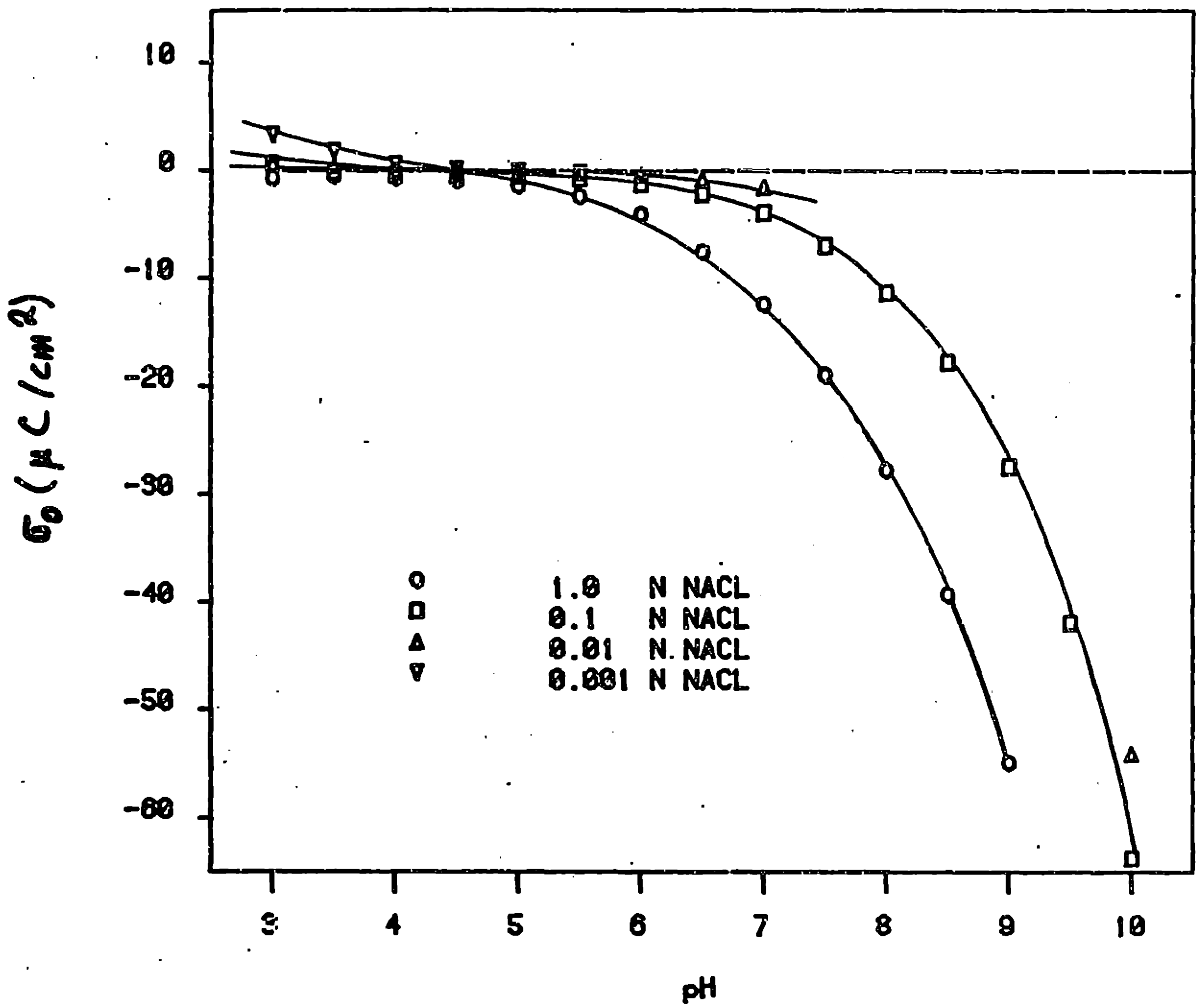

Figure 4.7 Surface charge, σ_o, versus pH for Quso G30.

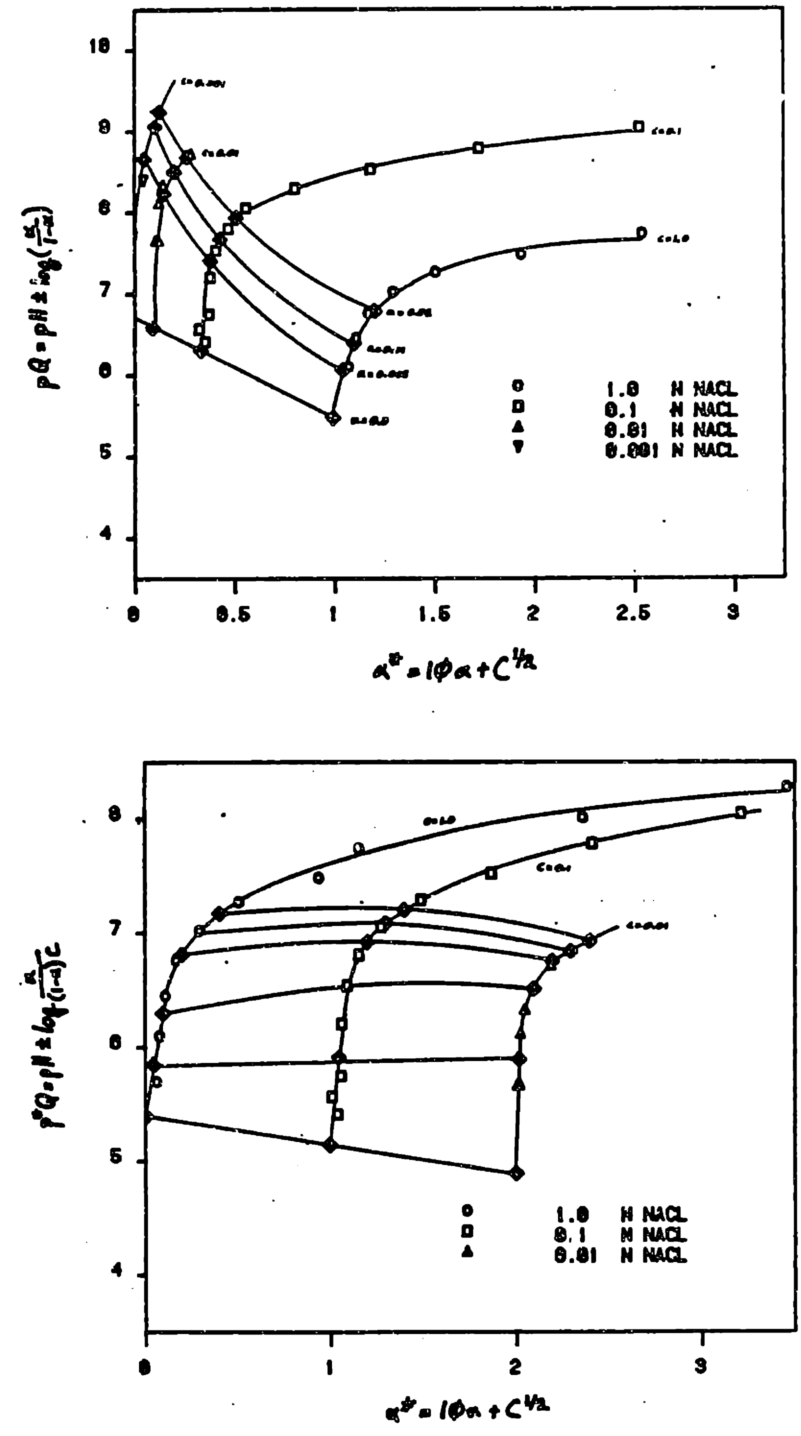

Figure 4.8 Double extrapolation plots for Quso G30.

a) yielding the ionization constant, pK_{a2}.

b) yielding the complexing constant, pK^{*}_{Na}.

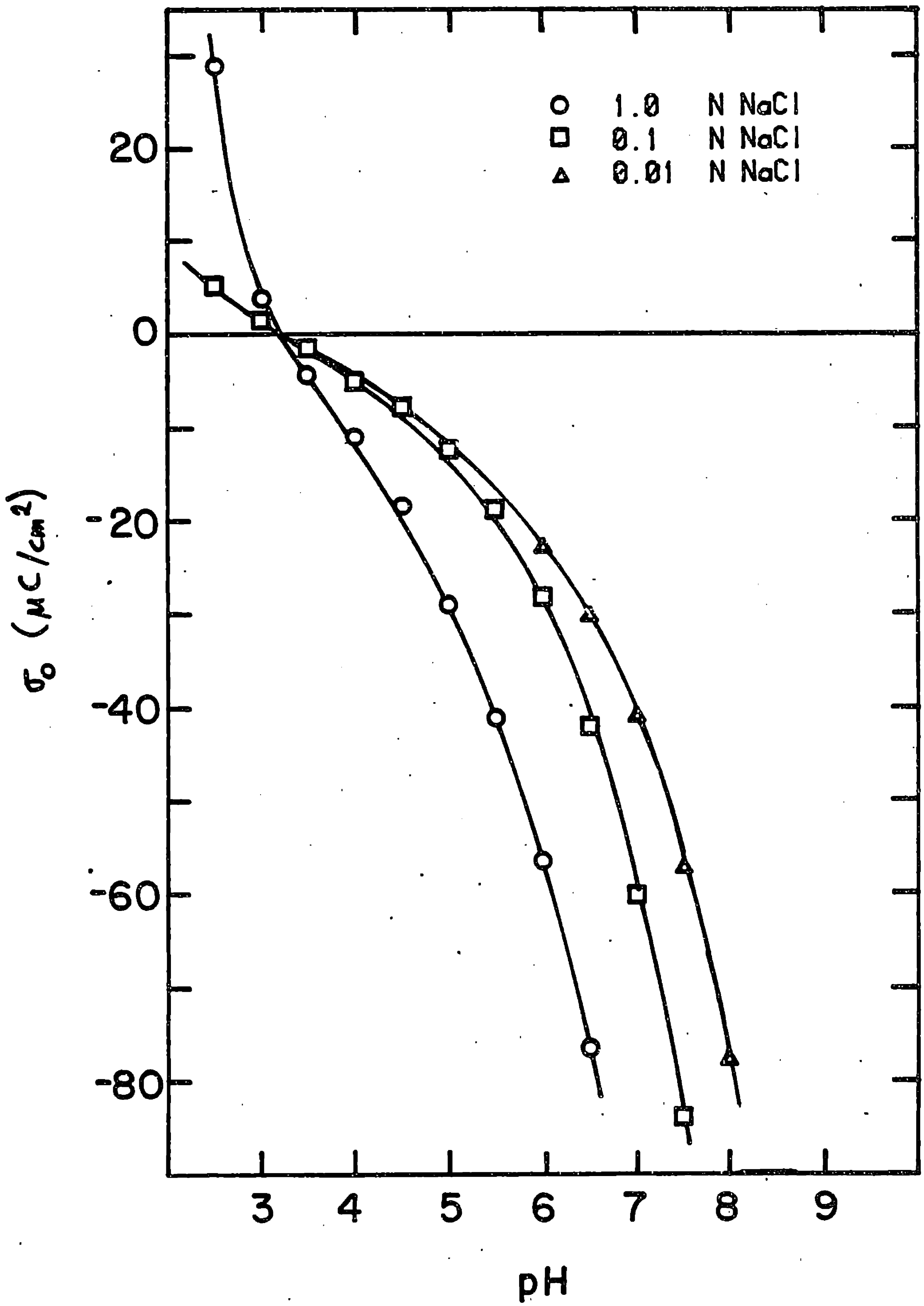

Figure 4.9 Surface charge versus pH for monosized silica.

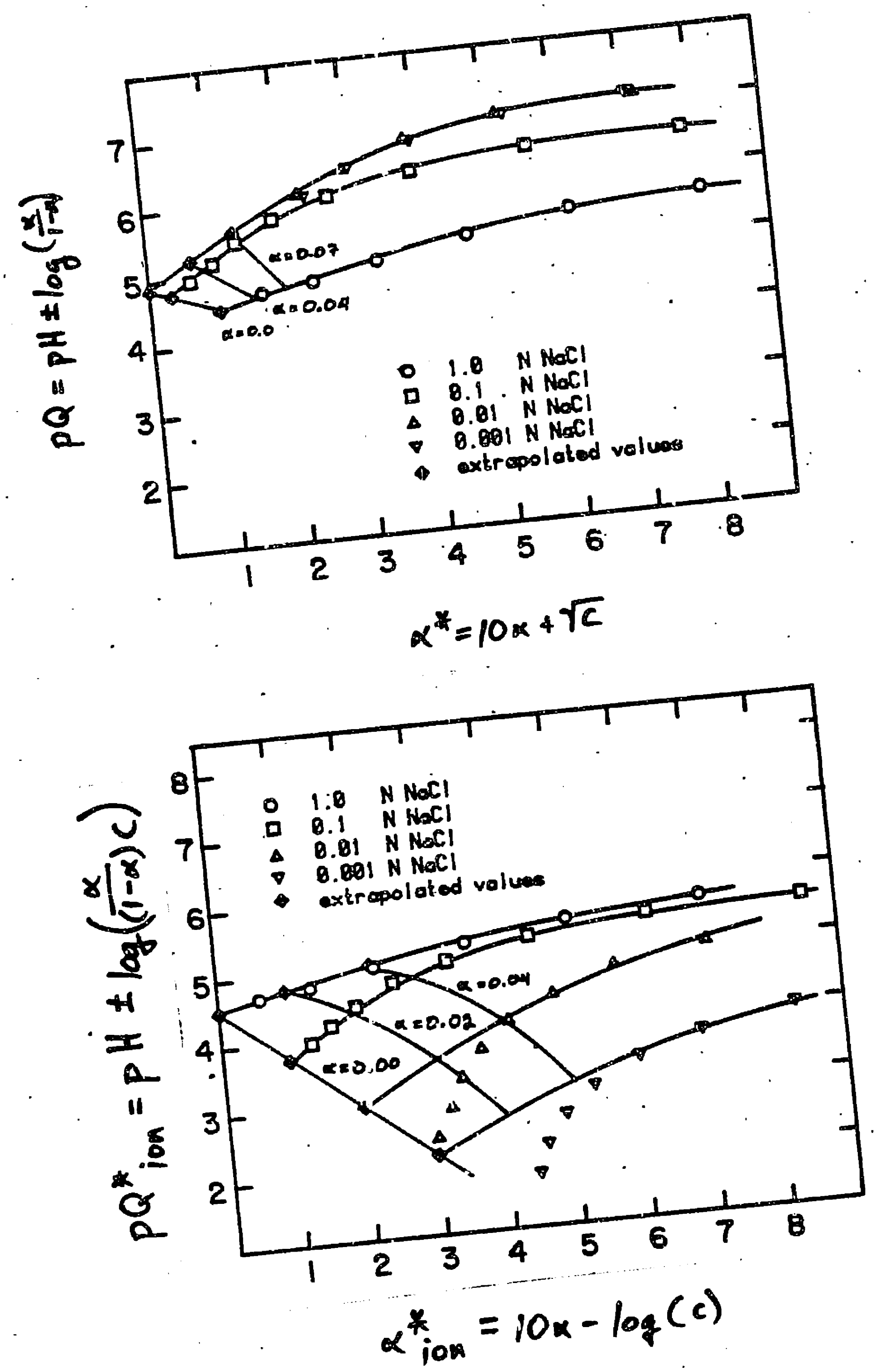

Figure 4.10 Double extrapolation plots for monosized silica.

a) yielding the ionization constant, pK_{a2}.

b) yielding the complexation constant, pK^*_{Na}.

Table 4.3

Silica Surface Properties

Material	Reference	Salt	pK_{a2}	$pK^*_{cat.}$	p.z.c.
Quso G30	this study	NaCl	6.6	5.4	4.25
monosized	this study	NaCl	4.9	4.5	3.2
SiO_2	Huang-77a	NaCl	6.7	-	2.0
SiO_2	Schindler-68a	NaCl	5.8	-	2.0
Cab-O-Sil	James-82a	KCl	7.2	6.7	3.0

4.2.2) Alumina

The surface charge profile for Meller 180, α-Al_2O_3, is shown in Figure 4.11; the p.z.c. is 8.75. The initial $R\sigma$ vs pH data for the corresponding unsoxhleted material yield a non-distinct intersection, implying surface or solution contamination. After soxhletion, the $R\sigma$-curves all intersected at a unique pH, implying good data. The ionization constants for Meller 180, determined from the plots of pQ vs $\alpha*$ in Figure 4.12 are pK_{a1} = 5.0 and pK_{a2} = 10.7. Corresponding complexation constants are $pK*_{Cl}$ = 7.1 and $pK*_{Na}$ = 10.2; see Figure 4.13.

The surface charge profile for Meller 182, the transition-phase, $\alpha\gamma$-Al_2O_3, is given in Figure 4.14. The curves are seen to be asymmetric about $R\sigma$ = 0, since the intersection does not occur at $R\sigma$ = 0. Rather, the intersection occurs between pH-values 8.0 and 9.0 while the point where $R\sigma$ = 0 occurs at pH = 7.0. Using this $R\sigma$ data, the calculated ionization and complexation constants are; pK_{a1} = 4.2, $pK*_{Cl}$ = 6.34, and $pK*_{Na}$ = 7.0 as determined in Figures 4.15 and 16. pK_{a2} is estimated to be 9.8 from extrapolation of the data to $\alpha*$=0. Full DJL extrapolation could not be made for pK_{a2} due to poor data separation and linearity. When the surface charge curves are shifted by $\Delta\sigma$ = -11.24, the intersection occurs at $R\sigma$ = 0, with a p.z.c. of 8.2. When the pQ values are recalculated using this new p.z.c., no distinct ionization or complexation constants could be determined in the double extrapolation plots. This implies that the unshifted $R\sigma$ curve represents the actual surface charge for the Meller 182.

Although the data for Meller 182 do not exhibit a distinct intersection and yields poor pK-curves, in all of our other studies of soxhleted materials the $R\sigma$ curves did not require $\Delta\sigma$ shifts, implying that surface impurities were removed. Other possible causes for the $\Delta\sigma$ shift in the data are surface dissolution and reprecipitation that occur during the titration, and specific adsorption of the electrolyte cation (REF Huang-81a). Surface dissolution and reprecipitation probably does not occur for the Meller 182 system as discussed in section 4.1. If specific adsorption of the cation occurs, surface charge curves shift such that the intersection occurs at negative $R\sigma$ (REF Huang-81a). In this case the unshifted σ curves represent the actual charge profile of the material as a function of pH and electrolyte concentration.

A comparison of the e.d.l. properties for the two aluminas in this study to those of other works are shown in Table 4.4. The difference in the properties of these materials are again caused by different preparation techniques that lead to different crystal habits. The differences in reactivity changes the relative amounts of sites ionized and complexed yielding different surface charges as a function of pH and electrolyte concentration, shifting calculated pK-values. If specific adsorption occurs on the $\alpha\gamma$-Al_2O_3 surface, then shifts in the determined values make direct comparison of the data with those in the literature questionable.

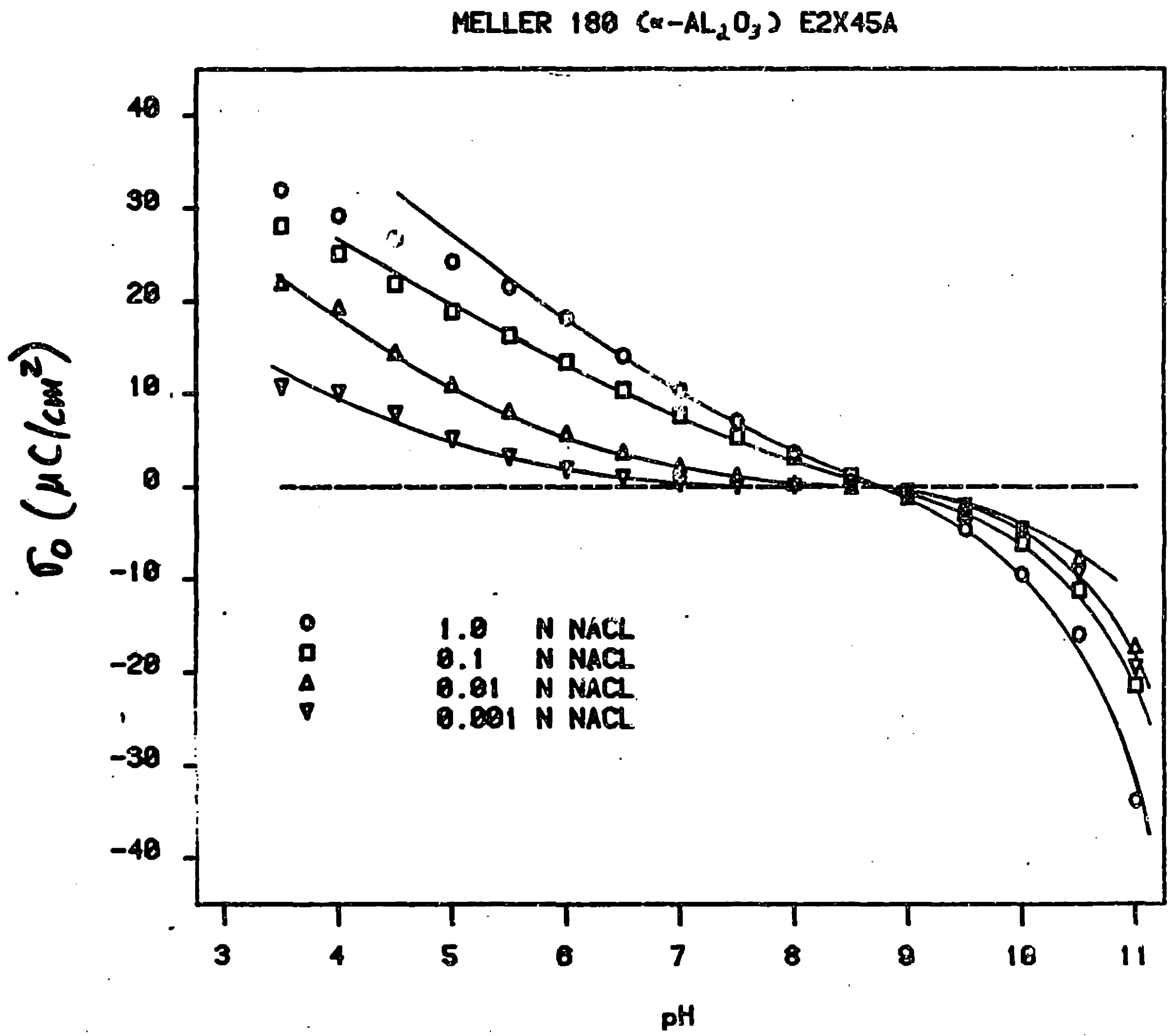

Figure 4.11 Surface charge versus pH for Meller 180 α-Al_2O_3.

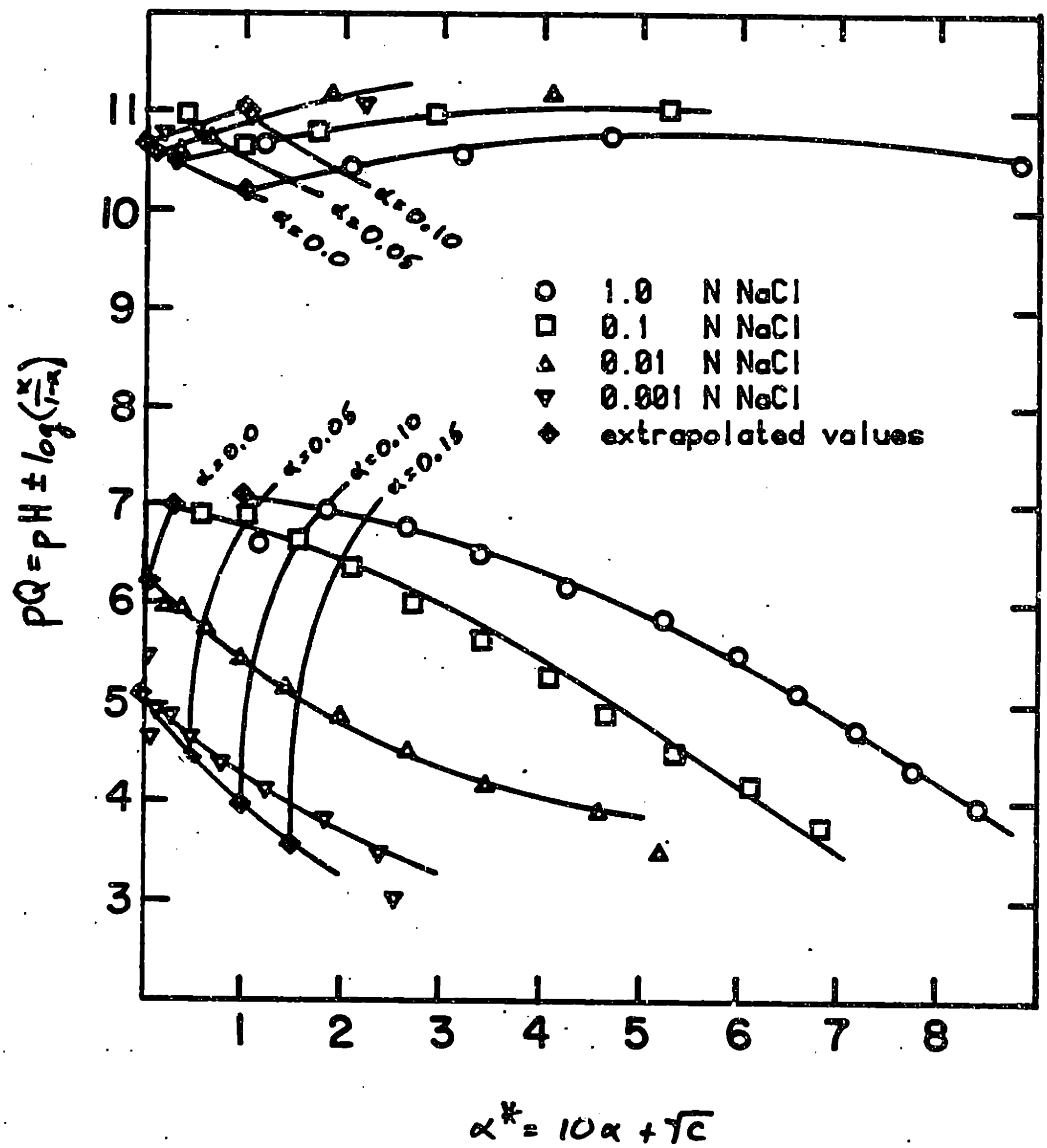

Figure 4.12 Double extrapolation plots for Meller 180 yielding the ionization constants, $pK_{a1,a2}$.

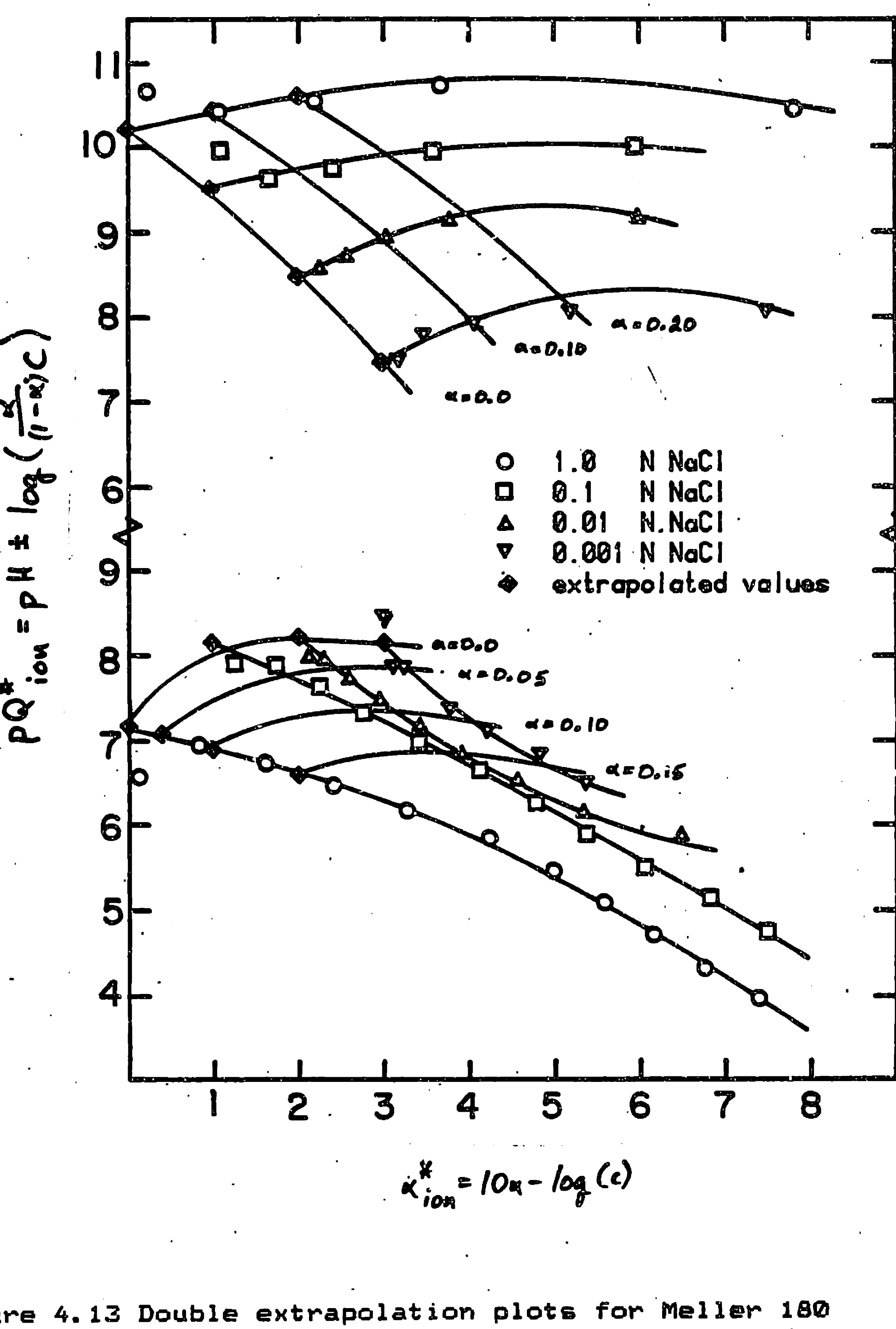

Figure 4.13 Double extrapolation plots for Meller 180 yielding the complexation constants, $pK^*_{Cl,Na}$.

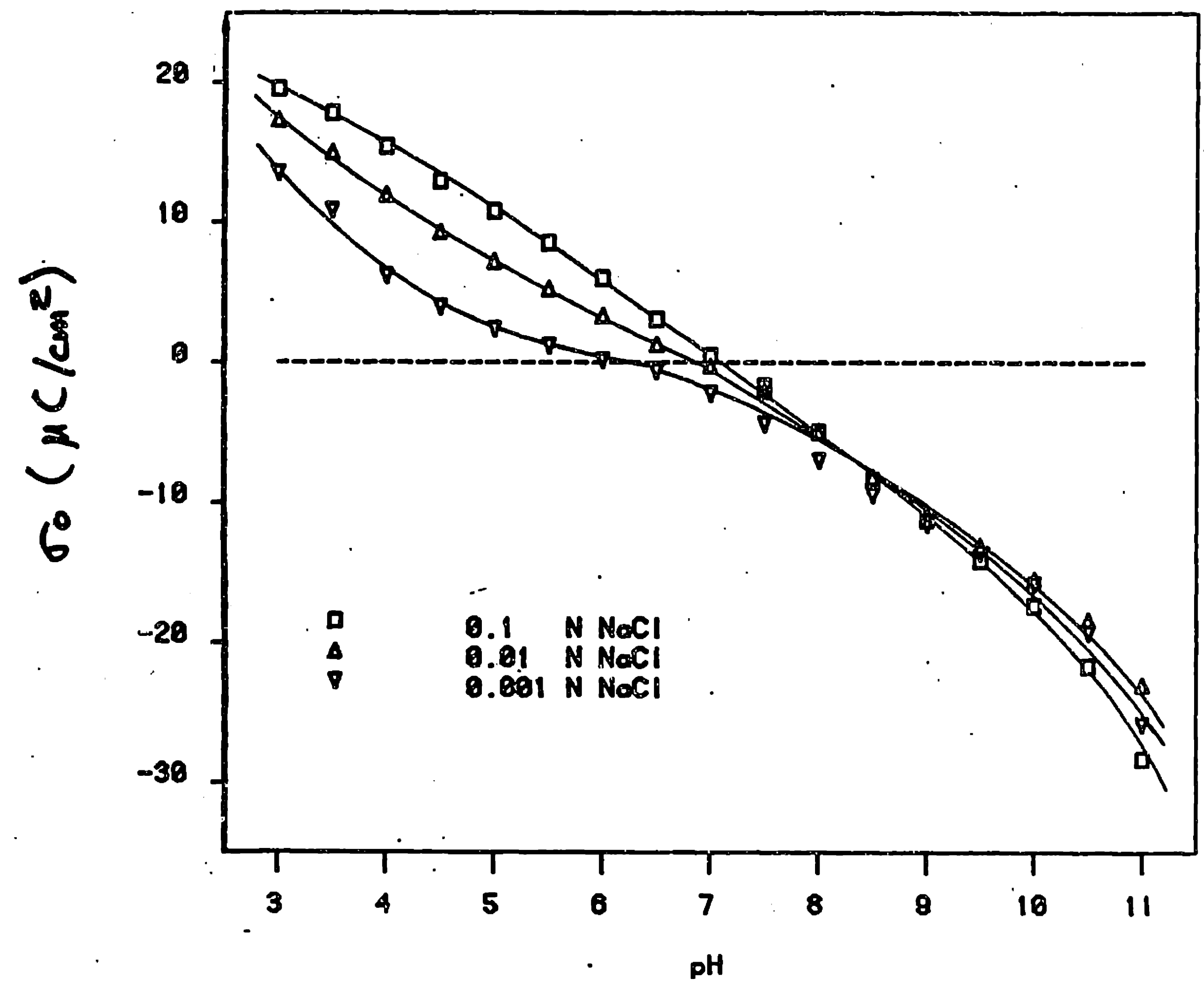

Figure 4.14 Surface charge profile versus pH for Meller 182, $\alpha\gamma$-Al_2O_3.

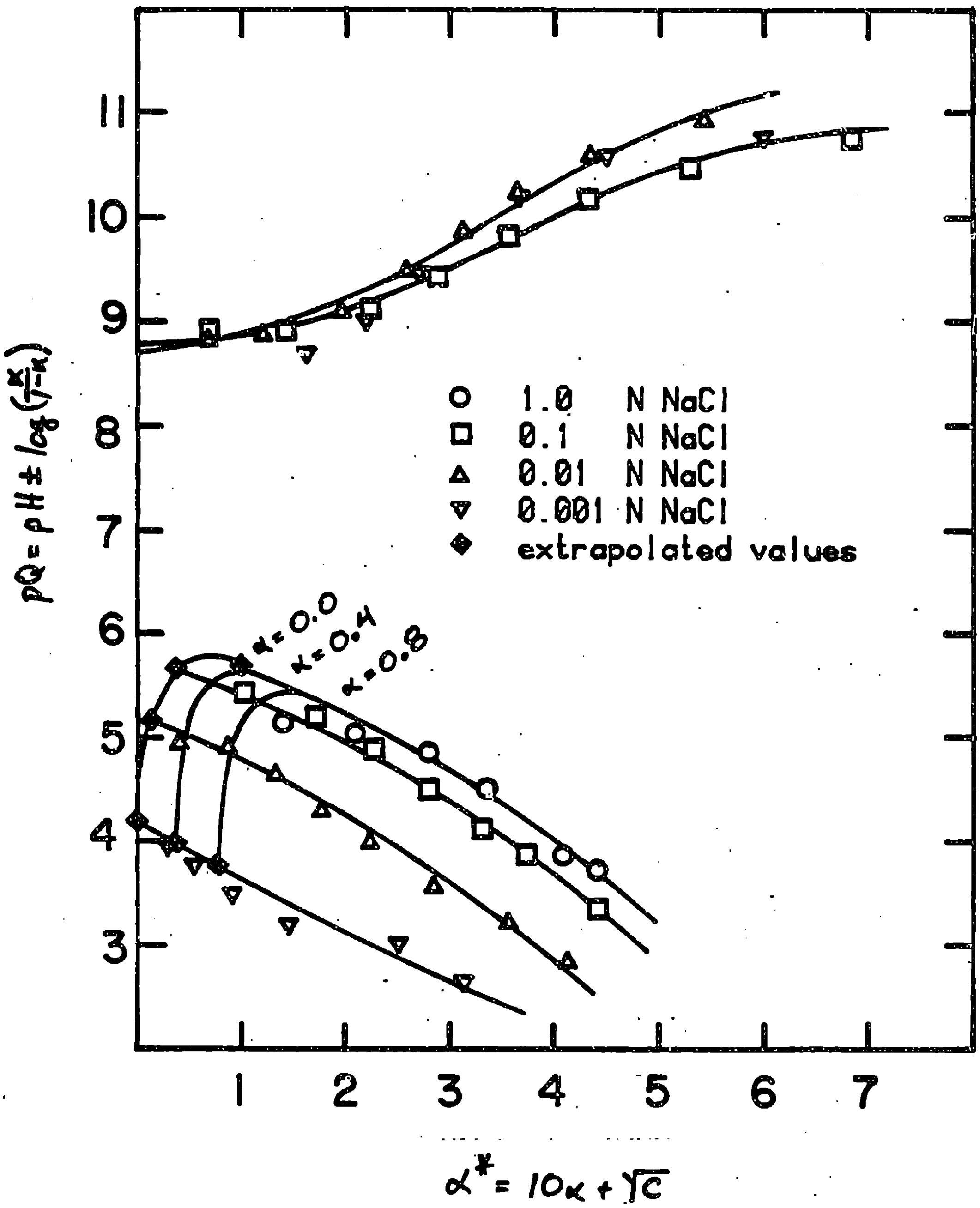

Figure 4.15 Double extrapolation plots for Meller 182 yielding the ionization constants, $pK_{a1,a2}$.

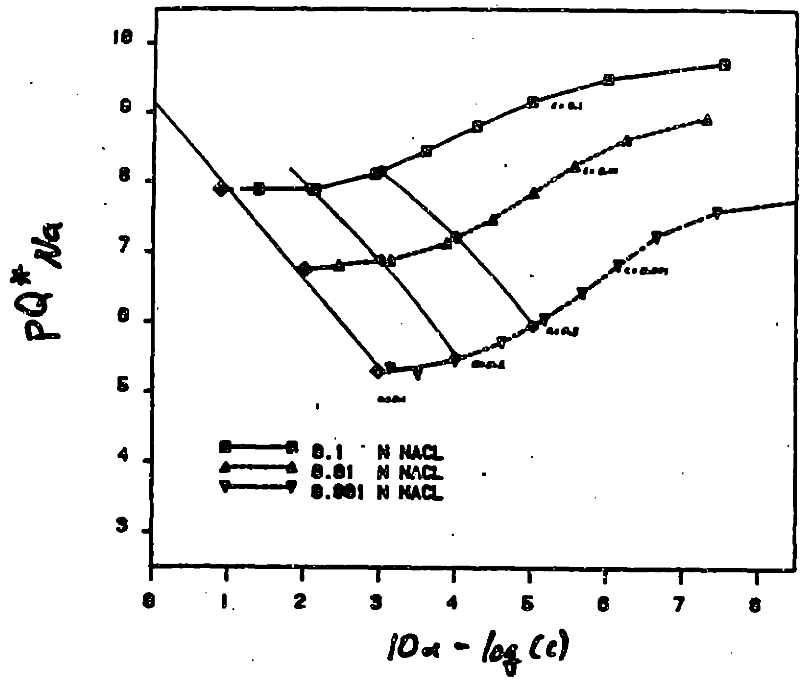

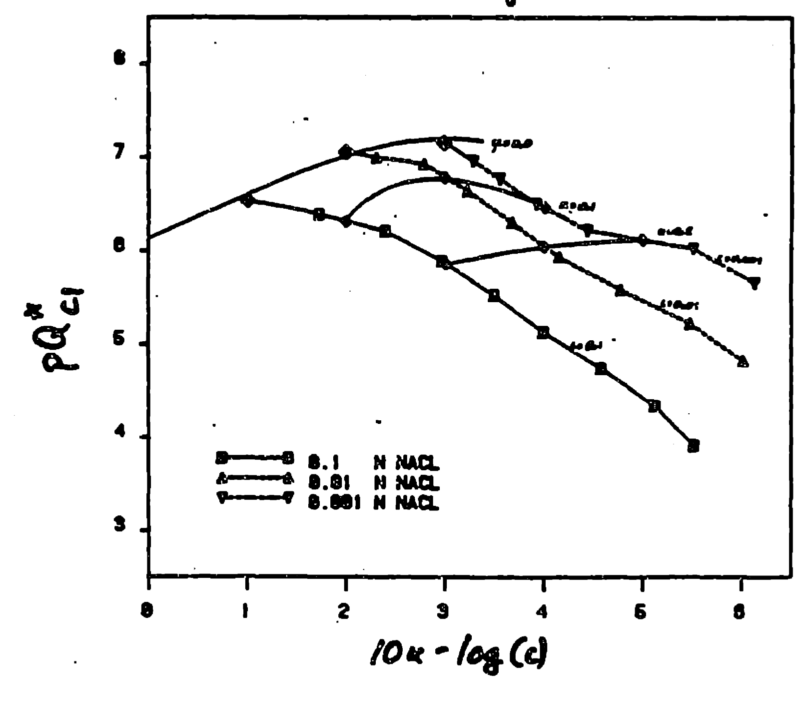

Figure 4.16 Double extrapolation plots for Meller 182 yielding the complexation constants, $pK^{\#}_{Cl,Na}$.

Table 4.4

Alumina Surface Properties

Material	Reference	pK_{a1}	pK_{a2}	pK^*_{Cl}	pK^*_{Na}	p.z.c.
α-Al_2O_3 (in NaCl)						
Meller	this study	5.0	10.7	7.1	10.2	8.75
-	Yorpps-64a	8.5	9.7	-	-	9.10
γ-Al_2O_3 (in NaCl)						
Meller	this study	4.2	9.8	6.34	9.2	7.0
Cabot	James-82a	5.2	11.8	7.9	9.2	8.5
Cabot	Huang-73a	7.7	9.3	-	-	8.5
Cabot	Davis-78a	5.7	11.5	-	-	8.6

4.2.3) Mullite

The surface charge profile for Baikowski's mullite, $3Al_2O_3 \cdot 2SiO_2$, is shown in Figure 4.17 with a p.z.c. of 8.50. This value is close to that determined by Smolik-66a for mullite; p.z.c. = 8.1. No shift in the $R\sigma$ curves for our material was required, $\Delta\sigma = 0$, implying that surface impurity were not present after soxhleting and that $\sigma_o = R\sigma$. The ionization and complexation constants for mullite can not be determined since the DJL model double extrapolation technique is invalid for mixed oxide surfaces. However, a first estimate for these constants can be made using the values for the pure alumina and silica surfaces calculated earlier. Caution must be exercised in interpreting these values because the interaction effects of oppositely charged alumina and silica sites cannot be suitably treated for in the calculations. If DJL double extrapolation plots are made for mullite, "effective" reaction constants can be determined, however these calculations are phenomenological rather than physically justified for the mixed oxide.

The σ_o-curves for our mullite appear compressed towards $\sigma_o = 0$ in the pH region where the surface is positive, i.e. for pH-values below the p.z.c., and expanded in the negative surface charge region. For pH-values below 8.5, the p.z.c. of mullite, surface silicate species are negatively charged, since the pH is greater than the p.z.c. for SiO_2 (see Figure 4.7). On the other hand, surface Al sites are positively charged at pH-values less than 9.0, the p.z.c. of Al_2O_3 (see Figure 4.11). Thus, the sum of the positive Al and negative

Si sites reduces the net σ_o-values owing to neutralization by the oppositely charged species. In the same manner, at pH-values above the p.z.c. of mullite, the silicate and aluminate sites are both negaively charged, causing the charge profile to be more negative than that for either single oxide component.

The experimentally determined p.z.c, 8.5, is very close to that of alumina (compare Figures 4.11 and 4.17), implying that Al_2O_3 sites dominate the aqueous surface chemistry of mullite. This apparent dominance by alumina-type sites has been found by other researchers (REF Iler-76a, Katsanis-83a, Pyman-79a, Smolik-66a, and Tschapek-74a). One proposed reason for this effect is that, since the structure of the $Al(OH)_4^-$ tetrahedra resembles the $Si(OH)_4$ complex, the Al-ion can be inserted or exchanged into a SiO_2 surface, producing an aluminosilicate site with a fixed negative charge (REF Iler-76a). Highlighting this postulate, Iler-76a found that only 0.66 wt% of Al_2O_3 was required to significantly change the surface properties of silica. This corresponds to approximately one aluminosilicate site per 20 silanol groups on the surface. If evenly distributed, the sites are 15 A apart, thus the effect of alumina is very large as compared to the Si site.

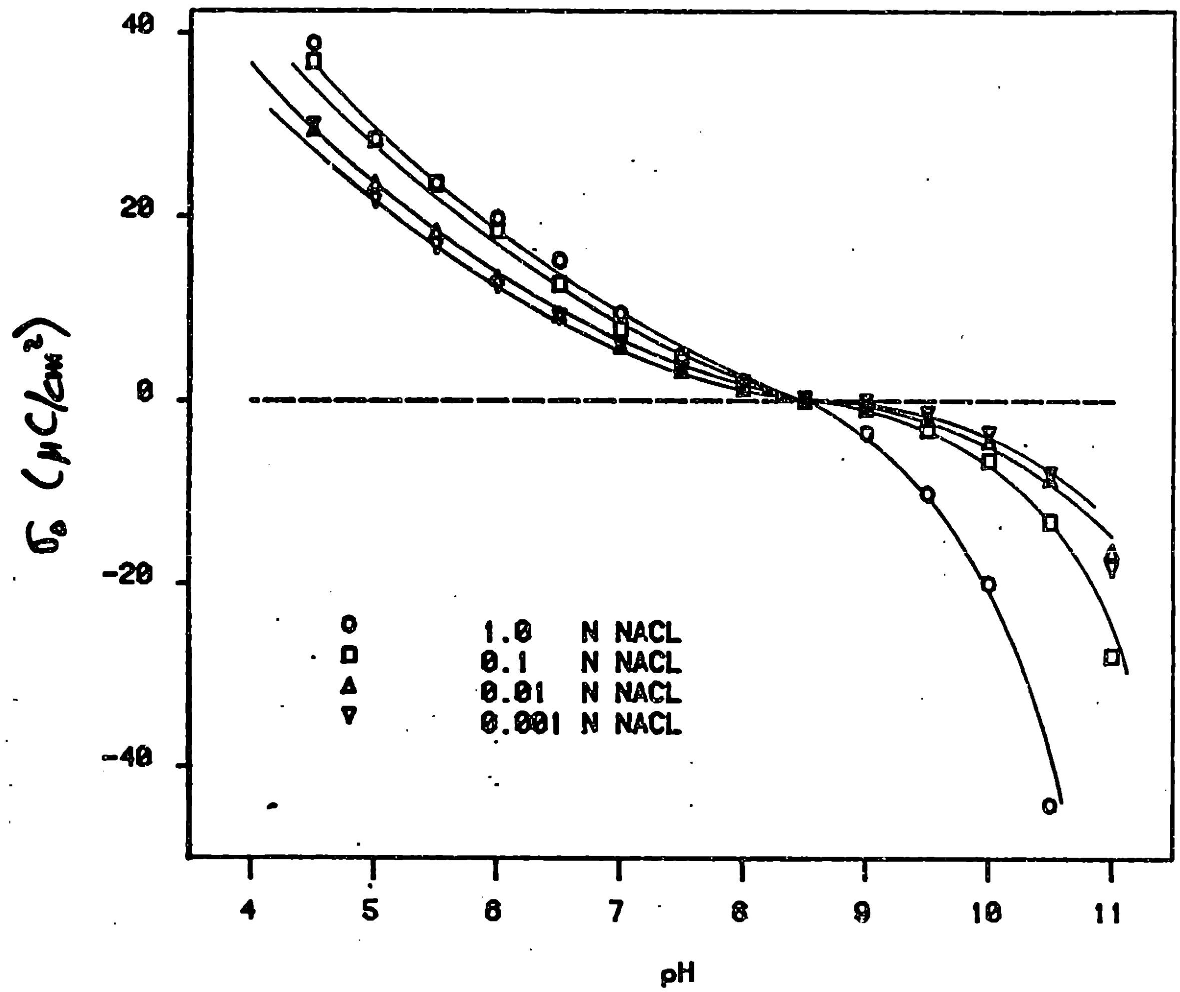

Figure 4.17 Surface charge versus pH for Baikowski mullite, $3Al_2O_3.2SiO_2$.

4.2.4) Zirconia

The surface charge profile for m-ZrO_2 shown in Figure 4.6 is given in Figure 4.18. The curves do not have an obvious intersection nor do they exhibit symmetry about an apparent p.z.c. Several explanations for these atypical results occur. First, if unknown and nonquantified surface or solution impurities result from the synthesis (REF Bleier-82a) and react with titrant, then incorrect adsorption curves would result. Since this powder was washed using the repeated, dilute-centrifuge-decant method, residual impurities could be retained, though Bleier and Cannon (REF Bleier-82a) feel that this is not likely. Second, the TEM figures of this powder (Figure 4.6) show that the "particles" consist of very small particles, somewhat as a particluate gel would. If the inner regions of the particles are accesible to solution species, then a finite time would be required for pore surface reaction, thus lengthening the normal equilibrium time. This kinetic effect on the surface reactions would not be properly taken into account in data reduction, leading to incorrect interpretation of the titration curves yielding incorrect σ_o curves. A study of the effect of titration rate on the $R\sigma$ values is required to describe the surface reaction kinetics in this system. Preliminary data taken by the author (REF Bleier-83c) suggest that this effect is important for this ZrO_2.

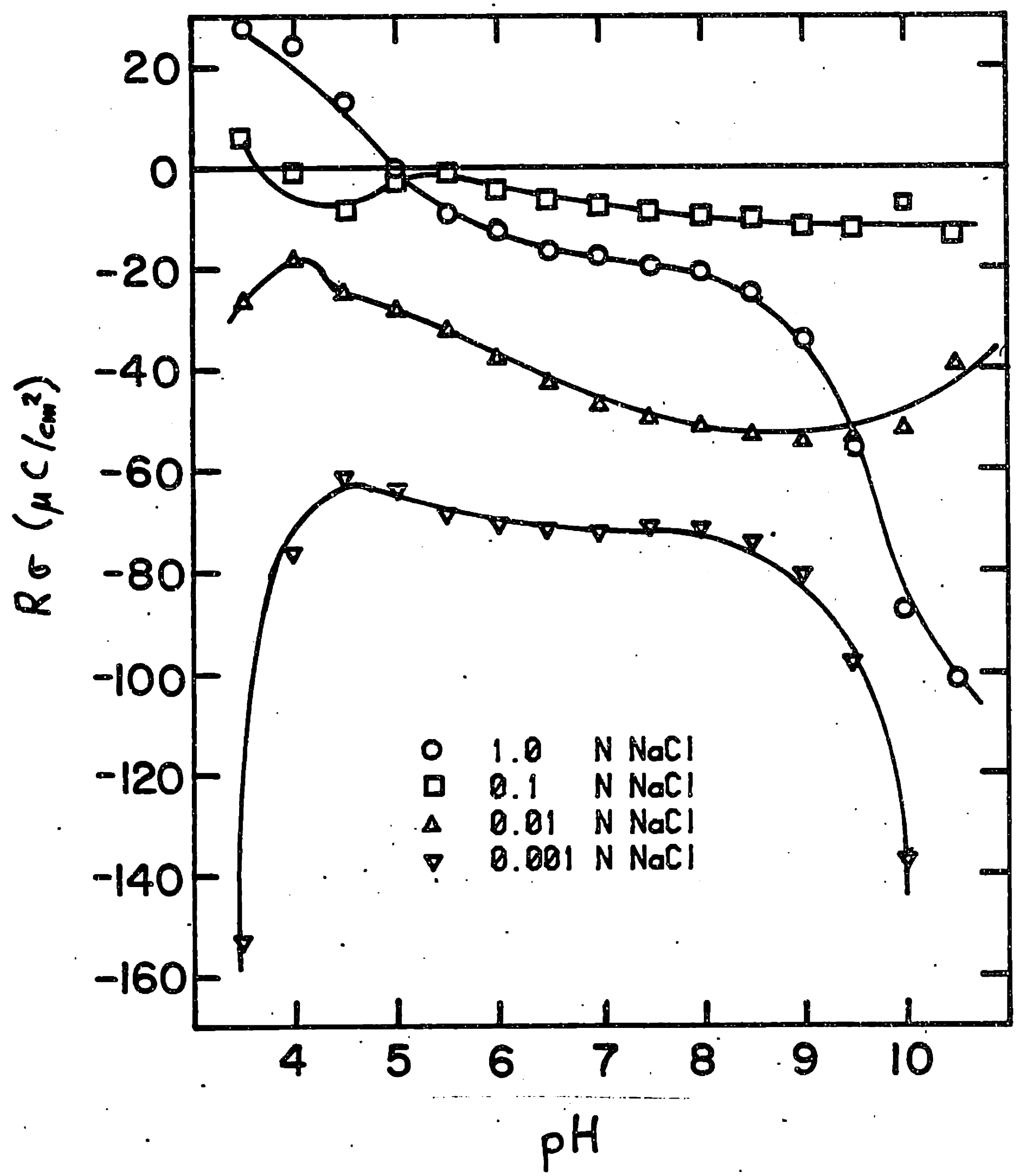

Figure 4.18 Surface charge versus pH for uniform ZrO_2.

4.3) Electrophoresis Experiments

The electrophoretic mobility was measured for Meller 180, α-Al_2O_3, for 0.1, 0.01, and 0.001 N NaCl suspensions in air for pH-values between 4 and 11. The ζ-potential was calculated and plotted in Figure 4.22 as a comparison to the theoretically calculated OHP potential, Ψ_2. The lack of good experimental fit to the theoretical curves may arise from CO_2 induced pH-shifts and species adsorption at the oxide surface. Further studies on the ζ-potential in systems where CO_2 is excluded are required for further verification of the theoretically calculated potential distribution in the e.d.l.

4.4) Theoretical Electrical Double Layer Calculations

This section deals with theoretical estimates of the chemical species and distributions of charge and potential in the e.d.l. determined using SITECAL, listed in appendix II, a modification of Westall's computer program MICROQL (Ref Westall-79a,b). As discussed earlier in section 2.3, this computer program solves a given set of reaction equations for the e.d.l. to calculate the equilibrium distribution of species, charge, and potential in the e.d.l. The tableau describing the surface reactions, reaction constants, and known concentrations of species is entered into the program and the e.d.l. properties are determined.

Ionization and complexation constants for Quso G30 and Meller 180 were considered representative of SiO_2 and Al_2O_3

surfaces and were choosen for a theoretical study since the experimental data appeared to be the best of the single oxides studied (Figures 4.7, 4.8, 4.11, 4.12, and 4.13). Values of the inner and outer layer capacitances were those of James-82a. The reaction tableau includes the electrolyte ions as both system components and chemical species in order to calculate the concentration of adsorbed species and remove them from the bulk solution. In Westall's original program, the bulk solution is considered to be an infinite source of ions, a invalid assumption for low electrolyte concentrations.

The reaction tableau for SiO_2 is given in Table 4.5. The first ionization and complexation constants are estimated from the experimentally determined second ionization and complexation reactions since p.z.c. = $(pK_1+pK_2)/2$. The predicted charge distributions for the surface, σ_0, IHP, σ_1, and OHP, σ_2, as a function of pH for 1.0 to 0.001 N NaCl are plotted in Figures 4.19. The experimentally determined σ_o-values are compared to the theoretical values in Figure 4.19a. The theoretical and experimentally determined p.z.c.-values are both found to be 4.25. The theoretical σ_o-values predict the experimentally determined values for low electrolyte concentrations and pH-values near the p.z.c. The experimentally determined σ_o curves appear to increase in the negative direction much more sharply towards the p.z.c. than do the theoretical ones. The theoretical potential distributions of the electrical double layer are shown in Figure 4.20.

The reaction taleau for α-Al_2O_3 is given in Table 4.6. The theoretical charge distributions for the surface, IHP, and OHP as a function of pH for 1.0 to 0.001 N NaCl are plotted in Figures 4.21. The experimentally determined surface charges, σ_o, are compared to the theoretical values in Figure 4.21a. The theoretical and experimentally determined p.z.c.-values are both 8.75. The theoretical σ_o curves are shown to be only slightly lower than the experimentally determined data for pH-values below the p.z.c. The theoretical potential disribution of the e.d.l. is shown in Figure 4.22. The experimentally determined ζ-potential is compared to the theoretical Ψ_2 in Figure 4.22c. The theoretical-values lie within the range of the experimental data, however discrepencies are probably due to CO_2 adsorption phenomina occuring in the experimental system.

The theoretical surface charge curves, σ_0, for Al_2O_3 and SiO_2 at all electrolyte concentrations intersect at the p.z.c. and have positive values for the conditions of pH < p.z.c. and negative values for the conditions of pH > p.z.c. as do the corresponding experimental curves. The IHP and OHP charges, σ_1 and σ_2, are opposite in sign when compared to σ_0 for the same pH-values. This result occurs due to the electroneutrality constraint, $\sigma_0 + \sigma_1 + \sigma_2 = 0$. The potential distributions, Ψ_0, Ψ_1, and Ψ_2, decrease monotonically from the surface to the OHP since the surface potential is neutralized by the oppositely charged species in the e.d.l.

An attempt was made to calculate the e.d.l. charge and potential distribution for mullite using the tableau shown in Table 4.7. The ionization and complexation constants for the alumina and silica surface sites are those of Tables 4.6 and 4.7. The computer program was modified in our work to include a charge balance of alumina and silica sites. This calculation did not yield $R\sigma$ intersections, so the author doubts the correctness of his modifications to the computer program. Hence, the theoretical e.d.l. disributions will not be reported, though continued work on this point is in progress.

Table 4.6

The reaction tableau for Quso G30 silica.

	components							
species	SiOH	e^{-y_0}	e^{-y_1}	e^{-y_2}	Na^+	Cl^-	H^+	pK
H^+	0	0	0	0	0	0	+1	0
OH^-	0	0	0	0	0	0	−1	−14.0
SiOH	+1	0	0	0	0	0	0	0
$SiOH_2^+$	+1	+1	0	0	0	0	1	1.9
SiO^-	+1	−1	0	0	0	0	−1	− 6.6
$SiOH_2^+Cl^-$	+1	+1	−1	0	0	+1	+1	3.1
SiO^-Na^+	+1	−1	+1	0	1	0	−1	− 5.4
Na^+	0	0	0	0	+1	0	0	0
Cl^-	0	0	0	0	0	+1	0	0
TOT	0	0	0	0	C	C	0	
log free	−3	−1	−0.5	0	−pC	−pC	−pH	

site density = 5 sites nm^{-2}

surface area = 118.73 m^2 gm^{-1}

conc. of solids = 9.501 g l^{-1}

C_1 = 120 uF cm^{-2}

C_2 = 20 uF cm^{-2}

where, C is the concentration of electrolyte;
pC = −log[C].

site density from James-82a.

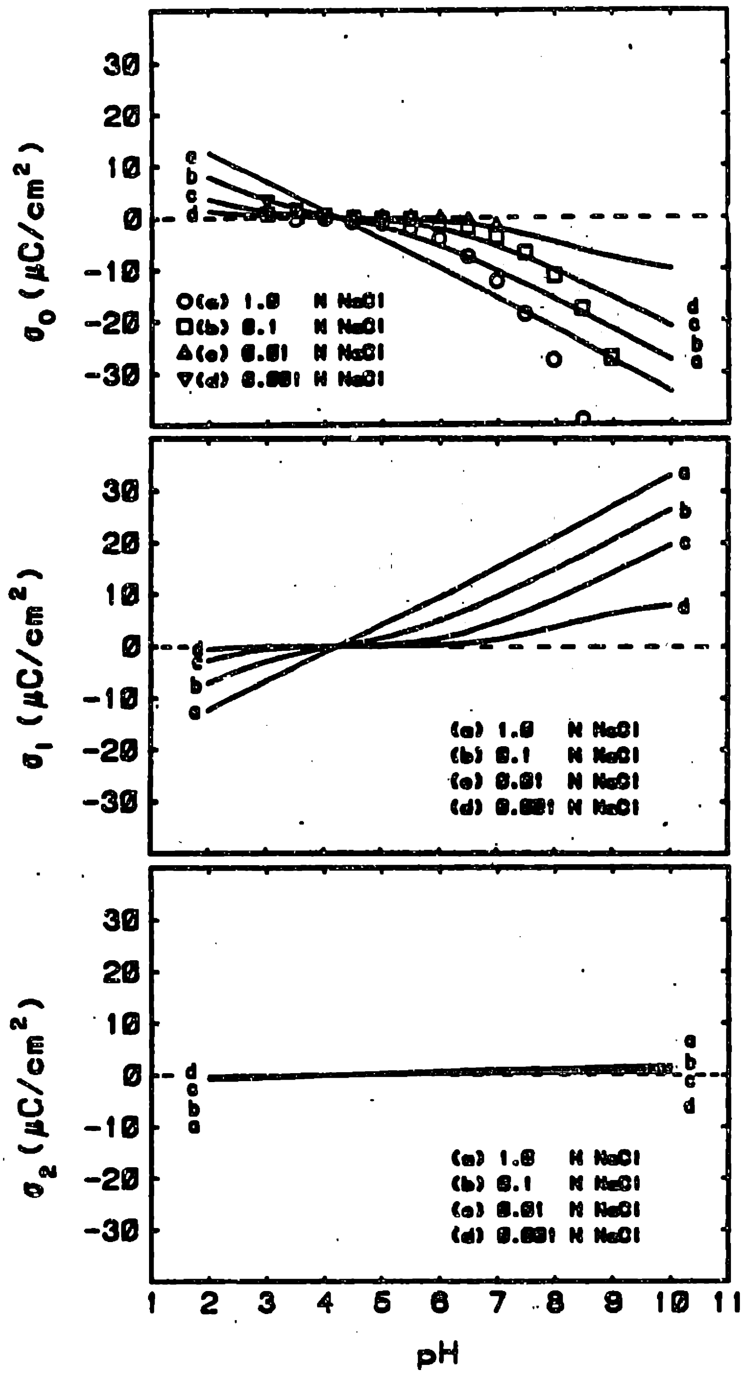

Figure 4.19 The theoretical charge distribution for Quso G30, amorph-SiO_2, at the surface, 0, IHP, 1, and OHP, 2.

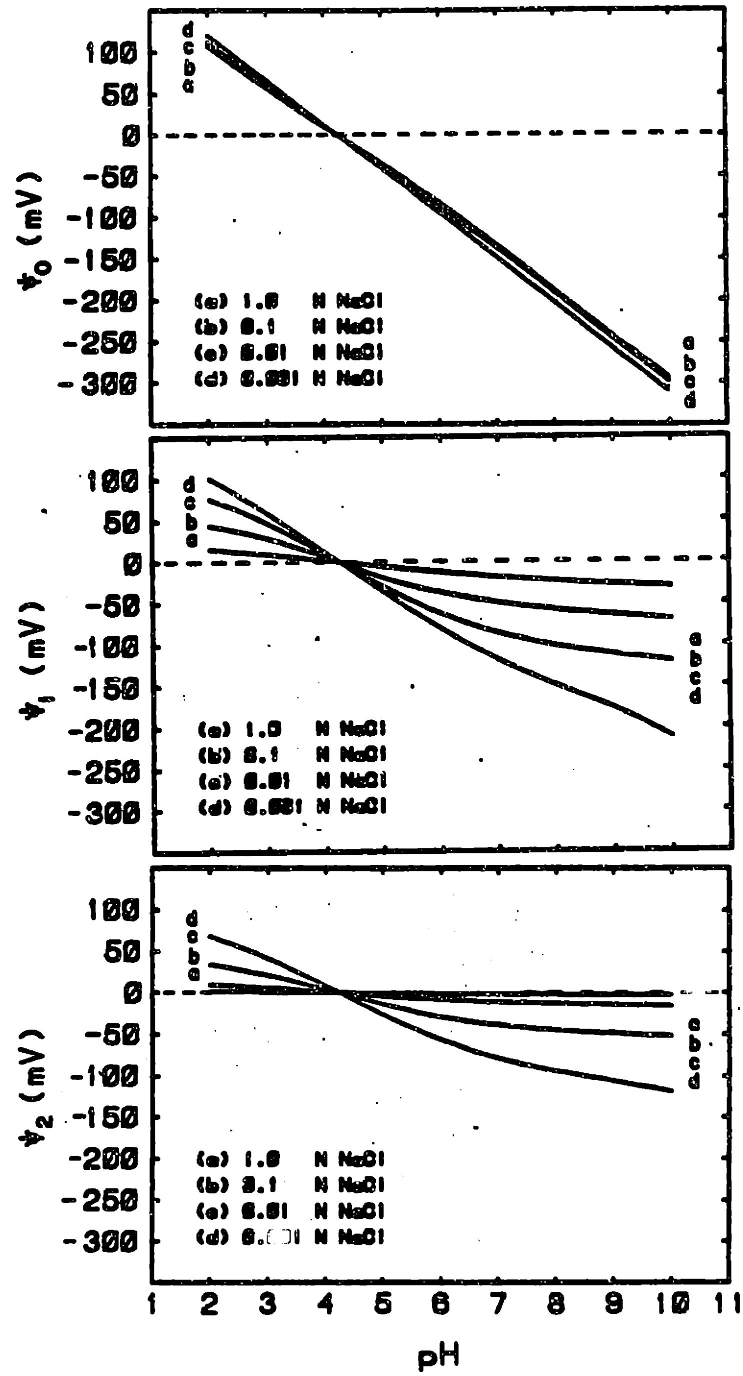

Figure 4.20 The theoretical potential distribution for Quso G30, amorph-SiO_2, at the surface, 0, IHP, 1, and OHP, 2.

Table 4.7

The reaction tableau for Meller 180 α-Al_2O_3.

components

species	AlOH	e^{-y_0}	e^{-y_1}	e^{-y_2}	Na^+	Cl^-	H^+	pK
H^+	0	0	0	0	0	0	+1	0
OH^-	0	0	0	0	0	0	−1	−14.0
AlOH	+1	0	0	0	0	0	0	0
$AlOH_2^+$	+1	+1	0	0	0	0	+1	5.0
AlO^-	+1	−1	0	0	0	0	−1	−10.7
$AlOH_2^+Cl^-$	+1	+1	−1	0	0	+1	+1	7.1
AlO^-Na^+	+1	−1	+1	0	+1	0	−1	−10.2
Na^+	0	0	0	0	+1	0	0	0
Cl^-	0	0	0	0	0	+1	0	0
TOT	0	0	0	0	C	C	0	
log free	−4	−1	−0.5	0	−pC	−pC	−pH	

site density = 2.7 sites nm^{-2}

surface area = 21.31 m^2 gm^{-1}

conc. of solids = 31.25 g l^{-1}

C_1 = 120 uF cm^{-2}

C_2 = 20 uF cm^{-2}

where, C is the concentration of electrolyte;
pC = −log[C].

site density from James-82a.

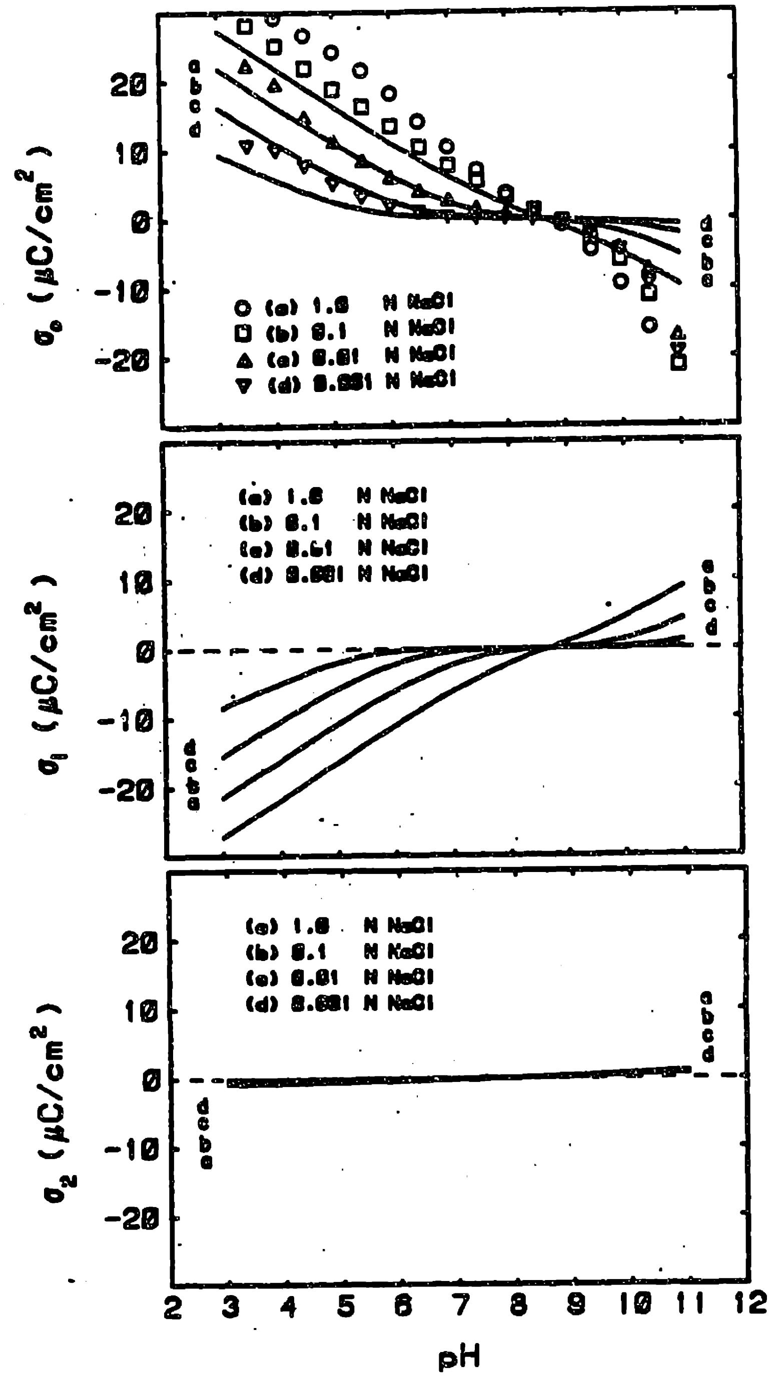

Figure 4.21 The theoretical charge distribution for Meller 180, α-Al_2O_3, at the surface, 0, IHP, 1, and OHP, 2.

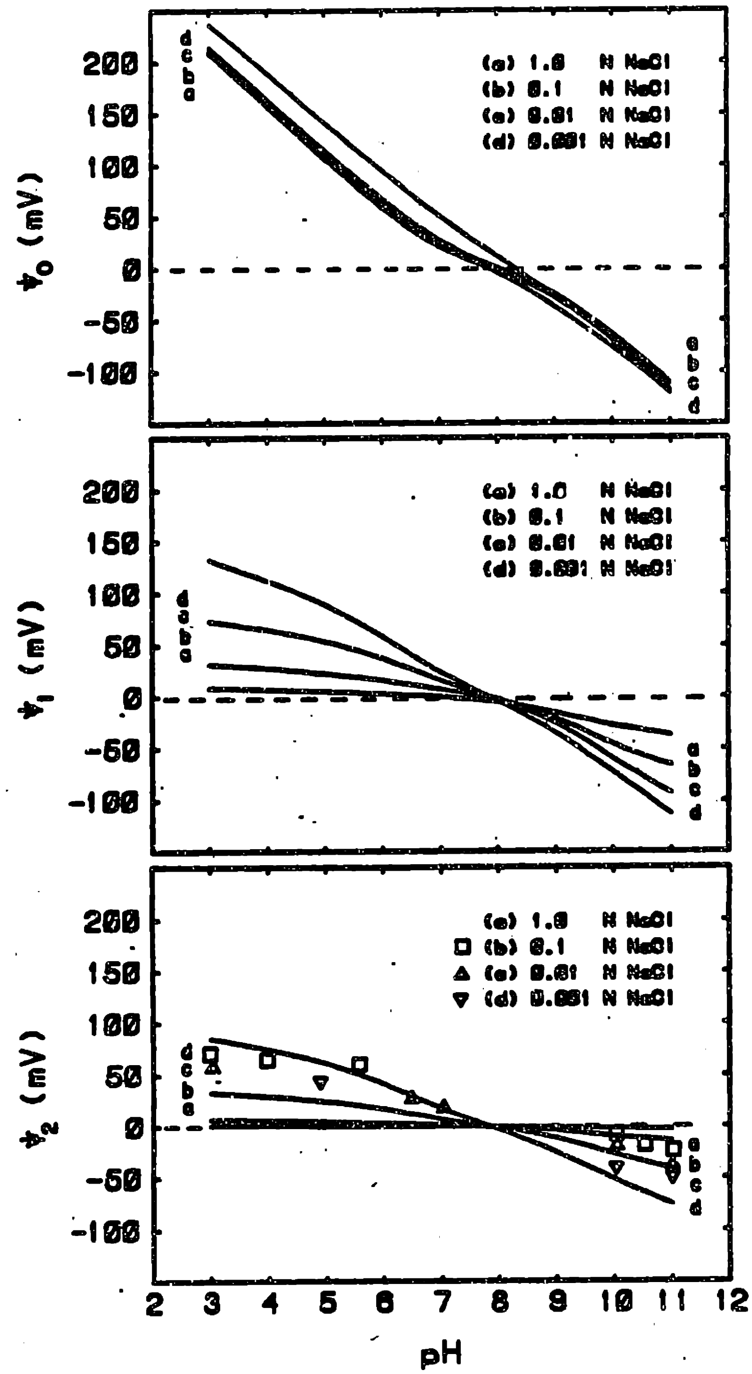

Figure 4.22 The theoretical potential distribution for Meller 180, α-Al_2O_3, at the surface, 0, IHP, 1, and OHP, 2.

Table 4.8

The reaction tableau for Baikowski mullite, $3Al_2O_3.2SiO_2$.

components

species	SiOH	AlOH	e^{-y_0}	e^{-y_1}	e^{-y_2}	Na^+	Cl^-	H^+	pK
H^+	0	0	0	0	0	0	0	+1	0
OH^-	0	0	0	0	0	0	0	−1	−13.8
SiOH	+1	0	0	0	0	0	0	0	0
SiO^-	+1	0	−1	0	0	0	0	−1	− 6.6
$SiONa^+$	+1	0	−1	+1	0	+1	0	−1	− 5.4
$AlOH_2^+$	0	+1	+1	0	0	0	0	+1	5.0
AlOH	0	+1	0	0	0	0	0	0	0
AlO^-	0	+1	−1	0	0	0	0	−1	−10.7
$AlOH_2^+Cl^-$	0	+1	+1	−1	0	0	+1	+1	7.1
AlO^-Na^+	0	+1	−1	+1	0	+1	0	−1	−10.2
Na^+	0	0	0	0	0	+1	0	0	0
Cl^-	0	0	0	0	0	0	+1	0	0
TOT	0	0	0	0		C	C	0	
log free	−3	−3	−1		−0.5	−pC	−pC	−pH	

site density = 5 sites nm^{-2}

surface area = 6.87 m^2 gm^{-1}

conc. of solids = 90.75 g l^{-1}

C_1 = 120 uF cm^{-2}

C_2 = 20 uF cm^{-2}

Al/Si = 3

where, C is the concentration of electrolyte;
pC = −log[C].

4.5) Future Work

In all of the titration studies mentioned, the DJL model explains the data well. With increasing salt concentration, for pH-values greater than the p.z.c., the amount of cation binding increases and for pH-values below the p.z.c. anion binding increases. This effect is seen experimentally with increasing surface charge with increasing electrolyte. Because of charge neutralization in the IHP by the complexed ion, the OHP potential decreases as seen by decreasing ζ-potential with increases salt concentration. Theoretical charge and potential calculations using the DJL model back predict the experimental data accurately.

Future work in this area includes:

1) Experiments on soxhleted monosize silica to remove possible alcohol blocking of surface sites and high temperature calcination to remove surface porosity and gel-layer.

2) Determine if soxhletion or some other cleaning technique removes the nonintersection Rσ problems for m-ZrO_2 . If not, the nonintersection is due to kinetic equilibrium attainment effects which must be studied.

3) The mixed site model for mullite and other multisite oxides should be completed to predict the experimental e.d.l. species, charge, and potential distributions for these systems.

4) Electrophoresis experiments must be made under N_2 to

exclude CO_2 effects, ensuring calculated ζ-potentials that can be directly compared to the theoretically predicted Ψ_d-values.

5) Conductometric and specific ion titrations can be made to provide secondary checks on the concentration of species in the bulk solution, providing a check on the calculated adsorption concentration of species in the e.d.l.

6) Once the intrinsic ionization and complexation constants have been determined for a material in a particular electrolyte, inclusion of the CO_2 equilibria would predict real ceramic processing e.d.l. charge and potential distributions. The inclusion of solubility and reprecipitation could also be included in the reaction tableau for more accurate results.

7) It is desired to apply the DJL model to more to other ceramic systems to predict suspension properties.

5) Conclusions

The surface charge, σ_o, for several silicas, aluminas, mullite, and zirconia aqueous suspensions were determined as a function of pH and NaCl electrolyte concentration. The σ_o-values of these materials were graphed and the point of zero charge determined. The p.z.c. values of the amorphous silicas were 4.25 for Quso G30, and 3.20 for the monosized silica. These values compare favorably with the literature values. The p.z.c.-values of the aluminas were 8.75 for Meller 180, α-Al_2O_3, while Meller 182, $\alpha\gamma$-Al_2O_3, had $R\sigma = 0$ at pH = 7.0 while the intersection of the $R\sigma$ curves occurred between pH 8.0 and 9.0. This result implies that solution cations specifically adsorb on the surface of the $\alpha\gamma$-Al_2O_3.

The p.z.c. for Baikowski mullite, $3Al_2O_3 \cdot 2SiO_2$, was determined to be 8.5, again in accordance with the literature reported value of 8.1 for crystalline mullite. Surface charge curves for mullite are skewed towards zero charge for pH-values less than the p.z.c. since positively charged alumina sites partially neutralize the negatively charged silica sites. For pH-values greater than the p.z.c. of mullite, both the alumina and silica sites are negatively charged, hence the σ_o curves are greater than for an average single oxide. The surface charge profile for uniform ZrO_2 was plotted, however the p.z.c. could not be determined since the $R\sigma$ curves did not crossover at a distinct point. This effect is probably due to the kinetics of equilibrium for solution species reacting at surface sites in the porous particles.

Ionization and complexation constants were determined for the aluminas and silicas studied using the double extrapolation technique of Davis, James, and Leckie. For Quso G30, the second ionization, pK_{a2}, and Na complexation, pK^*_{Na}, constants were determined to be 6.6 and 5.4. The valued determined for the laboratory produced, monosized silica were pK_{a2} = 4.9 and pK^*_{Na} = 4.5. The first ionization and chlorine complexation constants are, in general, difficult to determine for silica suspensions since they occur at pH-values of 0.0 to 2.5, where reliable pH measurements are difficult to obtain.

For the aluminas, Meller 180 and 182, α-Al_2O_3 and $\alpha\gamma$-Al_2O_3 respectively, both ionization and complexation constants were determined. For Meller 180 the reaction constants were determined to be pK_{a1} = 5.0, pK_{a2} = 10.7, pK^*_{Cl} = 7.1, and pK^*_{Na} = 10.2. For Meller 182 the reaction constants were determined to be pK_{a1} = 4.2, pK_{a2} = 9.8, pK^*_{Cl} = 6.34, and pK^*_{Na} = 9.2. The calculated reaction constants are within the range of values reported in the literature.

The reaction constants for Baikowski mullite could not be determined using the DJL model double extrapolation technique because it only applies for single oxide surfaces. A first estimate of the reaction constants can be made by using the values for pure alumina and silica since mullite, $3Al_2O_3 \cdot 2SiO_2$, is composed of these two end members. The values of the reaction constants for uniform m-ZrO_2 could not be determined since the Rσ curves did not yield a p.z.c., hence the DJL model could not be applied.

The differences between the p.z.c. and surface reaction constants determined for the two aluminas and silicas are due to differences in surface reactivity. These differences occur because the surfaces of the particles have different crystal habits and degrees of hydration resulting from different processing techniques. Crystal habit influences the local site-configuration, thereby affecting the local electrostatic field and the relative reactivity of the surface site. Hydration affects site reactivity by changing the ionization state of the surface site.

Surface reaction constants determined for Quso G30, amorph-SiO_2, and Meller 180, α-Al_2O_3, were used in the computer program SITECAL to calculate the e.d.l. site, charge and potential distributions. The undetermined first ionization and chlorine complexation constants for Quso G30 were estimated to be 1.9 and 3.1, since p.z.c. = $(pK_1+pK_2)/2$. These reaction constants must be included in the calculation otherwise the theoretical curves will not intersect at $R\sigma=0$ because neutralization of the negative and positive surface sites will not occur if the reaction decribing this transittion is not included.

The theoretical σ_o curves predicted the experimentally determined p.z.c. very well for both SiO_2 and α-Al_2O_3. The theoretical surface charge profile for SiO_2 increases more gradually than that of the experimental data. Experimental

σ_o-values are less than theoretical below pH 6.0, above which the former began to rise more rapidly with increasing pH. This effect may be due to surface dissolution during titration, though dissolution analysis suggest that this effect is small. The theoretical σ_o and relative curve-shape for α-Al_2O_3 match the experimental data quite well, however, the experimental values are slightly larger than the theoretical ones.

Soxhletion adequately removed surface impurities that cause large $\Delta\sigma$-shifts in the data or poor Rσ-crossover. The Rσ curves for unsoxhleted Quso G30 required a large $\Delta\sigma$ shift to cause the intersection to occur at σ_o=0. After soxhleting, curves intersected at σ_o=0, implying that the major expected soluble impurity, Na, had been removed. Poor Rσ-intersection was found for Meller 180, α-Al_2O_3, for unsoxhleted material. After soxhleting, the data behaived well.

Solubilities of the oxides in aqueous solution were determined, but not quantitatively taken into account because they were low or pH-independent. Normally, the effects of solubility must be included in the Rσ-calculations because titrant is consumed by the soluble metal species as they change ionization state and concentration as a function of pH.

A method for calculating surface charge, potential and reactive site pk is presented and described in detail for oxide surfaces. The DJL model incorporates specific ion adsorption and dissolution on the surface. Calculated pK-values are useful to predict colloidal properties of oxides. Pertinent prediction can be made for electrophoresis, coagulation, and ordering because the reactions at the surface determine the surface/electrolyte interfacial properties. These models can be applied to ceramic processing in order to produce high quality technical pieces for the future.

Appendix I

Supercalc spreadsheet for σ_o and pK calculations.

Constants

B1 = volume of the suspension
E1 = volume of the control electrolyte
B2 = concentration of the base used for the suspension
E2 = conc. of the base used for the control electrolyte
B3 = concentration of the acid used for the suspension
E3 = conc. of the acid used for the control electrolyte
H5 = concentration of electrolyte
B6 = weight of oxide powder in suspension
E6 = determined p.z.c.
B7 = surface area of oxide powder (m^2/gm)
E7 = determined $\Delta\sigma$ shift for the σ_o curves
B8 = surface site density (sites/nm2)
B10 = total volume of the suspension

Calculated for each titration pH

A12 = pH of the data point
B12 = volume of titrant required at pH for suspension
C12 = volume of titrant required for this pH for the control
D12 = calculated mEQ of titrant for the suspension
= IF(B12<0,B12*B2,B12*B3)
E12 = mEQ solubility correction for the suspension = 0
F12 = calculated mEQ of titrant for the control electrolyte
= IF(C12<0,C12*E2*B1/E1,C12*E3*B1/E1)
G12 = total mEQ difference including solubility
= D12-E12-F12
H12 = relative surface charge of the oxide at this pH
= 9648.456*G12/(B6*B7)
I12 = surface charge of the system after removing $\Delta\sigma$ effects
= H12-E7
K12 = fractional percent ionized on the surface, α
= .062416*ABS(I12/B8)
L12 = effective ionization constant, pQ
= IF(I12<0,A12-LOG10(K12/(1-K12)),A12+LOG10(K12/(1-K12)))
M12 = effective α, α* - ionization constant
= 10*K12+SQRT(H5)
N12 = effective α, α^*_{ion} -complexation constant
= 10*K12-LOG10(H5)
O12 = effective pQ, pQ* - complexation constant
= IF(I12<0,L12+LOG10(H5),L12-LOG10(H5))

Program SITECAL for the calculation of surface equilibria.

```
100 PAGE
110 PRINT "***********************************************"
120 PRINT "*                                             *"
130 PRINT "* PROGRAM *** SITECAL.BAS *** 12/14/83        *"
140 PRINT "*                                             *"
150 PRINT "*   TAPE FILE #3 AND DISK SCRATCHLIB/SITECAL  *"
160 PRINT "*                                             *"
170 PRINT "* CALCULATES THE EQUILIBRIUM CONCENTRATIONS   *"
180 PRINT "* OF AQUEOUS AND EDL SPECIES IN SOLUTION      *"
190 PRINT "* INCLUDES TITRATION COMPUTATIONS             *"
200 PRINT "* MODIFICATION OF J.WESTALL's  MICROQL-MIC8   *"
210 PRINT "* FROM JOHN WESTALL  MICROQL- 2. COMPUTATION  *"
220 PRINT "* OF ADSORPTION EQUILIBRIA IN BASIC- MIC8.BAS *"
230 PRINT "* SWISS FEDERAL INSTITUTE OF TECHNOLOGY EAWAG *"
240 PRINT "* CH-8600 DUEBENDORF, SWITZERLAND             *"
250 PRINT "*                                             *"
254 PRINT "*  WITH MATRIX CORRECTIONS FROM DR. R. JAMES  *"
256 PRINT "*                                             *"
260 PRINT "* MODIFIED FOR THE TEKTRONIX BY ** WAYNE HASZ *"
280 PRINT "*                                             *"
290 PRINT "***********************************************"
300 PRINT "HIT ANY KEY TO CONTINUE"
310 INPUT Z$
320 INIT
330 REM ** DEFINE THE THERMODYNAMIC CONSTANTS **
340 B1=6.022E+23 : REM AVOGADROS #
350 B2=0.1174     : REM (8EEoRE)^1/2
360 B3=19.46      : REM F/2RT
370 B4=0.0256     : REM RT/F
380 B5=0.05916    : REM LOG RT/F
390 B6=96487      : REM F
400 DEF FNS(X)=(EXP(X)-EXP(-X))/2
410 DEF FNC(X)=(EXP(X)+EXP(-X))/2
420 REM ** DEFINE THE SURFACE COMPONENTS **
430 L0=2 : REM EXP(-Y0) TERM
440 L1=3 : REM EXP(-Y1) TERM
450 L2=4 : REM EXP(-Y2) TERM
460 L3=1 : REM SOH SITE TERM
470 REM ** PROGRAM CONTROL **
490 I9=100     : REM ITERATION MAXIMUM
500 E9=1.0E-4 : REM TOLERANCE FOR CONBERGENCE
501 REM ** ENTER THE TITRATION CONDITIONS"
502 PH1=4.0   : REM BEGINNING PH
503 PH2=10.0  : REM ENDING PH
504 PH3=0.2   : REM INCREMENT PH
510 PAGE
520 PRINT "SITECAL MAIN MENU"
530 PRINT "1 RE/ENTER THE PARAMETERS"
540 PRINT "2 SOLVE THE MATRIX FOR ALL CONCENTRATIONS"
560 PRINT "3 PRINT THE SOLUTION"
```

```
570 PRINT "4 STOP"
580 PRINT "ENTER YOUR CHOICE    ";
590 INPUT Z1
600 IF Z1<1 OR Z1>4 THEN 510
610 GO TO Z1 OF 620,3290,4510,4790
620 PAGE
780 PRINT "MENU FOR THE EXAMPLES"
800 PRINT "1 USE THE DATA OF QUSO G30"
810 PRINT "2 USE THE DATA OF MELLER 180"
820 PRINT "3 GOTO THE MAIN MENU"
830 PRINT "  ENTER YOUR CHOICE"
840 INPUT Z2
850 IF Z2<1 OR Z2>3 THEN 780
860 GO TO Z2 OF 880,1180,510
880 PAGE
890 PRINT "USING THE DATA OF QUSO G30"
892 M$="QUSO G30"
894 P$="pH,SiOH,SiOH2+,SiO- // SiOH2+Cl-,SiO-Na+,
       psi0,1 // 2,sig 0,1,2"
900 M1=9      : rem M1=TOT NUMBER OF SPECIES (Y)
910 N1=7      : rem N1=TOT NUMBER OF COMPONENTS (X)
920 K1=N1-1   : rem # COMP WHICH TOT CONC IS KNOWN
930 DELETE A,K,T,X
940 DIM A(M1,N1),K(M1),T(N1),X(N1)
950 DATA 0,0,0,0,0,0,1
960 DATA 0,0,0,0,0,0,-1
970 DATA 1,0,0,0,0,0,0
975 DATA 1,1,0,0,0,0,1
980 DATA 1,-1,0,0,0,0,-1
985 DATA 1,1,-1,0,0,1,1
993 DATA 1,-1,1,0,1,0,-1
992 DATA 0,0,0,0,0.1,0.1,0
994 DATA 0,0,0,0,-1,-1,0
1000 FOR I=1 TO 9
1010 FOR J=1 TO 7
1020 READ A(I,J)
1030 NEXT J
1040 NEXT I
1050 C1=5*1.0E+18
1060 C2=118.73
1070 C3=9.501
1080 C4=0.1
1090 C5=120*0.01
1100 C6=20*0.01
1110 READ K
1120 DATA 0,-14,0,1.9,-6.6,3.1,-5.4,0,0
1130 READ T
1140 DATA 0,0,0,0,0.1,0.1,0
1150 READ X
1160 DATA -4,-1,-0.5,0,-1,-1,-7
1170 GO TO 2780
1180 PAGE
1190 PRINT "USING THE DATA OF MELLER 180"
1192 M$="Meller 180"
1194 P$="pH,AlOH,AlOH2+,AlO- // AlOH2+Cl-,AlO-Na+,
```

```
            psi0,1 // 2,sig0,1,2"
1200 M1=9
1210 N1=7
1220 K1=N1-1
1230 DELETE A,K,T,X
1240 DIM A(M1,N1),K(M1),T(N1),..(N1)
1250 DATA 0,0,0,0,0,0,1
1260 DATA 0,0,0,0,0,0,-1
1265 DATA 1,0,0,0,0,0,0
1270 DATA 1,1,0,0,0,0,1
1290 DATA 1,-1,0,0,0,0,-1
1300 DATA 1,1,-1,0,0,1,1
1310 DATA 1,-1,1,0,1,0,-1
1312 DATA 0,0,0,0,0.1,0.1,0
1314 DATA 0,0,0,0,-1,-1,-7
1320 FOR I=1 TO 9
1330 FOR J=1 TO 7
1340 READ A(I,J)
1350 NEXT J
1360 NEXT I
1370 C1=2.7*1.0E+18 : REM SITE DENSITY
1380 C2=21.31       : REM SURFACE AREA (M2/G)
1390 C3=31.25       : REM CONC. OF SOLIDS (G/L)
1400 C4=0.1         : REM ELECTROLYTE CONC.
1410 C5=120*0.01    : REM INNER LAYER CAPACITANCE
1420 C6=20*0.01     : REM OUTER LAYER CAPACITANCE
1430 READ K    : REM REACTION CONSTANTS
1440 DATA 0,-14,0,5,-10.7,7.1,-10.2,0,0
1450 READ T    : REM TOT CONC. OF COMPONENTS.
1460 DATA 0,0,0,0,0.1,0.1,0
1470 READ X    : REM LOG FREE CONC. OF COMP.
1480 DATA -4,-1,-0.5,0,0.1,0.1,-7
1490 GO TO 2780
2780 PAGE
2790 PRINT "BEGINNING PH = ";PH1
2800 PRINT "ENDING PH    = ";PH2
2810 PRINT "INCREMENT PH = ";PH3
2820 GOTO 510
3290 PAGE
3300 PRINT "SOLVING THE TITRATION EQUATIONS"
3310 DELETE Z0,Y0,E,Y,Z,C,Q0
3320 DIM Z0(K1,K1),Y0(K1),Q0(K1)
3330 DIM E(N1),Y(N1),Z(N1,N1)
3340 DIM C(M1)
3350 R1=(P2-P1)/P3+1
3360 DELETE S1
3370 DIM S1(R1,12)
3380 REM DIM SPECIES AND EDL PSI AND SIGMA
3390 R1=0
3400 PRINT "ALL CONCENTRATIONS IN LOG"
3402 PRINT F$,M$
3403 PRINT C4,C5*100,C6*100
3404 PRINT "I=",R1,"J= ",12
3410 PRINT P$
3430 FOR P4=P2 TO P1 STEP -P3
```

```
3440 R1=R1+1
3442 X(5)=LGT(C4)
3444 X(6)=LGT(C4)
3450 X(N1)=-P4
3452 T(5)=C4
3454 T(6)=C4
3460 T(N1)=0
3470 GOSUB 3550
3480 REM SOLVE THE EQUATIONS
3490 NEXT P4
3510 PRINT S1
3520 PRINT "DONE, HIT ANY KEY TO CONTINUE"
3530 INPUT Z$
3540 GO TO 510
3550 REM ** BEGIN A CASE HERE **
3560 I8=0
3570 REM COMPLEXES
3580 C=A MPY X
3590 LET C=C+K
3600 FOR I=1 TO M1
3610 C(I)=10^C(I)
3620 NEXT I
3630 FOR J=1 TO N1
3640 LET E(J)=10^X(J)
3650 NEXT J
3660 GOSUB 4590
3670 REM MASS BALANCE
3680 I7=0
3690 FOR J=1 TO N1
3700 V8=-T(J)
3710 V9=ABS(T(J))
3720 IF J=L2 THEN 3740
3730 GO TO 3750
3740 V8=V8+D3*D4
3750 FOR I=1 TO M1
3760 V8=V8+A(I,J)*C(I)
3770 V9=V9+ABS(A(I,J))*C(I)
3780 NEXT I
3790 IF J>K1 THEN 3830
3800 IF ABS(V8)/V9>E9 THEN 3820
3810 GO TO 3830
3820 I7=1
3830 Y(J)=V8
3840 NEXT J
3850 REM COMPUTE Z
3860 FOR J=1 TO N1
3870 FOR Q=1 TO N1
3880 V9=0
3890 FOR I=1 TO M1
3900 V9=V9+A(I,J)*A(I,Q)*C(I)/E(Q)
3910 NEXT I
3920 Z(J,Q)=V9
3930 NEXT Q
3940 NEXT J
3950 GOSUB 4700
```

```
3960 REM MODIFY DERIVATIVES
3970 IF I7=0 THEN 4170
3980 I8=I8+1
3990 IF I8>I9 THEN 4170
4000 REM SOLUTION
4010 FOR J=1 TO K1
4020 FOR Q=1 TO K1
4030 Z0(J,Q)=Z(J,Q)
4040 NEXT Q
4050 Y0(J)=Y(J)
4060 NEXT J
4070 Z0=INV(Z0)
4080 Q0=Z0 MPY Y0
4085 Y0=Q0
4090 FOR J=1 TO K1
4100 E(J)=E(J)-Y0(J)
4110 IF E(J)<0 THEN 4130
4120 GO TO 4140
4130 E(J)=(E(J)+Y0(J))/10
4140 X(J)=LGT(E(J))
4150 NEXT J
4160 GO TO 3570
4170 REM END OF THE ROUTINE GOTO
4180 S1(R1,1)=-LGT(C(1))
4190 FOR J=2 TO 6
4200 S1(R1,J)=LGT(C(J+1))
4210 NEXT J
4220 S1(R1,7)=D0*1000
4230 S1(R1,8)=D1*1000
4240 S1(R1,9)=D2*1000
4250 S1(R1,10)=T(L0)*100/D4
4260 S1(R1,11)=T(L1)*100/D4
4270 S1(R1,12)=T(L2)*100/D4
4290 RETURN
4300 PAGE
4520 PRINT "ROUTINE TO PRINT THE DATA"
4530 PRINT @51:F$,M$
4532 PRINT @51:C4,C5*100,C6*100
4540 PRINT @51:"I= ",R1,"J= ",12
4550 PRINT @51:P$
4570 PRINT @51:S1
4580 GO TO 510
4590 REM ** MODIFY THE MASS BALANCE **
4600 D0=-B5*X(L0)
4610 D1=-B5*X(L1)
4620 D2=-B5*X(L2)
4630 D3=-B2*SQR(C4)*FNS(B3*D2)
4640 D4=C2*C3/B6
4650 T(L0)=(D0-D1)*C5*D4
4660 T(L2)=(D2-D1)*C6*D4
4670 T(L1)=-T(L0)-T(L2)
4680 T(L3)=C1*C2*C3/B1
4690 RETURN
4700 REM ** MODIFY THE DERIVATIVES **
4710 Z(L1,L2)=-C6*B4/E(L2)*D4
```

```
4720 Z(L2,L1)=-C6*B4/E(L1)*D4
4730 Z(L2,L2)=(C6+B3*B2*SQR(C4)*FNC(B3*D2))*B4/E(L2)*D4
4740 Z(L0,L1)=Z(L0,L1)-C5*B4/E(L1)*D4
4750 Z(L1,L0)=Z(L1,L0)-C5*B4/E(L0)*D4
4760 Z(L1,L1)=Z(L1,L1)+(C5+C6)*B4/E(L1)*D4
4770 Z(L0,L0)=Z(L0,L0)+C5*B4/E(L0)*D4
4780 RETURN
4790 STOP
4800 END
```

```
D0 = the surface potential
D1 = the potential at the IHP
D2 = the potential at the OHP
D3 = a conversion for sigma -> conc. of sites
A  - (subscripted) stoichiometry
C  - (subscripted) species conc.
D0 - (subscripted) correction to X
E  - (subscripted) component concentration
E9 - tolerance for convergence
I7 - flag for convergence
I8 - iteration counter
I9 - iteration maximum
K  - (subscripted) log stability constants
K1 - number of somponents (reduced)
M1 - number of species
N1 - number of components (total)
T  - (subscripted) total conc. of components
X  - (subscripted) log free conc. of components
Y  - (subscripted) error in material balance equation
Y0 - (subscripted) error in material balance eq. (reduced)
Z  - Jacobian
Z0 - Jacobian (reduced).
```

Appendix III

Titration Data and Calculations for σ, α, and pQ.

Data for Quso G30 SiO_2

V(susp)=	39.7228	V(std)=	40	material=	Quso G30
C(OH,sp)=	.1018	C(OH,sd)=	.1018	comments=	soxhleted (92x6-3)
C(H,sp)=	.11369	C(H,sd)=	.11369	titrants	.1N NaOH, 1% HCl
DATA	e2x51-4,51-3	DATA	e2x43-3,51-2	salt=	1N NaCl
TABLE	e2x73	TABLE	e2x65	conc.=	1
Ms =	.3774	pH(pzc)=	4	file #	e3x5a
As =	118.731	dsigmax = 0		date=	4/17/83
Ns =	5	assumed			

pH	VT(sp)	VT(std)	mEQsus	mEQ	mEQstd	dlta mEQ	dsigma	sigma	alpha	pQ	alpha*	alpha*ion	pQ*ion
9.50	-3.55	-.024	-.36139	0	-.002426	-.358964	-77.2934	-77.2934	.9648689	8.061224	10.64869	9.648689	8.061224
9.00	-2.507	-.0062	-.255213	0	-.000627	-.254586	-54.8184	-54.8184	.6843085	8.664011	7.843085	6.843085	8.664011
8.50	-1.789	0	-.182120	0	0	-.182120	-39.2148	-39.2148	.4895261	8.518198	5.895261	4.895261	8.518198
8.00	-1.264	0	-.128675	0	0	-.128675	-27.7068	-27.7068	.3458697	8.276752	4.458697	3.458697	8.276752
7.50	-.861	.001	-.087650	0	.0001129	-.087763	-18.8974	-18.8974	.2358999	8.010423	3.358999	2.358999	8.010423
7.00	-.561	.002	-.057110	0	.0002258	-.057336	-12.3457	-12.3457	.1541140	7.739470	2.541140	1.541140	7.739470
6.50	-.338	.004	-.034408	0	.0004516	-.034860	-7.50619	-7.50619	.0937012	7.455526	1.937012	.9370121	7.455526
6.00	-.178	.0065	-.018120	0	.0007339	-.018854	-4.05977	-4.05977	.0506789	7.272586	1.506789	.5067891	7.272586
5.50	-.098	.0082	-.009976	0	.0009258	-.010902	-2.34750	-2.34750	.0293043	7.020151	1.293043	.2930433	7.020151
5.00	-.0512	.01	-.005212	0	.0011290	-.006341	-1.36541	-1.36541	.0170446	6.760946	1.170446	.1704469	6.760946
4.50	-.0245	.0143	-.002494	0	.0016145	-.004109	-.884679	-.884679	.0110436	6.452065	1.110436	.1104362	6.452065
4.00	0	.026	0	0	.0029355	-.002935	-.632073	-.632073	.0078903	6.099466	1.078903	.0789029	6.099466
3.50	.0395	.0605	.0044908	0	.0068306	-.002340	-.503819	-.503819	.0062893	5.698659	1.062893	.0628928	5.698659
3.00	.135	.1646	.0153482	0	.0185837	-.003236	-.696688	-.696688	.0086969	5.056842	1.086969	.0869690	5.056842

V(susp)=	39.7228	V(std)=	40	material=	Quso G30
C(OH,sp)=	.1018	C(OH,sd)=	.1018	comments=	soxhleted (e2x6-3)
C(H,sp)=	.11369	C(H,sd)=	.11369	titrants	.1N NaOH, 1% HCl
DATA	e2x51-4,51-3	DATA	e2x43-3,51-2	salt=	0.1N NaCl
TABLE	e2x73	TABLE	e2x65	conc.=	.1
Ms =	.3774	pH(pzc)=	4	file #	e3x5b
As =	118.731	dsigmax = 0		date=	4/17/83
Ns =	5	assumed			

pH	VT(sp)	VT(std)	mEQsus	mEQ	mEQstd	dlta mEQ	dsigma	sigma	alpha	pQ	alpha*	alpha*ion	pQ*ion
10.00	-2.953	-.0472	-.300615	0	-.004772	-.295844	-63.7022	-63.7022	.7952068	9.410835	8.248296	8.952068	8.410835
9.50	-1.925	-.0157	-.195965	0	-.001587	-.194378	-41.8541	-41.8541	.5224737	9.460933	5.340965	6.224737	8.460933
9.00	-1.255	-.005	-.127759	0	-.000505	-.127254	-27.4007	-27.4007	.3420484	9.284106	3.736712	4.420484	8.284106
8.50	-.81	-.0017	-.082458	0	-.000172	-.082286	-17.7182	-17.7182	.2211793	9.046693	2.528020	3.211793	8.046693
8.00	-.516	-.001	-.052529	0	-.000101	-.052428	-11.2889	-11.2889	.1409219	8.785054	1.725447	2.409219	7.785054
7.50	-.3165	0	-.032220	0	0	-.032220	-6.93766	-6.93766	.0866043	8.523120	1.182270	1.866043	7.523120
7.00	-.1777	.0005	-.018090	0	.0000565	-.018146	-3.90733	-3.90733	.0487760	8.290077	.8039077	1.487760	7.290077
6.50	-.094	.0047	-.009569	0	.0005306	-.010100	-2.17473	-2.17473	.0271476	8.034315	.5877043	1.271476	7.034315
6.00	-.049	.0065	-.004988	0	.0007339	-.005722	-1.23210	-1.23210	.0153805	7.806298	.4700328	1.153805	6.806298
5.50	-.024	.0082	-.002443	0	.0009258	-.003369	-.725425	-.725425	.0090556	7.539131	.4067840	1.090556	6.539131
5.00	-.0097	.0115	-.000987	0	.0012984	-.002286	-.492194	-.492194	.0061442	7.208861	.3776494	1.061442	6.208861
4.50	0	.0185	0	0	.0020887	-.002089	-.449744	-.449744	.0056142	6.748263	.3723702	1.056142	5.748263
4.00	.0255	.0385	.0028991	0	.0043467	-.001448	-.311711	-.311711	.0038911	6.408229	.3551392	1.038911	5.408229
3.50	.0955	.099	.0108574	0	.0111773	-.000320	-.068885	-.068885	.0008599	6.565173	.3248269	1.008599	5.565173
3.00	.31	.2842	.0352439	0	.0320868	.0031571	.6798017	.6798017	.0084861	.9324093	.4010888	1.084861	1.932409

V(susp)= 39.7228 | V(std)= 40 | material= Quso G30
C(OH,sp)= .1018 | C(OH,sd)= .1018 | comments= scrubleted (e2x6-3)
C(H,sp)= .11369 | C(H,sd)= .11369 | titrants .1N NaOH, 1% HCl
DATA e2x51-4,51-3 | DATA e2x43-3,51-2 | salt= 0.01M NaCl
TABLE e2x73 | TABLE e2x65 | conc.= .01
Ms = .3774 | pH(pzc)= 4 | file 0 e3x5c
As = 118.731 | dsigmax = 0 | date= 4/17/83
Ns = 5 assumed

pH	VT(sp)	VT(std)	mE0sus	mE0	mE0std	dlta mE0	dsigma	sigma	alpha	p0	alpha*	alpha*ion	p0*ion
10.00	-2.5	-.039	-.2545	0	-.003943	-.250557	-53.9509	-53.9509	.6734802	9.685585	6.834802	8.734802	7.685585
7.00	-.065	.0025	-.006617	0	.0002823	-.006899	-1.48557	-1.48557	.0165447	8.723651	.2854471	2.185447	6.723651
6.50	-.0322	.0017	-.003278	0	.0001919	-.003470	-.747150	-.747150	.0093268	8.526197	.1932683	2.093268	6.526197
6.00	-.0132	.0032	-.001344	0	.0003613	-.001705	-.367137	-.367137	.0045830	8.336851	.1458304	2.045830	6.336851
5.50	-.004	.0042	-.000407	0	.0004742	-.000881	-.189784	-.189784	.0023691	8.124385	.1236911	2.023691	6.124385
5.00	0	.007	0	0	.0007903	-.000790	-.170174	-.170174	.0021243	7.671859	.1212431	2.021243	5.671859
4.50	.0107	.013	.0012165	0	.0014677	-.000251	-.054099	-.054099	.0006753	7.670192	.1067533	2.006753	5.670192
4.00	.036	.0315	.0040928	0	.0035564	.0005364	.1155046	.1155046	.0014419	1.159552	.1144187	2.014419	3.159552
3.50	.1105	.094	.0125427	0	.0106128	.0019499	.4198693	.4198693	.0052413	1.221722	.1524131	2.052413	3.221722
3.00	.343	.3162	.0389957	0	.0356997	.0032960	.7097105	.7097105	.0088595	.9512719	.1885946	2.088595	2.951272

V(susp)= 39.7228 | V(std)= 40 | material= Quso G30
C(OH,sp)= .1018 | C(OH,sd)= .1018 | comments= scrubleted (e2x6-3)
C(H,sp)= .11369 | C(H,sd)= .11369 | titrants .1N NaOH, 1% HCl
DATA e2x51-4,51-3 | DATA e2x43-3,51-2 | salt= 0.001M NaCl
TABLE e2x73 | TABLE e2x65 | conc.= .001
Ms = .3774 | pH(pzc)= 4 | file 0 e3x5d
As = 118.731 | dsigmax = 0 | date= 4/17/83
Ns = 5 assumed

pH	VT(sp)	VT(std)	mE0sus	mE0	mE0std	dlta mE0	dsigma	sigma	alpha	p0	alpha*	alpha*ion	p0*ion
5.50	0	.0042	0	0	.0004742	-.000474	-.102104	-.102104	.0012746	8.394077	.0443486	3.012746	5.394077
5.00	.0065	.0057	.0007390	0	.0006435	.0008954	.0205511	.0205511	.0002565	1.409273	.0341882	3.002565	4.409273
4.50	.0182	.0098	.0020692	0	.0011064	.0009627	.2072958	.2072958	.0025877	1.914042	.0574999	3.025877	4.914042
4.00	.049	.0225	.0055708	0	.0025403	.0030305	.6525410	.6525410	.0081458	1.914486	.1130808	3.001458	4.914486
3.50	.152	.0785	.0172809	0	.0088628	.0084181	1.812608	1.812600	.0226272	1.864570	.2578943	3.226272	4.864570
3.00	.495	.3593	.0542766	0	.0405657	.0157168	3.382911	3.382911	.0422295	1.644355	.4539183	3.422295	4.644355

V(susp)= 39.7359 V(std)= 10 material= Monosized SiO2 from TEOS
C(OH,sp)= .1018 C(OH,sd)= .1018 comments= (a2x19-1) 0.4 um (Huang corrction)
C(H,sp)= .11369 C(H,sd)= .11369 titrants .1N NaOH (a2x), 1% HCl (a2x)
DATA a3x30-1,xx-x DATA a3x30-2,II-I salt= 1N NaCl
TABLE a3x34 TABLE a3x44 conc.= 1
Ms = .4611 pH(pzc)= 3.2 file # a3x45a
As = 41.46 dsigmax = 82 date= 6/08/83
Ns = 5 assumed

pH	VT(sp)	VT(std)	mEQsus	mEQ	mEQstd	dlta mEQ	dsigma	sigma	alpha	pQ	alpha*	alpha*ion	pQ*ion
12.00	N/A	N/A	N/A	0	N/A	N/A	N/A	N/A	N/A	N/A	N/A	N/A	N/A
11.50	N/A	N/A	N/A	0	N/A	N/A	N/A	N/A	N/A	N/A	N/A	N/A	N/A
11.00	N/A	N/A	N/A	0	N/A	N/A	N/A	N/A	N/A	N/A	N/A	N/A	N/A
10.50	N/A	N/A	N/A	0	N/A	N/A	N/A	N/A	N/A	N/A	N/A	N/A	N/A
10.00	N/A	N/A	N/A	0	N/A	N/A	N/A	N/A	N/A	N/A	N/A	N/A	N/A
9.50	N/A	N/A	N/A	0	N/A	N/A	N/A	N/A	N/A	N/A	N/A	N/A	N/A
9.00	N/A	N/A	N/A	0	N/A	N/A	N/A	N/A	N/A	N/A	N/A	N/A	N/A
8.50	N/A	.019	N/A	0	.0085534	N/A	N/A	N/A	N/A	N/A	N/A	N/A	N/A
8.00	N/A	.0357	N/A	0	.0161277	N/A	N/A	N/A	N/A	N/A	N/A	N/A	N/A
7.50	N/A	.042	N/A	0	.0189738	N/A	N/A	N/A	N/A	N/A	N/A	N/A	N/A
7.00	N/A	.0452	N/A	0	.0204194	N/A	N/A	N/A	N/A	N/A	N/A	N/A	N/A
6.50	.29	.0492	.0329701	0	.0222265	.0107436	5.422313	-76.5777	.9559346	5.163670	10.55935	9.559346	5.163670
6.00	.659	.054	.0749217	0	.0243949	.0505268	25.50089	-56.4991	.7052897	5.621028	8.052897	7.052897	5.621028
5.50	.941	.0575	.1069823	0	.0259761	.0810062	40.88386	-41.1161	.5132610	5.476958	6.132610	5.132610	5.476939
5.00	1.156	.0585	.1314256	0	.0264278	.1049978	52.99242	-29.0076	.3621075	5.245919	4.621075	3.621075	5.245910
4.50	1.345	.0597	.1529131	0	.0269699	.1259431	63.56351	-18.4365	.2301464	5.024404	3.301464	2.301464	5.024404
4.00	1.491	.0637	.1695118	0	.0287769	.1407348	71.02889	-10.9711	.1369346	4.799457	2.369546	1.369546	4.799457
3.50	1.637	.074	.1861105	0	.0334301	.1526805	77.05785	-4.94215	.0616938	4.682103	1.616938	.6169379	4.682103
3.00	1.91	.105	.2171479	0	.0474345	.1697134	85.65436	3.654336	.0456181	1.679415	1.456181	.4561805	1.679415
2.50	2.68	.189	.3046892	0	.0853822	.2193070	110.6863	28.68429	.3580717	2.246484	4.580717	3.580717	2.246484

V(susp)= 39.7359 V(std)= 10 material= monosized SiO2 from TEOS
C(OH,sp)= .1018 C(OH,sd)= .1018 comments= (a2x19-1) 0.4um (Huang correction)
C(H,sp)= .11369 C(H,sd)= .11369 titrants .1N NaOH (a2x), 1% HCl (a2x)
DATA a3x30-1,II-I DATA a3x30-2,II-I salt= 0.1N NaCl
TABLE a3x34 TABLE a3x44 conc.= .1
Ms = .4611 pH(pzc)= 3.2 file # a3x45b
As = 41.46 dsigmax = 82 date= 6/08/83
Ns = 5 assumed

pH	VT(sp)	VT(std)	mEQsus	mEQ	mEQstd	dlta mEQ	dsigma	sigma	alpha	pQ	alpha*	alpha*ion	pQ*ion
12.00	N/A	N/A	N/A	0	N/A	N/A	N/A	N/A	N/A	N/A	N/A	N/A	N/A
11.50	N/A	N/A	N/A	0	N/A	N/A	N/A	N/A	N/A	N/A	N/A	N/A	N/A
11.00	N/A	N/A	N/A	0	N/A	N/A	N/A	N/A	N/A	N/A	N/A	N/A	N/A
10.50	N/A	N/A	N/A	0	N/A	N/A	N/A	N/A	N/A	N/A	N/A	N/A	N/A
10.00	N/A	N/A	N/A	0	N/A	N/A	N/A	N/A	N/A	N/A	N/A	N/A	N/A
9.50	N/A	N/A	N/A	0	N/A	N/A	N/A	N/A	N/A	N/A	N/A	N/A	N/A
9.00	N/A	.0025	N/A	0	.0011294	N/A	N/A	N/A	N/A	N/A	N/A	N/A	N/A
8.50	N/A	.028	N/A	0	.0126492	N/A	N/A	N/A	N/A	N/A	N/A	N/A	N/A
8.00	N/A	.0402	N/A	0	.0181606	N/A	N/A	N/A	N/A	N/A	N/A	N/A	N/A
7.50	.148	.0452	.0168261	0	.0204194	-.093593	-1.81535	-83.8135	1.046261	ERROR	10.77884	11.46261	ERROR
7.00	.571	.0485	.0649170	0	.0219102	.0430068	21.70551	-60.2945	.7526481	6.516677	7.842909	8.526481	5.516677
6.50	.903	.0527	.1026621	0	.0238076	.0788545	39.79785	-42.2021	.3268179	6.453368	5.584406	6.268179	5.453368
6.00	1.16	.0567	.1318804	0	.0256146	.1062658	53.63234	-28.3677	.3541192	6.261003	3.857420	4.541192	5.261003
5.50	1.332	.0582	.1514351	0	.0262923	.1251428	63.15958	-18.8404	.2351887	6.012138	2.668115	3.351887	5.012138
5.00	1.449	.059	.1647368	0	.0266537	.1380831	69.69057	-12.3091	.1536611	5.740980	1.852839	2.536611	4.740980
4.50	1.5315	.0607	.1741162	0	.0274217	.1466946	74.03676	-7.96324	.0994067	5.457113	1.310295	1.994067	4.457113
4.00	1.603	.066	.1822451	0	.0298160	.1524291	76.93097	-5.06903	.0632777	5.170360	.9490046	1.632777	4.170360
3.50	1.702	.08	.1935004	0	.0361406	.1573598	79.41950	-2.58050	.0322129	4.977750	.6383567	1.322129	3.977750
3.00	1.938	.123	.2203312	0	.0555662	.1647651	83.15694	1.156941	.0144423	1.165955	.4606510	1.144423	2.165955
2.50	2.523	.2526	.2868399	0	.1141139	.1727259	87.17480	5.174801	.0645981	1.339221	.9622085	1.645981	2.339221

V(susp)=	39.7359	V(std)=	10	material=	monosized SiO2 from TEOS
C(OH,sp)=	.1018	C(OH,sd)=	.1018	comments=	(s2x19-1) 0.4 um (Huang correction)
C(H,sp)=	.11369	C(H,sd)=	.11369	titrants	.1N NaOH (s2x), 1% HCl (s2x)
DATA	e3x30-1,II-I	DATA	e3x30-2,II-I	salt=	0.01N NaCl
TABLE	e3x34	TABLE	e3x44	conc.=	.01
Ms =	.4611	pH(pzc)= 3.2		file 8	e3x45c
As =	41.46	dsigmax = 82		date=	6/08/83
Ns =	5 assumed				

pH	VT(sp)	VT(std)	mEQsus	mEQ	mEQstd	dlta mEQ	dsigma	sigma	alpha	pQ	alpha*	alpha*ion	pQ*ion
12.00	N/A	N/A	N/A	0	N/A	N/A	N/A	N/A	N/A	N/A	N/A	N/A	N/A
11.50	N/A	N/A	N/A	0	N/A	N/A	N/A	N/A	N/A	N/A	N/A	N/A	N/A
11.00	N/A	N/A	N/A	0	N/A	N/A	N/A	N/A	N/A	N/A	N/A	N/A	N/A
10.50	N/A	N/A	N/A	0	N/A	N/A	N/A	N/A	N/A	N/A	N/A	N/A	N/A
10.00	N/A	N/A	N/A	0	N/A	N/A	N/A	N/A	N/A	N/A	N/A	N/A	N/A
9.50	N/A	N/A	N/A	0	N/A	N/A	N/A	N/A	N/A	N/A	N/A	N/A	N/A
9.00	N/A	.005	N/A	0	.0022588	N/A	N/A	N/A	N/A	N/A	N/A	N/A	N/A
8.50	N/A	.03	N/A	0	.0135527	N/A	N/A	N/A	N/A	N/A	N/A	N/A	N/A
8.00	.237	.041	.0269445	0	.0185221	.0084225	4.250824	-77.7492	.9705585	6.481938	9.805585	11.70559	4.481938
7.50	.618	.046	.0702604	0	.0207808	.0494796	24.97235	-57.0277	.7110876	7.107151	7.210876	9.110876	5.107151
7.00	.912	.0492	.1036853	0	.0222265	.0814588	41.11227	-40.8877	.5104097	6.981914	5.204097	7.104097	4.981914
6.50	1.118	.0537	.1271054	0	.0242594	.1028460	51.90641	-30.0936	.3756643	6.720618	3.856643	5.756643	4.720618
6.00	1.261	.0572	.1433631	0	.0258405	.1175226	59.31365	-22.6863	.2831982	6.403309	2.931982	4.831982	4.403309
5.50	1.359	.0582	.1545047	0	.0262923	.1282124	64.70883	-17.2912	.2158492	6.060269	2.258492	4.158492	4.060269
5.00	1.423	.059	.1617809	0	.0266537	.1351272	68.19870	-13.8013	.1722843	5.681635	1.822843	3.722843	3.681635
4.50	1.47	.0607	.1671243	0	.0274217	.1397026	70.50793	-11.4921	.1434578	5.276025	1.534578	3.434578	3.276025
4.00	1.519	.0665	.1726951	0	.0300419	.1426532	71.99711	-10.0029	.1248681	4.845622	1.348681	3.248681	2.845622
3.50	1.621	.0835	.1842915	0	.0377217	.1465697	73.97377	-8.02623	.1001931	4.453312	1.101931	3.001931	2.453312
3.00	1.938	.143	.2203312	0	.0646013	.1557299	78.59190	-3.40310	.0424816	4.352947	.5248157	2.424816	2.352967
2.50	2.953	.3317	.3357266	0	.1498479	.1858786	93.81296	11.81296	.1474636	1.737972	1.574636	3.474636	3.737972

V(susp)=	39.7359	V(std)=	10	material=	monosized SiO2 from TEOS
C(OH,sp)=	.1018	C(OH,sd)=	.1018	comments=	(s2x19-1) 0.4 um (Huang correction)
C(H,sp)=	.11369	C(H,sd)=	.11369	titrants	.1N NaOH (s2x), 1% HCl (s2x)
DATA	e3x30-1,II-I	DATA	e3x30-2,II-I	salt=	0.001N NaCl
TABLE	e3x34	TABLE	e3x44	conc.=	.001
Ms =	.4611	pH(pzc)= 3.2		file 8	e3x45d
As =	41.46	dsigmax = 82		date=	6/08/83
Ns =	5 assumed				

pH	VT(sp)	VT(std)	mEQsus	mEQ	mEQstd	dlta mEQ	dsigma	sigma	alpha	pQ	alpha*	alpha*ion	pQ*ion
12.00	N/A	N/A	N/A	0	N/A	N/A	N/A	N/A	N/A	N/A	N/A	N/A	N/A
11.50	N/A	N/A	N/A	0	N/A	N/A	N/A	N/A	N/A	N/A	N/A	N/A	N/A
11.00	N/A	N/A	N/A	0	N/A	N/A	N/A	N/A	N/A	N/A	N/A	N/A	N/A
10.50	N/A	N/A	N/A	0	N/A	N/A	N/A	N/A	N/A	N/A	N/A	N/A	N/A
10.00	N/A	N/A	N/A	0	N/A	N/A	N/A	N/A	N/A	N/A	N/A	N/A	N/A
9.50	N/A	N/A	N/A	0	N/A	N/A	N/A	N/A	N/A	N/A	N/A	N/A	N/A
9.00	N/A	N/A	N/A	0	N/A	N/A	N/A	N/A	N/A	N/A	N/A	N/A	N/A
8.50	N/A	.0155	N/A	0	.0070022	N/A	N/A	N/A	N/A	N/A	N/A	N/A	N/A
8.00	.25	.034	.0284225	0	.0153598	.0130627	6.592770	-75.4072	.9413235	6.794725	9.444858	12.41324	3.794725
7.50	.607	.0417	.0690098	0	.0188383	.0501715	25.32158	-56.6784	.7075280	7.116341	7.106903	10.07528	4.116341
7.00	.87	.0455	.0989103	0	.0205550	.0783553	39.54595	-42.4541	.5299624	6.947807	5.331247	8.299624	3.947807
6.50	1.077	.049	.1224441	0	.0221361	.1003080	50.62547	-31.3745	.3916546	6.691247	3.948169	6.916546	3.691247
6.00	1.225	.0535	.1392703	0	.0241690	.1151012	58.09160	-23.9084	.2984533	6.371180	3.016156	5.984533	3.371180
5.50	1.324	.0557	.1505256	0	.0251629	.1253627	63.27055	-18.7294	.2338034	6.015489	2.369657	5.338034	3.015489
5.00	1.3915	.0565	.1581996	0	.0255243	.1326753	66.96126	-15.0387	.1877316	5.636162	1.908939	4.877316	2.636162
4.50	1.436	.0575	.1632598	0	.0259761	.1372828	69.28664	-12.7134	.1587034	5.224363	1.618657	4.587034	2.224363
4.00	1.4735	.0615	.1675222	0	.0277831	.1397391	70.52636	-11.4736	.1432278	4.776038	1.463901	4.432278	1.776038
3.50	1.53	.0765	.1739457	0	.0345594	.1393863	70.34826	-11.6517	.1454510	4.269020	1.486133	4.454510	1.269020
3.00	1.693	.134	.1924772	0	.0605355	.1319417	66.59098	-15.4090	.1923539	3.623120	1.955162	4.923539	.6231200
2.50	2.254	.3086	.2562573	0	.1394123	.1168449	58.97164	-23.0284	.2874676	2.894216	2.906299	5.874676	-.105784

Data for Meller 180 α-Al_2O_3

V(susp)=	39.5656	V(std)=	40	material=	Meller 180 soxhleted (a2x6-)
C(OH,sp)=	.1018	C(OH,sd)=	.1018	comments=	
C(H,sp)=	.011369	C(H,sd)=	.011369	titrants	.1N NaOH (a2x), 1% HCl (a2x)
DATA	a2x43-1,43-4	DATA	a2x43-3,51-2	salt=	1N NaCl
TABLE		TABLE	a2x63	conc.=	1
Ms =	1.2365	pH(pzc)=	8.75	file #	a2x45a
As =	21.31	dsigmax = 0		date=	4/17/83
Ns =	2.7 assumed				

pH	VT(sp)	VT(std)	mEQsus	mEQ	mEQstd	dlta mEQ	dsigma	sigma	alpha	pQ	alpha*	alpha*ion	pQ*ion
12.00	N/A	N/A	N/A	0	N/A	N/A	N/A	N/A	N/A	N/A	N/A	N/A	N/A
11.50	N/A	N/A	N/A	0	N/A	N/A	N/A	N/A	N/A	N/A	N/A	N/A	N/A
11.00	-1.776	-.8788	-.180797	0	-.088490	-.092307	-33.7997	-33.7997	.7813485	10.44691	8.813485	7.813485	10.44691
10.50	-.655	-.23	-.066679	0	-.023160	-.043519	-15.9354	-15.9354	.3683783	10.73416	4.683783	3.683783	10.73416
10.00	-.326	-.074	-.033187	0	-.007451	-.025735	-9.42348	-9.42348	.2178430	10.55315	3.178430	2.178430	10.55315
9.50	-.147	-.024	-.014965	0	-.002417	-.012548	-4.59465	-4.59465	.1062147	10.42505	2.062147	1.062147	10.42505
9.00	-.03	-.0062	-.003054	0	-.000624	-.002430	-.889676	-.889676	.0205667	10.67781	1.205667	.2056667	10.67781
8.50	.135	0	.0015348	0	0	.0015348	.5620000	.5620000	.0129918	6.619348	1.129918	.1299177	6.619348
8.00	.875	0	.0099479	0	0	.0099479	3.642592	3.642592	.0842059	6.963545	1.842059	.8420594	6.963545
7.50	1.69	0	.0192136	0	0	.0192136	7.035407	7.035407	.1626378	6.788308	2.626378	1.626378	6.788308
7.00	2.5	.0005	.0284225	0	.0000056	.0284169	10.40535	10.40535	.2405408	6.500684	3.405408	2.405408	6.500684
6.50	3.41	.023	.0387683	0	.0002586	.0385096	14.10099	14.10099	.3259732	6.184505	4.259732	3.259732	6.184505
6.00	4.425	.043	.0503078	0	.0004836	.0498243	18.24405	18.24405	.4217483	5.862936	5.217483	4.217483	5.862936
5.50	5.24	.0597	.0595736	0	.0006714	.0589022	21.56809	21.56809	.4985904	5.497551	5.985904	4.985904	5.497551
5.00	5.9	.0867	.0670771	0	.0009750	.0661021	24.20447	24.20447	.5595356	5.103917	6.595356	5.595356	5.103917
4.50	6.565	.1485	.0746375	0	.0016700	.0729675	26.71836	26.71836	.6176494	4.708280	7.176494	6.176494	4.708280
4.00	7.34	.323	.0834485	0	.0036323	.0798162	29.22611	29.22611	.6756211	4.318651	7.756211	6.756211	4.318651
3.50	8.537	.8567	.0970572	0	.0096340	.0874231	32.01153	32.01153	.7400118	3.954285	8.400118	7.400118	3.954285

V(susp)=	39.5656	V(std)=	40	material=	Meller 180 soxhleted (a2x6-)
C(OH,sp)=	.1018	C(OH,sd)=	.1018	comments=	
C(H,sp)=	.011369	C(H,sd)=	.011369	titrants	.1N NaOH (a2x), 1% HCl (a2x)
DATA	a2x43-1,43-4	DATA	a2x43-3,51-2	salt=	0.1N NaCl
TABLE		TABLE	a2x65	conc.=	.1
Ms =	1.2365	pH(pzc)=	8.75	file #	a2x45b
As =	21.31	dsigmax = 0		date=	4/17/83
Ns =	2.7 assumed				

pH	VT(sp)	VT(std)	mEQsus	mEQ	mEQstd	dlta mEQ	dsigma	sigma	alpha	pQ	alpha*	alpha*ion	pQ*ion
12.00	N/A	N/A	N/A	0	N/A	N/A	N/A	N/A	N/A	N/A	N/A	N/A	N/A
11.50	N/A	N/A	N/A	0	N/A	N/A	N/A	N/A	N/A	N/A	N/A	N/A	N/A
11.00	-1.063	-.4982	-.108722	0	-.050166	-.058556	-21.4415	-21.4415	.4956635	11.00753	5.272863	5.956635	10.00753
10.50	-.44	-.141	-.044792	0	-.014198	-.030594	-11.2026	-11.2026	.2589702	10.95659	2.905930	3.589702	9.956586
10.00	-.21	-.0472	-.021378	0	-.004753	-.016625	-6.08762	-6.08762	.1407278	10.78575	1.723506	2.407278	9.785751
9.50	-.093	-.0157	-.009467	0	-.001581	-.007886	-2.88778	-2.88778	.0667570	10.64550	.9837974	1.667570	9.645498
9.00	-.017	-.005	-.001731	0	-.000503	-.001227	-.449335	-.449335	.0103873	10.97896	.4201007	1.103873	9.978963
8.50	.265	-.0017	.0030128	0	-.000171	.0031840	1.165866	1.165866	.0269514	6.942446	.5857414	1.269514	7.942846
8.00	.765	-.001	.0086973	0	-.000101	.0087980	3.221538	3.221538	.0744724	6.905606	1.060952	1.744724	7.905606
7.50	1.29	0	.0146660	0	0	.0146660	5.370222	5.370222	.1241436	6.651491	1.557664	2.241436	7.651491
7.00	1.855	0	.0210895	0	0	.0210895	7.722296	7.722296	.1785166	6.337080	2.101394	2.785166	7.337080
6.50	2.5	.0055	.0284225	0	.0000619	.0283606	10.38476	10.38476	.2400649	5.999552	2.716876	3.400649	6.999552
6.00	3.255	.016	.0370061	0	.0001799	.0368262	13.48456	13.48456	.3117231	5.656006	3.433458	4.117231	6.656006
5.50	3.95	.0295	.0449076	0	.0003317	.0445758	16.32223	16.32223	.3773216	5.282448	4.089443	4.773216	6.282448
5.00	4.6	.0575	.0522974	0	.0006466	.0516508	18.91286	18.91286	.4372092	4.890342	4.688320	5.372092	5.890342
4.50	5.39	.143	.0612789	0	.0016081	.0596708	21.84953	21.84953	.5050964	4.508854	5.367192	6.050964	5.508854
4.00	6.42	.385	.0729890	0	.0043295	.0686594	25.14089	25.14089	.5811828	4.142288	6.128056	6.811828	5.142288
3.50	7.87	1.128	.0894740	0	.0126850	.0767891	28.11769	28.11769	.6499977	3.768841	6.816205	7.499977	4.768841

V(susp)=	39.5656	V(std)=	40	material=	Moller 180 soxhleted (s2x6-)
C(OH,sp)=	.1018	C(OH,sd)=	.1018	comments=	
C(H,sp)=	.011369	C(H,sd)=	.011369	titrants	.1N NaOH (s2x), 1% HCl (s2x)
DATA	e2x43-1,43-4	DATA	e2x43-3,51-2	salt=	0.01N NaCl
TABLE		TABLE	e2x65	conc.=	.01
Ms =	1.2365	pH(pzc)=	8.75	file #	e2x43c
As =	21.31	dsigmax = 0		date=	4/17/83
Ns =	2.7 assumed				

pH	VT(sp)	VT(std)	mEQsus	mEQ	mEQstd	dlta mEQ	dsigma	sigma	alpha	pQ	alpha*	alpha*ion	pQ*ion
12.00	N/A	N/A	N/A	0	N/A	N/A	N/A	N/A	N/A	N/A	N/A	N/A	N/A
11.50	N/A	N/A	N/A	0	N/A	N/A	N/A	N/A	N/A	N/A	N/A	N/A	N/A
11.00	-.9085	-.4519	-.092485	0	-.045504	-.046981	-17.2031	-17.2031	.3976849	11.18028	4.076849	5.976849	9.180285
10.50	-.339	-.134	-.034510	0	-.013493	-.021017	-7.69580	-7.69580	.1779042	11.16474	1.879042	3.779042	9.164736
10.00	-.158	-.039	-.016084	0	-.003927	-.012157	-4.45162	-4.45162	.1029082	10.94039	1.129082	3.029082	8.940397
9.50	-.075	-.0097	-.007635	0	-.000977	-.006658	-2.43804	-2.43804	.0563603	10.72303	.6636032	2.563603	8.723033
9.00	-.029	0	-.002952	0	0	-.002952	-1.08100	-1.08100	.0249895	10.59125	.3498954	2.249895	8.591251
8.50	0	0	0	0	0	0	0	0	0	ERROR	.1	2	ERROR
8.00	.105	0	.0011937	0	0	.0011937	.4371111	.4371111	.0101047	6.008935	.2010471	2.101047	8.008935
7.50	.305	0	.0034675	0	0	.0034675	1.269704	1.269704	.0293518	5.980573	.3935179	2.293518	7.980573
7.00	.56	0	.0063666	0	0	.0063666	2.331259	2.331259	.0538918	5.755582	.6389180	2.538918	7.755582
6.50	.92	.0047	.0104595	0	.0000529	.0104066	3.810572	3.810572	.0880891	5.484970	.9808914	2.880891	7.484970
6.00	1.4	.0105	.0159166	0	.0001181	.0157985	5.784911	5.784911	.1337300	5.188576	1.437300	3.337300	7.188576
5.50	1.98	.022	.0225106	0	.0002474	.0222632	8.152076	8.152076	.1884518	4.865886	1.984518	3.884518	6.865886
5.00	2.7	.0515	.0306963	0	.0005791	.0301172	11.02793	11.02793	.2549332	4.534231	2.649332	4.549332	6.534231
4.50	3.615	.135	.0410989	0	.0015181	.0395808	14.49321	14.49321	.3350402	4.202301	3.450402	5.350402	6.202301
4.00	5.115	.46	.0581524	0	.0051729	.0529795	19.39939	19.39939	.4484564	3.910140	4.584564	6.484564	5.910140
3.50	6.864	1.578	.0780368	0	.0177455	.0602914	22.07676	22.07676	.5103493	3.517981	5.203493	7.103493	5.517981

V(susp)=	39.5656	V(std)=	40	material=	Moller 180 soxhleted (s2x6-)
C(OH,sp)=	.1018	C(OH,sd)=	.1018	comments=	
C(H,sp)=	.011369	C(H,sd)=	.011369	titrants	.1N NaOH (s2x), 1% HCl (s2x)
DATA	e2x43-1,43-4	DATA	e2x43-3,51-2	salt=	0.001N NaCl
TABLE		TABLE	e2x65	conc.=	.001
Ms =	1.2365	pH(pzc)=	8.75	file #	e2x43d
As =	21.31	dsigmax = 0		date=	4/17/83
Ns =	2.7 assumed				

pH	VT(sp)	VT(std)	mEQsus	mEQ	mEQstd	dlta mEQ	dsigma	sigma	alpha	pQ	alpha*	alpha*ion	pQ*ion
12.00	N/A	N/A	N/A	0	N/A	N/A	N/A	N/A	N/A	N/A	N/A	N/A	N/A
11.50	N/A	N/A	N/A	0	N/A	N/A	N/A	N/A	N/A	N/A	N/A	N/A	N/A
11.00	-1.079	-.5635	-.109842	0	-.056741	-.053101	-19.4438	-19.4438	.4494039	11.08806	4.526461	7.494839	8.088056
10.50	-.44	-.19	-.044792	0	-.019132	-.025660	-9.39589	-9.39589	.2172051	11.05678	2.203674	5.172051	8.056778
10.00	-.187	-.065	-.019037	0	-.006543	-.012491	-4.57397	-4.57397	.1057367	10.92724	1.088990	4.057367	7.927240
9.50	-.0785	-.023	-.007991	0	-.002316	-.005675	-2.07812	-2.07812	.0480400	10.79702	.5120232	3.480400	7.797015
9.00	-.03	-.0097	-.003054	0	-.000977	-.002077	-.760627	-.760627	.0175834	10.74719	.2074573	3.175834	7.747192
8.50	-.0035	-.0047	-.000356	0	-.000473	.0001170	.0428284	.0428284	.0009901	5.496095	.0415234	3.009901	8.496095
8.00	0	-.003	0	0	-.000302	.0003021	.1106132	.1106132	.0025570	5.408851	.0571933	3.025570	8.408851
7.50	0	-.0017	0	0	-.000171	.0001712	.0626808	.0626808	.0014490	4.661697	.0461127	3.014490	7.661697
7.00	.085	0	.0009664	0	0	.0009664	.3538518	.3538518	.0081800	4.916321	.1134228	3.081800	7.916321
6.50	.245	0	.0027854	0	0	.0027854	1.019926	1.019926	.0235777	4.882863	.2673994	3.235777	7.882863
6.00	.465	0	.0052866	0	0	.0052866	1.935778	1.935778	.0447494	4.670670	.4791172	3.447494	7.670670
5.50	.78	0	.0088678	0	0	.0088678	3.247181	3.247111	.0750636	4.409317	.7822586	3.750636	7.409317
5.00	1.27	.0207	.0144386	0	.0002328	.0142058	5.201725	5.201725	.1202485	4.135720	1.234107	4.202485	7.135720
4.50	1.97	.068	.0223969	0	.0009896	.0214073	7.838674	7.838674	.1812069	3.845001	1.843692	4.812069	6.845001
4.00	2.915	.495	.0331406	0	.0055665	.0275741	10.09675	10.09675	.2334069	3.483549	2.365692	5.334069	6.483549
3.50	4.603	2.037	.0523315	0	.0229072	.0294244	10.77425	10.77425	.2490688	3.020719	2.522311	5.490688	6.020719

Data for Meller 182 $\alpha\gamma$-Al_2O_3

V(susp)= 39.55 | V(std)= 40 | material= Meller 182 soxhleted (s2x6-2)
C(OH,sp)= .1018 | C(OH,sd)= .1018 | comments=
C(H,sp)= .11369 | C(H,sd)= .11369 | titrants .1N NaOH (s2x), 1% HCl (s2x)
DATA e2x43-2,44-3 | DATA e2x43-3,51-2 | salt= 1N NaCl
TABLE e2x72 | TABLE e2x65 | conc.= 1
Ms = .8769 | pH(pzc)= 7.1 | file # s3x10a
As = 79.678 | dsigmax = 0 | date= 4/17/83
Ns = 2.7 assumed

pH	VT(sp)	VT(std)	mEQmeas	mEQ	mEQstd	dlta mEQ	dsigma	sigma	alpha	pQ	alpha*	alpha*ion	pQ*ion
12.00	N/A	N/A	N/A	0	N/A	N/A	N/A	N/A	N/A	N/A	N/A	N/A	N/A
11.50	N/A	N/A	N/A	0	N/A	N/A	N/A	N/A	N/A	N/A	N/A	N/A	N/A
11.00	N/A	-.8788	N/A	0	-.0086679	N/A	N/A	N/A	N/A	N/A	N/A	N/A	N/A
10.50	N/A	-.23	N/A	0	-.0023209	N/A	N/A	N/A	N/A	N/A	N/A	N/A	N/A
10.00	N/A	-.074	N/A	0	-.0007467	N/A	N/A	N/A	N/A	N/A	N/A	N/A	N/A
9.50	N/A	-.024	N/A	0	-.0002422	N/A	N/A	N/A	N/A	N/A	N/A	N/A	N/A
9.00	N/A	-.0062	N/A	0	-.0000626	N/A	N/A	N/A	N/A	N/A	N/A	N/A	N/A
8.50	N/A	0	N/A	0	0	N/A	N/A	N/A	N/A	N/A	N/A	N/A	N/A
8.00	N/A	0	N/A	0	0	N/A	N/A	N/A	N/A	N/A	N/A	N/A	N/A
7.50	N/A	.001	N/A	0	.0001127	N/A	N/A	N/A	N/A	N/A	N/A	N/A	N/A
7.00	N/A	.002	N/A	0	.0002254	N/A	N/A	N/A	N/A	N/A	N/A	N/A	N/A
6.50	.127	.004	.0144386	0	.0004508	.0139878	1.931614	1.931614	.0446532	5.169691	1.446532	.4465318	5.169691
6.00	.32	.0065	.0363808	0	.0007325	.0356483	4.922752	4.922752	.1137994	5.108608	2.137994	1.137994	5.108608
5.50	.506	.0082	.0575271	0	.0009241	.0566030	7.815441	7.816441	.1806930	4.843495	2.806930	1.806930	4.843495
5.00	.661	.01	.0751491	0	.0011270	.0740221	10.22180	10.22180	.2362997	4.490540	3.362997	2.362997	4.490540
4.50	.8032	.0143	.0913158	0	.0016115	.0897043	12.38746	12.38746	.2863615	4.103436	3.863615	2.863615	4.103436
4.00	.967	.026	.1099382	0	.0029301	.1070082	14.77700	14.77700	.3416004	3.715029	4.416004	3.416004	3.715029
3.50	N/A	.0605	N/A	0	.0068181	N/A	N/A	N/A	N/A	N/A	N/A	N/A	N/A
3.00	1.384	.1646	.1573470	0	.0185496	.1387973	19.16684	19.16684	.4430805	2.900690	5.430805	4.430805	2.900690

V(susp)= 39.65 | V(std)= 40 | material= Meller 182
C(OH,sp)= .1018 | C(OH,sd)= .1018 | comments= soxhleted s2x6-2
C(H,sp)= .11369 | C(H,sd)= .11369 | titrants .1N NaOH (s2x), 1% HCl (s2x)
DATA e2x43-2,44-3 | DATA e2x43-3,51-2 | salt= 0.1N NaCl
TABLE e2x72 | TABLE e2x65 | conc.= .1
Ms = .8769 | pH(pzc)= 7.1 | file # s3x10b
As = 79.678 | dsigmax = 0 | date= 4/17/83
Ns = 2.7 assumed

pH	VT(sp)	VT(std)	mEQmeas	mEQ	mEQstd	dlta mEQ	dsigma	sigma	alpha	pQ	alpha*	alpha*ion	pQ*ion
12.00	N/A	N/A	N/A	0	N/A	N/A	N/A	N/A	N/A	N/A	N/A	N/A	N/A
11.50	N/A	N/A	N/A	0	N/A	N/A	N/A	N/A	N/A	N/A	N/A	N/A	N/A
11.00	-2.507	-.4982	-.255213	0	-.050273	-.204940	-28.3006	-28.3006	.6542254	10.72307	6.858482	7.542254	9.723066
10.50	-1.68	-.141	-.171024	0	-.014228	-.156796	-21.6523	-21.6523	.5005367	10.49907	5.321573	6.005367	9.499068
10.00	-1.28	-.0472	-.130304	0	-.004763	-.125541	-17.3363	-17.3363	.4007628	10.17471	4.323835	5.007628	9.174711
9.50	-1.022	-.0157	-.104040	0	-.001584	-.102455	-14.1483	-14.1483	.3270665	9.813336	3.506093	4.270665	8.813336
9.00	-.805	-.005	-.081949	0	-.000505	-.081444	-11.2468	-11.2468	.2599938	9.454272	2.916166	3.599938	8.454272
8.50	-.597	-.0017	-.060775	0	-.000172	-.060603	-8.36881	-8.36881	.1934621	9.120029	2.250849	2.934621	8.120029
8.00	-.352	-.001	-.035834	0	-.000101	-.035733	-4.93441	-4.93441	.1140689	8.890233	1.456917	2.140689	7.890233
7.50	-.12	0	-.012216	0	0	-.012216	-1.68694	-1.68694	.0389969	8.891694	.7061972	1.389969	7.891694
7.00	.0315	.0005	.0035812	0	.0000563	.0035249	.4867597	.4867597	.0112524	5.056161	.4287522	1.112524	6.056161
6.50	.204	.0047	.0231928	0	.0005297	.0226631	3.129590	3.129590	.0723470	5.392035	1.039698	1.723470	6.392035
6.00	.391	.0065	.0444528	0	.0007325	.0437203	6.037431	6.037431	.1395675	5.210068	1.711903	2.395675	6.210068
5.50	.551	.0082	.0626432	0	.0009241	.0617191	8.522920	8.522926	.1970248	4.889819	2.286476	2.970248	5.889819
5.00	.6985	.0115	.0794125	0	.0012960	.0781165	10.78728	10.78728	.2493699	4.521418	2.809927	3.493699	5.521418
4.50	.842	.0185	.0957270	0	.0020849	.0936421	12.93125	12.93125	.2989322	4.129813	3.305550	3.989322	5.129813
4.00	1.0225	.0385	.1162480	0	.0043388	.1119093	15.45380	15.45380	.3572461	3.744923	3.888689	4.572461	4.744923
3.50	1.233	.099	.1401798	0	.0111568	.1290229	17.81707	17.81707	.4118779	3.345301	4.435006	5.118779	4.345301
3.00	1.525	.2842	.1733773	0	.0320280	.1413493	19.51924	19.51924	.4512279	2.915002	4.828498	5.512270	3.915002

V(susp)= 39.65	V(std)= 40	material= Meller 182
C(OH,sp)= .1018	C(OH,sd)= .1018	comments= soxhleted s2x6-2
C(H,sp)= .11369	C(H,sd)= .11369	titrants .1N NaOH (s2x), 1% HCl (s2x)
DATA e2x43-2,44-3	DATA e2x43-3,51-2	salt= 0.01N NaCl
TABLE e2x72	TABLE e2x65	conc.= .01
Ms = .8769	pH(pzc)= 7.1	file # e3x10c
As = 79.678	dsigmax = 0	date= 4/17/83
Ns = 2.7 assumed		

pH	VT(sp)	VT(std)	mEQsus	mEQ	mEQstd	dlta mEQ	dsigma	sigma	alpha	pQ	alpha*	alpha*ion	pQ*ion
12.00	N/A	N/A	N/A	0	N/A	N/A	N/A	N/A	N/A	N/A	N/A	N/A	N/A
11.50	N/A	N/A	N/A	0	N/A	N/A	N/A	N/A	N/A	N/A	N/A	N/A	N/A
11.00	-2.083	-.4519	-.212049	0	-.045601	-.166449	-22.9853	-22.9853	.5313509	10.94547	5.413509	7.313509	8.945466
10.50	-1.44	-.134	-.146592	0	-.013522	-.133070	-18.3760	-18.3760	.4247977	10.63164	4.347977	6.247977	8.631638
10.00	-1.137	-.039	-.115747	0	-.003935	-.111811	-15.4403	-15.4403	.3569329	10.25567	3.669329	5.569329	8.255670
9.50	-.94	-.0097	-.095692	0	-.000979	-.094713	-13.0792	-13.0792	.3023514	9.863125	3.123514	5.023514	7.863125
9.00	-.767	0	-.078081	0	0	-.078081	-10.7823	-10.7823	.2492554	9.478848	2.592554	4.492554	7.478848
8.50	-.58	0	-.059044	0	0	-.059044	-8.15352	-8.15352	.1884852	9.134019	1.984852	3.884852	7.134019
8.00	-.352	0	-.035834	0	0	-.035834	-4.94834	-4.94834	.1143910	8.888850	1.243910	3.143910	6.888850
7.50	-.142	0	-.014456	0	0	-.014456	-1.99621	-1.99621	.0461464	8.815344	.5614638	2.461464	6.815344
7.00	-.01	.0025	-.001018	0	.0002817	-.001300	-.179484	-.179484	.0041491	9.380237	.1414913	2.041491	7.380237
6.50	.086	.0017	.0097773	0	.0001916	.0095858	1.323719	1.323719	.0306005	4.999225	.4060046	2.306005	6.999225
6.00	.219	.0032	.0248981	0	.0003606	.0245375	3.388437	3.388437	.0783306	4.929356	.8833062	2.783306	6.929356
5.50	.342	.0042	.0388820	0	.0004733	.0384087	5.303939	5.303939	.1226113	4.645339	1.326113	3.226113	6.645339
5.00	.469	.007	.0533206	0	.0007889	.0525317	7.254227	7.254227	.1676962	4.304241	1.776962	3.676962	6.304241
4.50	.606	.013	.0688961	0	.0014650	.0674311	9.311713	9.311713	.2152592	3.938236	2.252592	4.152592	5.938236
4.00	.797	.0315	.0906109	0	.0035499	.0870610	12.02245	12.02245	.2779235	3.585342	2.879235	4.779235	5.585342
3.50	1.05	.094	.1193745	0	.0105933	.1087812	15.02183	15.02183	.3472603	3.225915	3.572603	5.472603	5.225915
3.00	1.419	.3162	.1613261	0	.0356342	.1256919	17.35708	17.35708	.4012442	2.826159	4.112442	6.012442	4.826159

V(susp)= 39.65	V(std)= 40	material= Meller 182
C(OH,sp)= .1018	C(OH,sd)= .1018	comments= soxhlete s2x6-2
C(H,sp)= .11369	C(H,sd)= .11369	titrants .1N NaOH (s2x), 1% HCl (s2x)
DATA e2x43-2,44-3	DATA e2x43-3,51-2	salt= 0.001N NaCl
TABLE e2x72	TABLE e2x65	conc.= .001
Ms = .8769	pH(pzc)= 7.1	file # e3x10d
As = 79.678	dsigmax = 0	date= 4/17/83
Ns = 2.7 assumed		

pH	VT(sp)	VT(std)	mEQsus	mEQ	mEQstd	dlta mEQ	dsigma	sigma	alpha	pQ	alpha*	alpha*ion	pQ*ion
12.00	N/A	N/A	N/A	0	N/A	N/A	N/A	N/A	N/A	N/A	N/A	N/A	N/A
11.50	N/A	N/A	N/A	0	N/A	N/A	N/A	N/A	N/A	N/A	N/A	N/A	N/A
11.00	-2.397	-.5635	-.244015	0	-.056862	-.187152	-25.8443	-25.8443	.5974431	10.82853	6.006053	8.974431	7.828531
10.50	-1.56	-.19	-.158808	0	-.019173	-.139635	-19.2825	-19.2825	.4457553	10.59460	4.489176	7.457553	7.594605
10.00	-1.19	-.065	-.121142	0	-.006559	-.114583	-15.8230	-15.8230	.3657811	10.23902	3.689434	6.657811	7.239018
9.50	-.992	-.023	-.100986	0	-.002321	-.098665	-13.6248	-13.6248	.3149657	9.837449	3.181280	6.149657	6.837449
9.00	-.832	-.0097	-.084698	0	-.000979	-.083719	-11.5609	-11.5609	.2672541	9.438329	2.704164	5.672541	6.438329
8.50	-.675	-.0047	-.068715	0	-.000474	-.068241	-9.42352	-9.42352	.2178438	9.055148	2.210060	5.178438	6.055148
8.00	-.5	-.003	-.0509	0	-.000303	-.050597	-6.98709	-6.98709	.1615209	8.715264	1.646831	4.615209	5.715264
7.50	-.312	-.0017	-.031762	0	-.000172	-.031590	-4.36234	-4.36234	.1008444	8.450183	1.040067	4.008444	5.450183
7.00	-.157	0	-.015983	0	0	-.015983	-2.20707	-2.20707	.0510210	8.269508	.5418327	3.510210	5.269508
6.50	-.042	.0017	-.004276	0	.0001916	-.004467	-.616883	-.616883	.0142605	8.339627	.1742279	3.142605	5.339627
6.00	.0145	.0032	.0016485	0	.0003606	.0012879	.1778463	.1778463	.0041113	3.615766	.0727356	3.041113	6.615766
5.50	.0817	.0042	.0092885	0	.0004733	.0088152	1.217304	1.217304	.0281405	3.961728	.3130275	3.281405	6.961728
5.00	.1582	.0057	.0179858	0	.0006424	.0173434	2.394989	2.394989	.0553650	3.767972	.5852732	3.553650	6.767972
4.50	.2635	.0098	.0299573	0	.0011044	.0288529	3.984362	3.984362	.0921067	3.506256	.9526893	3.921067	6.506256
4.00	.419	.0225	.0476361	0	.0025356	.0451005	6.228025	6.228025	.1439733	3.225795	1.471358	4.439733	6.225795
3.50	.77	.0785	.0875413	0	.0088466	.0786947	10.86713	10.86713	.2512159	3.025691	2.543782	5.512159	6.025691
3.00	1.219	.3593	.1385881	0	.0404914	.0980967	13.54640	13.54640	.3131526	2.658896	3.163148	6.131526	5.658896

Data for Baikowski's Mullite

V(susp)= 38.7074 | V(std)= 40 | material= Baikowski Mullite
C(OH,sp)= .1018 | C(OH,sd)= .1018 | comments= soxhleted (s2x6-4)
C(H,sp)= .11369 | C(H,sd)= .11369 | titrants .1N NaOH (s2x), 1% HCl (s2x)
DATA e2x71-2,71-1 | DATA e2x43-3,51-2 | salt= 1N NaCl
TABLE e2x74 | TABLE e2x65 | conc.= 1
Ms = 3.5128 | pH(pzc)= 8.5 | file # e3x15a
As = 6.87 | dsigmax = 0 | date= 4/13/83
Ns = N/A

pH	VT(sp)	VT(std)	mEQsus	mEQ	mEQstd	dlta mEQ	dsigma	sigma
12.00	N/A	N/A	N/A	0	N/A	N/A	N/A	N/A
11.50	N/A	N/A	N/A	0	N/A	N/A	N/A	N/A
11.00	N/A	-.8788	N/A	0	-.086571	N/A	N/A	N/A
10.50	-1.306	-.23	-.132951	0	-.022657	-.110293	-44.0958	-44.0958
10.00	-.56	-.074	-.057008	0	-.007290	-.049718	-19.8776	-19.8776
9.50	-.272	-.024	-.027690	0	-.002364	-.025325	-10.1252	-10.1252
9.00	-.0915	-.0062	-.009315	0	-.000611	-.008704	-3.47987	-3.47987
8.50	0	0	0	0	0	0	0	0
8.00	.045	0	.0051161	-0	0	.0051161	2.045420	2.045420
7.50	.1082	.001	.0123013	0	.0001100	.0121912	4.874113	4.874113
7.00	.2105	.002	.0239317	0	.0002200	.0237117	9.480049	9.480049
6.50	.34	.004	.0386546	0	.0004401	.0382145	15.27834	15.27834
6.00	.442	.0065	.0502510	0	.0007151	.0495359	19.80467	19.80467
5.50	.5285	.0082	.0600852	0	.0009021	.0591830	23.66164	23.66164
5.00	.637	.01	.0724205	0	.0011002	.0713204	28.51420	28.51420
4.50	.87	.0143	.0989103	0	.0015732	.0973371	38.91580	38.91580
4.00	3.068	.026	.3488009	0	.0028604	.3459405	138.3086	138.3086

V(susp)= 38.7074 | V(std)= 40 | material= Baikowski Mullite
C(OH,sp)= .1018 | C(OH,sd)= .1018 | comments= soxhleted s2x6-4
C(H,sp)= .11369 | C(H,sd)= .11369 | titrants .1N NaOH (s2x), 1% HCl (s2x)
DATA e2x71-2,71-1 | DATA e2x43-3,51-2 | salt= 0.1N NaCl
TABLE e2x74 | TABLE e2x65 | conc.= .1
Ms = 3.5128 | pH(pzc)= 8.5 | file # e3x15b
As = 6.87 | dsigmax = 0 | date= 4/13/83
Ns = N/A

pH	VT(sp)	VT(std)	mEQsus	mEQ	mEQstd	dlta mEQ	dsigma	sigma
12.00	N/A	N/A	N/A	0	N/A	N/A	N/A	N/A
11.50	N/A	N/A	N/A	0	N/A	N/A	N/A	N/A
11.00	-1.167	-.4982	-.118801	0	-.049078	-.069723	-27.8755	-27.8755
10.50	-.46	-.141	-.046828	0	-.013890	-.032938	-13.1688	-13.1688
10.00	-.205	-.0472	-.020869	0	-.004650	-.016219	-6.48435	-6.48435
9.50	-.09	-.0157	-.009162	0	-.001547	-.007615	-3.04467	-3.04467
9.00	-.025	-.005	-.002545	0	-.000493	-.002052	-.820578	-.820578
8.50	.002	-.0017	.0002274	0	-.000167	.0003948	.1578618	.1578618
8.00	.0417	-.001	.0047409	0	-.000099	.0048394	1.934807	1.934807
7.50	.0945	0	.0107437	0	0	.0107437	4.295381	4.295381
7.00	.1725	.0005	.0196115	0	.0000550	.0195565	7.818783	7.818783
6.50	.284	.0047	.0322880	0	.0005171	.0317709	12.70214	12.70214
6.00	.412	.0065	.0468403	0	.0007151	.0461252	18.44105	18.44105
5.50	.5255	.0082	.0597441	0	.0009021	.0588420	23.52528	23.52528
5.00	.637	.0115	.0724205	0	.0013652	.0711553	28.44823	28.44823
4.50	.83	.0185	.0943627	0	.0020353	.0923274	36.91291	36.91291
4.00	2.931	.0385	.3332254	0	.0042356	.3289898	131.5316	131.5316

V(susp)=	38.7074	V(std)=	40	material=	Baikowski Mullite
C(OH,sp)=	.1018	C(OH,sd)=	.1018	comments=	soxhlet s2x6-4
C(H,sp)=	.11369	C(H,sd)=	.11369	titrants	.1N NaOH (s2x), 1% HCl (s2x)
DATA	e2x71-2,71-1	DATA	e2x43-3,51-2	salt=	0.01N NaCl
TABLE	e2x74	TABLE	e2x65	conc.=	.01
Ms =	3.5128	pH(pzc)=	8.5	file #	o3x15c
As =	6.87	dsigmax =	0	date=	4/13/83
Ns =	N/A				

pH	VT(sp)	VT(std)	mEQsus	mEQ	mEQstd	dlta mEQ	dsigma	sigma
12.00	N/A	N/A	N/A	0	N/A	N/A	N/A	N/A
11.50	N/A	N/A	N/A	0	N/A	N/A	N/A	N/A
11.00	-.84	-.4519	-.085512	0	-.044517	-.040995	-16.3901	-16.3901
10.50	-.337	-.134	-.034307	0	-.013200	-.021106	-8.43836	-8.43836
10.00	-.145	-.039	-.014761	0	-.003842	-.010919	-4.36550	-4.36550
9.50	-.057	-.0097	-.005803	0	-.000956	-.004847	-1.93787	-1.93787
9.00	-.012	0	-.001222	0	0	-.001222	-.488401	-.488401
8.50	0	0	0	0	0	0	0	0
8.00	.0285	0	.0032402	0	0	.0032402	1.295432	1.295432
7.50	.0727	0	.0082653	0	0	.0082653	3.304489	3.304489
7.00	.1325	.0025	.0150639	0	.0002750	.0147889	5.912662	5.912662
6.50	.208	.0017	.0236475	0	.0001870	.0234605	9.379610	9.379610
6.00	.2975	.0032	.0338228	0	.0003521	.0334707	13.38175	13.38175
5.50	.4095	.0042	.0465561	0	.0004621	.0460940	18.42858	18.42858
5.00	.5275	.007	.0599715	0	.0007701	.0592014	23.66897	23.66897
4.50	.664	.013	.0754902	0	.0014302	.0740600	29.60950	29.60950
4.00	1.291	.0315	.1467738	0	.0034655	.1433083	57.29529	57.29529

V(susp)=	38.7074	V(std)=	40	material=	Baikowski Mullite
C(OH,sp)=	.1018	C(OH,sd)=	.1018	comments=	soxhlets s2x6-4
C(H,sp)=	.11369	C(H,sd)=	.11369	titrants	.1N NaOH (s2x), 1% HCl (s2x)
DATA	e2x71-2,71-1	DATA	e2x43-3,51-2	salt=	0.001N NaCl
TABLE	e2x74	TABLE	e2x65	conc.=	.001
Ms =	3.5128	pH(pzc)=	8.5	file #	o3x15d
As =	6.87	dsigmax =	0	date=	4/13/83
Ns =	N/A				

pH	VT(sp)	VT(std)	mEQsus	mEQ	mEQstd	dlta mEQ	dsigma	sigma
12.00	N/A	N/A	N/A	0	N/A	N/A	N/A	N/A
11.50	N/A	N/A	N/A	0	N/A	N/A	N/A	N/A
11.00	-.993	-.5635	-.101087	0	-.055511	-.045577	-18.2218	-18.2218
10.50	-.38	-.19	-.038684	0	-.018717	-.019967	-7.98291	-7.58291
10.00	-.15	-.065	-.01527	0	-.006403	-.008867	-3.54500	-3.54500
9.50	-.057	-.023	-.005803	0	-.002266	-.003537	-1.41405	-1.41405
9.00	-.012	-.0097	-.001222	0	-.000956	-.000266	-.106368	-.106368
8.50	0	-.0047	0	0	-.000463	.0004630	.1851089	.1851089
8.00	.0317	-.003	.0036040	0	-.000296	.0038995	1.559039	1.559039
7.50	.0742	-.0017	.0084358	0	-.000167	.0086033	3.439624	3.439624
7.00	.1305	0	.0148365	0	0	.0148365	5.931717	5.931717
6.50	.201	.0017	.0228517	0	.0001870	.0226647	9.061434	9.061434
6.00	.281	.0032	.0319469	0	.0003521	.0315948	12.63176	12.63176
5.50	.3745	.0042	.0425769	0	.0004621	.0421148	16.83770	16.83770
5.00	.4855	.0057	.0551965	0	.0006271	.0545694	21.81709	21.81709
4.50	.67	.0098	.0761723	0	.0010782	.0750941	30.02297	30.02297
4.00	1.108	.0225	.1259685	0	.0024754	.1234932	49.37312	49.37312

Bibliography

Abendroth-70a
R.P.Abendroth, "Behavior of a Pyrogenic Silica in Simple Electrolytes," J. Colloid Interface Sci., 34(1970)591.

Ahmed-66a
S.M. Ahmed, "Studies of the Double Layer at Oxide-Solution Interface," Can. J. Chem., 13(1966)1663.

Ahmed-75a
S.M.Ahmed, "Electrochamical Properties of the Oxide Solution Interface in Relation to Floatation," in "Advances in Interfacial Phenomina of Particulate/ Solution/ Gas Systems: Application to Floatation Research" AIChE Symposium Series #150 v.71 1975.

Allen-71a
L.H.Allen, E.Matijevic and L.Meites, "Exchange of Na^+ for the Silanolic Protons of Silica," J. Inorganic Nucl. Chem., 33(1971)1293.

Armistead-69a
C.G.Armistead and A.J.Tyler et al., J. Phys. Chem., 73(1969)3947.

Baran-83a
A.A.Baran, N.S.Mitina, and B.E.Platonov, "Electrical Surface Properties of Zirconium Dioxide in Aqueous 1:1 Electrolyte Solutions," Colloid J- USSR, 44(1983)849.

Barringer-82a
E.A.Barringer and H.K.Bowen, "Formation, Packing and Sintering of Monodispersed TiO_2 Powders," J. Am. Ceram. Soc., 65(1982)C-199.

Berube-68a
Y.G.Berube and P.L.De Bruyn, "Adsorption at the Rutile-Solution Interface," J. Colloid Interface Sci., 28(1968)92.

Bleier-82a
A.Bleier and R.M.Cannon, "Synthesis and Characterization of Uniform Zirconia," unpublished work.

Bleier-83a
A.Bleier, "Acid-Base Properties of Ceramic Powders," in "Advances in Material Characterization," Univ. Ser. Ceram. Sci., R.A.Condrate, D.R.Rossington, and R.L.Snyder eds, (Plenum Publishing Co., New York, 1983).

Bleier-83b
A.Bleier, "The Science of the Interactions of Colloidal Particles and Ceramics Processing," to appear in "Emergent Process Methods for High Technology Ceramics," Mat. Sci.

Res. Ser., R.F.Davis, H.Palmour, and R.L.Porter, eds., (Plenum Press, 1983).

Bleier-83c
A.Bleier and W.C.Hasz, "Structure and Processing Properties of m-ZrO_2," Bull. Am. Ceram. Soc., 62(1983)376.

Boehm-71a
H.P.Boehm, "Acidic and Basic Properties of Hydroxylated Metal Oxide Surfaces," in "Surface Chemistry of Oxides," Discuss of the Faraday Soc #52, The Faraday Society, London, (University Press, Aberdeen, 1972). p 264.

Bolt-57a
G.H.Bolt, "Determination of the Charge Density of Silica Sols," J. Phys. Chem., 61(1957)1166.

Bowden-77a
J.W.Bowden, A.M.Posner and J.P.Quirk, "Ionic Adsorption on Variable Charge Mineral Surfaces. Theoretical-Charge Development and Titration Curves," Aust. J. Soil Res., 15(1977)121.

Bowen-80a
H.K.Bowen, "Basic Research needs on High Temperature Ceramics for Energy Applications," Mat. Sci. and Eng., 44(1980)1.

Brook-81a
R.J.Brook, "Preparation and Electrical Behavior of Zirconia Ceramics," in Adv. in Ceramics v.3, "Science and Technology of Zirconia," eds. A.H.Heuer and L.W.Hobbs, (The Amer. Ceramic S. Inc., 1981).

Brunauer-38a
S.Brunner, P.Emmett, and E.Teller, "Adsorption of Gasses in Multimolecular Layers," J. Am. Ceram. Soc., 60(1938)309.

Chapman-13a
D.L.Chapman, Philos. Mag., 25(1913)475.

Chernoberezhskii-82a
Y.M.Chernoberezhskii, "The Suspension Effect," in "Surface and Colloid Science," v12, ed. E.Matijevic, (Plenum Press, New York, 1982).

Davis-78a
J.A.Davis, R.O.James and J.O.Leckie, "Surface Ionization and Complexation at the Oxide/Water Interface 1. Computation of Electrical Double Layer Properties in Simple Electrolytes," J. Colloid Interface Sci., 63(1978)480.

Davis-78b
J.A.Davis and J.O.Leckie, "Surface Ionization and Complexation at the Oxidation/Water Interface 2. Surface

Properties of Amorphous Iron Oxyhydroxide and Adsorption of Metal Ions," J. Colloid Interface Sci., 67(1978)90.

Evans-82a
A.G.Evans, "Structural Reliability: A Processing-Dependent Phenominon," J. Am. Ceram. Soc., 65(1982)127.

Evans-82b
A.G.Evans, "Considerations of Inhomogeneity Effects in Sintering," J. Am. Ceram. Soc., 65(1982)497.

Gouy-10a
C.Gouy, J. Phys. Chem., 9(1910)457.

Gray-71a
T.J.Gray, in General Discussion, Disscuss Faraday Soc., 52(1971)288.

Grahame-47a
D.C.Grahame, "The Electrical Double Layer and the Theory of Electrocapillarity," Chem. Rev., 41(1947)441.

Greenberg-57a
Greenberg and Price, J. Phys. Chem., 61(1957)1539.

Hair-67a
M.L.Hair, "Infrared Spectroscopy in Surface Chemistry," (Marcel Dekker, New York, 1967).

Healy-77a
T.W.Healy and D.E.Yates, "Nernstialn and Non-Nernstian Potential Differences at Aqueous Interfaces," J. Electroanal. Chem., 80(1977)57.

Healy-78a
T.W.Healy and L.R.White, "Ionizable Surface Group Models of Aqueous Interfaces," Adv. Colloid Interface Sci., 9(1978)303.

Hiemenz-77a
P.C.Hiemenz, "Principles of Colloid and Surface Chemistry," (Marcel Dekker, Inc., N.Y., 1977).

Hohl-76a
H.Hohl and W.Stumm, "Interaction of Pb^{2+} with Hydrous γ-Al_2O_3," J. Colloid Interface Sci., 55(1976)281.

Huang-71a
C.P.Huang, "The Chemistry of the Aluminum Oxide-Electrolyte Interface," Ph.D. Thesis, Harvard University, 1971.

Huang-73a
C.P.Huang and W.Stumm, "Specific Adsorption of Cations on Hydrous γ-Al_2O_3," J. Colloid Interface Sci., 43(1973)409.

Huang-73a
C.P.Huang, "The Determination of Surface Acidity by Alkalimetric Titration," Annual NSF Report (1977).

Huang-81a
C.P.Huang, " The Surface Acidity of Hydrous Solids", in "Adsorption of Inorganics at Solid-Liquid Interfaces," eds. M.A.Anderson and A.J.Rubin, (Ann Arbor Science Publ. Inc., Ann Arbor, Mich., 1981).

Hunter-71a
R.J.Hunter, "The Dependence of Electrokinetic Potential on Concentration of Electrolyte," J. Colloid Interface Sci., 37(1971)564.

Hunter-81a
R.J.Hunter, "Zeta Potential in Colloid Science- Principles and Applications," (Academic Press, New York, 1981).

Iler-76a
R.K.Iler, "The Effect of Surface Aluminosilicate Ions on the Properties of Colloidal Silica," J. Colloid Interface Sci., 55(1976)25.

Iler-79a
R.K.Iler, "The Chemistry of Silica- Solubility, Polymerization, Colloidal and Surface Properties, and Biochemistry ," (John Wiley and Sons, NY, 1979).

James-82a
R.O.James and G.A.Parks, "Characterization of Aqueous Colloids by Their Electrical Double-Layer and Intrinsic Surface Chemical Properties," in "Surface and Colloid Science" V12. ed. E.Matijevic, (Plenum Press, New York, 1982).

James-83a
R.O.James, personal communication, 1983.

Jubb-82a
N.J.Jubb, "The Processing of Boron-Doped Monodispersed SiO_2 Particles," M.S. Thesis, Ceramics Processing Research Laboratory, Report #17, MIT, Cambridge, Ma., July, 1982.

Katsanis-83a
E.P.Katsanis and E.Matijevic, "Properties of Aluminated Silica Sols," Colloid and Polymer Sci., 261(1983)255.

Knozinger-78a
H.Knozinger and P.Ratnasamy, "Catalytic Aluminas: Surface Models and Characterization of Surface Sites," Catal. Rev.-Sci. Eng., 17(1978)31.

Levine-71a
S.Levine and A.L.Smith, "Theory of the Differential Capacity

of the Oxide/Aqueous Electrolyte Interface," Discuss. Faraday Soc, 52(1971)290, "Surface Chemistry of Oxides," The Faraday Soc., London, (University Press, Aberdeen, 1972).

Lyklema-68a
J.Lyklema, "The Structure of the Electrical Double Layer on Porous Surfaces," J. Electroanal. Chem., 18(1968)341.

Lyklema-71a
J.Lyklema, "The Electrical Double Layer on Oxides," Croat. Chem. Acta., 43(1971)249.

Mandel-80a
F.S.Mandel and H.G.Spencer, "Point of Zero Charge of Synthetic Hydrous Zirconia Zr(IV) Oxide Sols," J. Colloid Interface Sci., 77(1980)577.

Meller-83a
"Alumina Powder for Ceramic Manufacturing," The Adolph Meller Co., RI.

Milonjic-83a
S.K.Milonjic, Z.E.Ilic and M.M.Kopecni, "Sorption of Alkali Cations at the Zirconium Oxide/ Aqueous Electrolyte Interface," Colloids and Surfaces, 6(1983)167.

Mikami-83a
N.Mikami etal., "Kinetics of the Adsorption-Desorption of Phosphate on the γ-Al_2O_3 Surface Using the Pressure- Jump Technique," J. Phys. Chem., 87(1983)1454.

Morel-81a
F.M.M.Morel, J.C.Westall and J.G.Yeasted, "Adsorption Models: A Mathematical Analysis in the Framework of General Equilibrium Calculations," in "Adsorption of Inorganics at Solid-Liquid Interfaces," eds. M.A.Anderson and A.J.Rubin, (Ann Arbor Science Publ. Inc., Ann Arbor, Mich., 1981).

Morterra-76a
G.Morterra, G.Ghiotti, E.Garrone, and F.Boccuzzi, J. Chem. S., Faraday Trans 1, 72(1976)2722.

Parfitt-72a
G.D.Parfitt and D.G.Wharton, J. Colloid Interface Sci., 38(1972)431.

Parks-62a
G.A.Parks and P.L. de Bruyn, "The Zero Point of Charge of Oxides," J. Phys. Chem., 66(1962)967.

Parks-65a
G.A.Parks, "The Isoelectric Points of Solid Oxides, Solid Hydroxides, and Aqueous Hydroxo Complex Systems," Chem. Rev., 65(1965)177.

Parks-67a
G.A. Parks, "Aqueous Surface Chemistry of Oxides and Complex Oxide Minerals," Advances in Chemistry Series No.67, (Amer. Chem. Soc., Washington. DC.,1967), p. 121.

Parkyns-72a
N.D.Parkyns, Proc. Int. Congr. Catal., 5th, Palm Beach, Fl., 1972, 1(1973)255.

Peri-65a
J.B.Peri, "Infrared and Gravimetric Study of the Surface Hydration of γ-Alumina," J. Phys. Chem., 69(1965)211.

Peri-65b
J.B.Peri, "A Model for the Surface of γ-Alumina," J. Phys. Chem., 69(1965)220.

Perram-73a
J.W.Perram, J. Chem. Soc. Faraday II, 69(1973)993.

Perram-74a
J.W.Perram, R.J.Hunter, and H.J.L.Wright, "The Oxide-Solution Interface," Austral. J. Chem., 27(1974)461.

Perrot-77a
K.W.Perrot, Clays and Clay Minerals, 25(1977)417.

PQ-78a
"Properties and Applications, Quso Micro-fine Precipitated Silicas" Technical Brochure #18-1, PQ Corporation, Valley Forge, PA.

Pyman-79a
M.A.F.Pyman, J.W.Bowden and A.M.Posner, "The Point of Zero Charge of Amorphous Coprecipitates of Silica with Hydrous Aluminum or Ferric Hydroxide," Clay Minerals, 14(1979)87.

Ray-75a
K.C.Ray and S.Khan, "Electrical Double Layer at Zirconium Oxide-Solution Interface," Indian J. of Chem., 13(1975)577.

Ratnasamy-71a
P.Ratnasamy and A.J.Leonard, in General Discussion, Discuss. Faraday Soc., 52(1971)113.

Regazzoni-83b
A.E.Regazzoni, M.A.Blesa and A.J.G.Maroto, "Interfacial Properties of Zirconium Dioxide and Magnetite in Water," J. Colloid Interface Sci., 91(1983)560.

Rijnten-70a
H.T.Rijnten, "Formation, Preparation and Properties of Hydrous Zirconia," in "Physical and Chemical Aspects of Adsorbents and Catalysts," ed B.G.Linsen, (Academic Press, NY, 1970).

Rhodes-81a
W.H. Rhodes, "Agglomerate and Particle Size Effects on Sintering Yttria-Stabilized Zirconia," J Am. Ceram. S., 64(1981)19.

Sadanaga-62a
R. Sadanaga, M. Tokonami and Y. Takeuchi, Acta Cryst., 15(1962)65.

Schindler-68a
P.W. Schindler and H.R. Kamber, "Die Aciditat von Silanolgruppen," Helv. Chim. Acta, 51(1968)1781.

Schindler-72a
P.W. Schindler and H. Gamsjagr, "Acid-Base Reactions of the TiO_2 (Anatase)- Water Interface and the Point of Zero Charge of TiO_2 Suspensions," Kolloid- Z. u. Z. Polymere, 250(1972)759.

Schindler-81a
P.W. Schindler, "Surface Complexes at Oxide-Water Interfaces," in "Adsorption of Inorganics at Solid-Liquid Interfaces," eds. M.A. Anderson and A.J. Rubin, (Ann Arbor Science Publ. Inc., Ann Arbor, Mich., 1981).

Smit-78a
W. Smit, C.L.M. Holten, H.N. Stein, J.J.M. De Goeij, and H.M.J.J. Theelen, "A Radiotracer Determination of the Adsorption of Sodium Ion in the Compact Part of the Double Layer of Vitreous Silica," J. Colloid Interface Sci., 63(1978)120.

Smit-78b
W. Smit, C.L.M. Holten, H.N. Stein, J.J.M. De Goeij, and H.M.J.J. Theelen, "A Radiotracer Determination of the Sorption of Sodium Ion by Microporous Silica Films," J. Colloid Interface Sci., 63(1978)120.

Smit-80a
W. Smit and C.L.M. Holten, "Zeta Potential and Radiotracer Adsorption Measurement on EFG α-Al_2O_3 Single Crystals in NaBr Solutions," J. Colloid Interface Sci., 78(1980)1.

Smith-81a
A.L. Smith, "Electrical Phenomena Associated with the Solid-Liquid Interface," ch. 3 p.99, in "Dispersion of Powders in Liquids," 3rd ed., G.D. Parfitt, ed., (Applied Sci. Publish Inc, Englewood, NJ, 1981).

Smolik-66a
T. Smolik, Harman and D.W. Fuerstenau, Trans. Soc. Mining Eng. AIME, 235(1966)367.

Sposito-83a

G. Sposito, "On the Surface Complexation Model of the Oxide-Aqueous Solution Interface," J. Colloid Interface Sci., 91(1983)329.

Stern-24a
O. Stern, "On the Theory of the Electrical Double Layer," Z. fur Electrochem., 30(1924)508.

Stober-68a
W. Stober, A. Fink and E. Bohn, "Controlled Growth of Monodisperse Silica Spheres in the Micron Size Range," J. Colloid Interface Sci., 26(1966)62.

Stumm-70a
W. Stumm, C. P. Huang, and S. R. Jenkins, "Specific Chemical Interaction Affecting the Stability of Dispersed Systems," Croat. Chem. Acta, 42(1970)223.

Stumm-76a
W. Stumm, H. Hohl, and F. Dalang, "Interaction of Metal Ions with Hydrous Oxide Surfaces," Croat. Chem. Acta, 48(1976)491.

Stumm-81a
W. Stumm and J. J. Morgan, "Aquatic Chemistry- An Introduction Emphasizing Chemical Equilibria in Natural Waters," (John Wiley and Sons, NY, 1981).

Tadros-68a
Th. F. Tadros and J. Lyklema, "Adsorption of Potential-Determining Ions at the Silica-Aqueous Electrolyte Interface and the Role of Some Cations," Electroanal. Chem. and Interfacial Electrochem., 17(1968)267.

Tadros-69a
Th. F. Tadros and J. Lyklema, "The Electrical Double Layer on Silica in the Presence of Bivalent Counter-Ions," Electroanal. Chem. and Interfacial Electrochem., 22(1969)1.

Tschapek-74a
M. Tschapek, L. Tcheichvili and C. Wasowski, "The Point of Zero Charge (pzc) of Kaolinite and SiO_2 +Al_2O_3 Mixtures," Clay Minerals, 10(1974)219.

Tschapek-76a
M. Tschapek, C. Wasowski and R. M. Torres Sanchez, "The PZC and IEP and gamma-Al_2O_3 and TiO_2," J. Electroanal. Chem, 74(1976)167.

Vogel-62a
A. I. Vogel, "A Text-Book of Quantitative Inorganic Analysis, Including Elementary Instrumental Analysis," 3rd ed., (John Wiley, NY, 1962).

Westall-76a

J. Westall, J. Zachary and F. Morel, "MINEQL: A Computer Program for the Calculation of Chemical Equilibrium Composition of Aqueous Systems," in Technical Note No. 18, Ralph Parsons Laboratory, MIT, Cambridge, MA (1976).

Westall-79a
J. Westall, "MICROQL I. A Chemical Equilibrium Program in Basic," Swiss Federal Institute of Technology EAWAG (1979).

Westall-79b
J. Westall, "MICROQL II. Computation of Adsorption Equilibria in Basic," Swiss Federal Institute of Technology EAWAG (1979).

Westall-80a
J. Westall and H. Hohl, "A Comparison of Electrostatic Models for the Oxide/Solution Interface," Adv. Colloid Interface Sci., 12(1980)265.

Wiese-71a
G. R. Wiese, R. O. James, and T. W. Healy, "Discreteness of Charge and Solvation Effects in Cation Adsorption at the Oxide/Water Interface," in "Surface Chem of Oxides," Discuss. Faraday Soc., 52(1971)302, The Faraday Soc, London, University Press, Aberdeen, 1972.

Wiese-73a
G. R. Wiese, "Cation Adsorption and Heterocoagulation in Oxide/Water Systems," Ph.D. Thesis, University of Melbourne, 1973.

Yates-74a
D. E. Yates, S. Levine and T. W. Healy, "Site-Binding Model of the Electrical Double Layer at the Oxide/ Water Interface," Trans. Faraday S., 70(1974)1807.

Yates-75a
D. E. Yates, "The Structure of the Oxide/Aqueous Electrolyte Interface," Ph.D. thesis, University of Melbourne, 1975.

Yates-76a
D. E. Yates and T. W. Healy, "The Structure of the Silica/Electrolyte Interface," J. Colloid Interface Sci., 55(1976)9.

Yoon-79a
R. H. Yoon, T. Salman and G. Donnay, "Predicting Points of Zero Charge of Oxides and Hydroxides," J. Colloid Intrface Sci., 70(1979)483.

Yorpps-64a
J. A. Yorpps and D. W. Fuerstenau, "The Zero Point of Charge of α-Al_2O_3," J. Colloid Interface Sci., 19(1964)61.